Vitamin B12 Transport in Bacteria

Rempel, Stephan

Vitamin B12 Transport in Bacteria

A structural and biochemical study to identify new transport systems

Stephan Rempel

Cover: The Power of Transport – engine room of the *MS Cap San Diego*, one of the last seaworthy pre-container era general cargo ships in the world.
Cover design: Stephan Rempel

ISBN (print version): 978-94-034-1284-9
ISBN (online version): 978-94-034-1283-2

Printed by: Optima Grafische Communicatie B.V. – The Netherlands

The research described in this thesis was carried out in the Membrane Enzymology Group of the Groningen Biomolecular and Biotechnology (GBB) Institute of the University of Groningen, The Netherlands. The Netherlands Organization for Scientific Research (NWO), the European Research Council (ERC), and the European Molecular Biology Organization (EMBO) funded the research. The Stichting Stimulering Biochemie Nederland (SSBN-NVBMB) and the German Science Foundation (DFG) supported the project with travel grants.

university of groningen

Vitamin B12 transport in bacteria

A structural and biochemical study to identify new transport systems

PhD thesis

to obtain the degree of PhD at the
University of Groningen
on the authority of the
Rector Magnificus Prof. E. Sterken
and in accordance with
the decision by the College of Deans.

This thesis will be defended in public on

Friday 18th of January 2019 at 16:15 hours

by

Stephan Rempel

born on 24 June 1989
in Wertheim, Germany

Supervisors
Prof. D.J. Slotboom
Prof. B. Poolman

Assessment Committee
Prof. S.J. Marrink
Prof. A.J.M. Driessen
Prof. M.A. Seeger

“Technology is a big destroyer of emotion and truth, […] it makes it easier and you can get home sooner; but it doesn’t make you a more creative person. That’s [what] we have to fight in any creative field:
ease of use.”

– Jack White –

Table of Contents

Chapter 1

ECF-type ABC transporters

Rempel, S.[1], Stanek, W.K.[1], and Slotboom, D.J.[1,2]

[1]*Groningen Biomolecular and Biotechnology Institute (GBB), University of Groningen, The Netherlands*

[2]*Zernike Institute for Advanced Materials, University of Groningen, The Netherlands*

Adapted from the manuscript in press, which will be published in *Annual Reviews in Biochemistry*, **88**, 2019.

Table 1 and Suppl. tables 2-4 have been published previously in the PhD thesis of Stanek, W.K.

Abstract

Energy coupling factor (ECF)-type ATP-binding cassette (ABC) transporters catalyze membrane transport of micronutrients in prokaryotes. Crystal structures and biochemical characterization have revealed that ECF-transporters are mechanistically distinct from other ABC transport systems. Notably, ECF transporters make use of small integral membrane subunits (S-components) that are predicted to topple over in the membrane, to carry bound substrate from the extracellular side of the bilayer to the cytosol. Here we review the phylogenetic diversity of ECF-transporters, as well as recent structural and biochemical advancements that have led to the postulation of conceptually different mechanistic models. These models can be described as Power Stroke and Thermal Ratchet. Structural data indicate, that the lipid composition and bilayer structure are likely to have great impact on the transport function. We argue that study of ECF transporters could lead to generic insight of membrane protein structure, dynamics and interaction.

Discovery of ECF-transporters

The name energy coupling factor (ECF) was first used in the late 1970s by Henderson *et al.*, in a series of studies on uptake of folate, biotin, and thiamine in the Gram-positive bacterium *Lactobacillus casei* (1–10). Transport of each of these substrates depended on a specific, membrane-bound binding protein (now named S-component), and a shared component, for which different S-components compete, termed the energy coupling factor (now named ECF module). In these studies, it was shown that transport was most likely dependent on ATP hydrolysis, and it was speculated that the energy coupling factor might resemble the HisP component of the histidine transport system from *Salmonella typhimurium* (7, 11). We now know that both the ECF module and the histidine transport system contain ATPases belonging to the ABC superfamily (**Box B1, Figure 1**), but that the ECF-type ABC transporters form a structurally and mechanistically distinct group within this superfamily (12, 13). Although the molecular identity of ECF-type ABC transporters remained elusive at the time, the results cumulated in the remarkably accurate description of the function of ECF-transporters by Henderson *et al.*, postulating the "[…] hypothesis that the folate, thiamine, and biotin transport systems of *L[actobacillus] casei* each function via a specific binding protein, and that they require, in addition, a common component […, which] may be a protein required for the coupling of energy to these transport processes." (7).

In the 2000s, new ABC transporters were identified for the import of biotin (BioMN), Co^{2+} and Ni^{2+} (CbiMNQO and NikMNQO, respectively) in *Senorhizobium meliloti*, or *Salmonella enterica* and *Rhodobacter capsulatus*, respectively (14–16). These ABC transporters did not appear to make use of identifiable periplasmic substrate binding proteins (SBPs, **Box B1**), which were invariably associated with bacterial ABC importers known at the time, but a connection with the earlier work on ECF transporters was not made (14, 15, 17). Additionally, the genes encoding S-components of ECF transporters were picked up, without initially being linked to Henderson's work (18–24). The protein RibU (initially named YpaA) was found to be involved in riboflavin transport in *Bacillus subtilis* and *Lactococcus lactis*, and was assumed to be a new transport system (22, 24). Later this assumption was found to be incorrect, when it was recognized that RibU is a S-component of an ECF transporter, nonetheless the incorrect assumption was propagated in the interpretation of the first

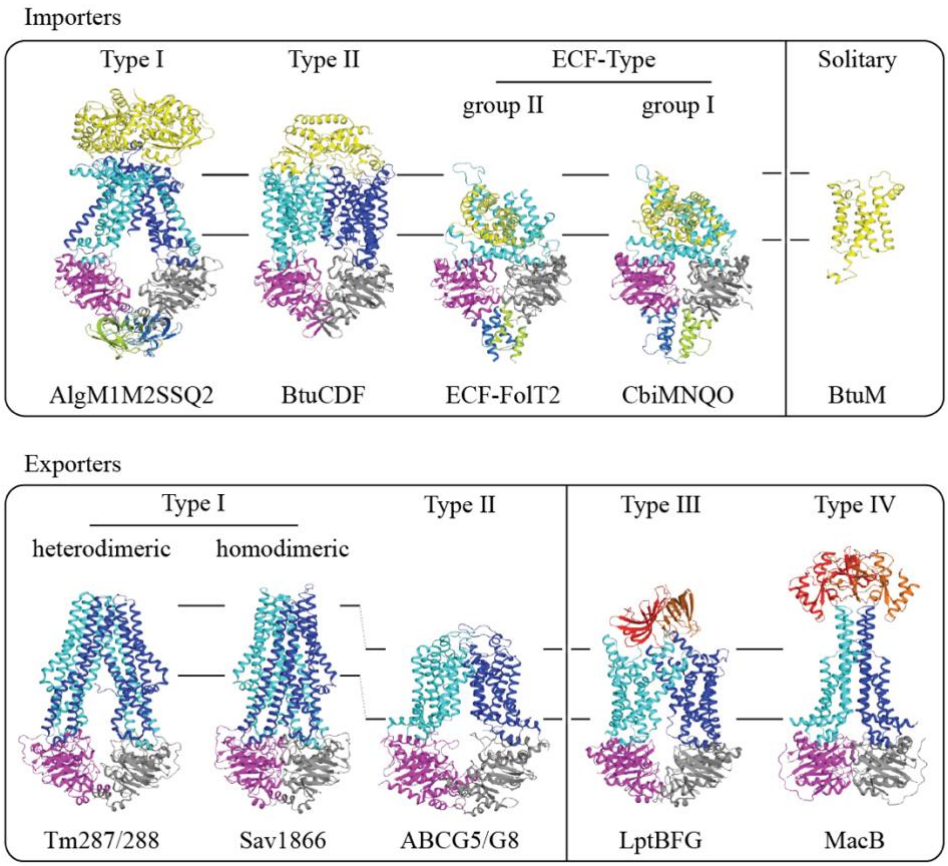

Figure 1: Comparison of the seven different structural classes of ABC-transporters, as well as solitary S-components. The color scheme is ATPase domains (magenta and grey), C-terminal domains (light blue and light green), integral membrane domains (cyan and dark blue), SBPs and S-components (yellow), and additional domains (orange and red). All structures were aligned on their NBDs in pymol showing the different distances of the NBDs from the membrane in various systems. On the top, ABC importers that are only known for prokaryotes are classified as type I, represented by the alginate transporter Alg M1M2SSQ2 (pdb: 4TQU), and type II represented by the cobalamin importer BtuCDF (pdb: 2QI9). Both types depend on an extracellular SBP. ECF-type ABC transporters are represented by the group II folate transporter ECF-FolT2 and group I Co^{2+} transporter CbiMNQO (CbiN missing in the structure; pdb :5JSZ and 5X3X, respectively) that have homologous or identical ATPases, respectively. Solitary S-components are represented by BtuM (pdb: 6FFV). On the bottom, ABC-exporters that are present in all kingdoms of life, are classified as type I that can be heterodimeric, sometimes with a degenerate ATPase site, or homodimeric, represented by the prokaryotic multidrug exporter Tm287/288 (pdb: 4Q4H) and Sav1866 (pdb: 2HYD), respectively. The human sterol exporter ABCG5/G8 (pdb: 5DO7) is a type II ABC-exporter. Type III and type IV ABC-exporters are also called ABC-mechanotransducers and export lipopolysaccharide in the case of LptBFG (pdb: 5X5Y) or antibiotics and enterotoxin in the case of MacB (pdb: 5LIL) (28–38).

crystal structure of RibU (25). The thiamine binding protein ThiT and folate binding protein FolT were the first to be associated with

Henderson's work (26). Then, in 2009, a comprehensive study combined bioinformatic and experimental data, and made the link with the energy coupling factor described by Henderson *et al.* in the 1970s (7, 13).

Box B1: Overview of the ABC transporter superfamily

ATP-binding cassette (ABC) transporters contain two conserved cytosolic nucleotide-binding domains (NBDs) or subunits that bind and hydrolyze ATP, and that are associated with a pair of integral membrane subunits (12, 13, 17, 40, 41). Seven different structural classes of membrane subunits have been discovered to date, which probably support different modes of transport (**Figure 1**). Four classes are dedicated to nutrient import in prokaryotes: type I importers, type II importers, ECF-type transporters, and solitary S-components. Type I and II importers make use of water-soluble substrate-binding proteins or domains (SBPs) that provide substrate specificity.

In ABC transporters, the binding and hydrolysis of ATP leads to conformational changes in the ATPase subunits, which are then transmitted to the transmembrane domains (TMDs) or subunits via α-helical structures on the cytoplasmic side of the membrane subunits (coupling helices). The transmembrane subunits cycle through different conformations that allow access of the transported substrate alternately to the extracellular side of the membrane and to the cytosol.

ECF-transporters are strict importers and widespread among prokaryotes (13). They are not present in eukaryotes, with a single possible exception in plants (27). ECF-transporters are specific for substrates that are needed in small quantities, including enzymatic cofactors or their precursors (such as B-type vitamins B1-3, 6-7, 9 and 12), the divalent cations nickel and cobalt, and a few other compounds such as tryptophan (**Table 1**). ECF transporters are genuine ABC-transporters (**Figure 1**) consisting of two ATP hydrolyzing nucleotide binding domains (NBDs), called ECF-A or A-component or EcfA, and two transmembrane proteins, termed ECF-T, T-component, or EcfT (**Box B2**), and S-component (13, 17, 27). The NBDs and ECF-T together form the tripartite ECF module (13). While the ECF-A subunits are similar to the NBDs from all other ABC transporters, the integral membrane subunits of ECF transporters are not related to those of other ABC transporters. ECF transporters do not make use of periplasmic or extracellular SBPs, which are essential components of

prokaryotic type I and type II ABC importers (13, 17, 39). Instead, the membrane embedded S-component solely confers substrate specificity to the uptake system.

ECF-type ABC transporters are classified into three groups: group I, group II, and solitary. Group I transporters are dedicated systems, where only a single S-component forms a complex with the ECF module. Group II transporters are modular, meaning that different S-components for various substrates can interact with a shared ECF-module (13, 39). The transport systems described by Henderson *et al.* in the 1970s belong to this group (7). Some organisms only encode an S-component, and do not contain genes coding for the ECF module (13, 30, 39, 43). It is still controversial whether these solitary S-components constitute *bona fide* transport systems themselves, but recent data supports a transport function and suggests that they may be more widespread than previously thought (30).

Here, we provide an overview of the phylogeny and diversity of ECF-transporters, and review recent structural and biochemical advancements that have led to more detailed mechanistic insights. We discuss different conceptual models for ATP-coupled transport, and show that the study of ECF transporters could lead to generic understanding of membrane protein structure, function, and dynamics.

Diversity and phylogeny of ECF-transporters

The highly curated SEED database (http://pseed.theseed.org/?page=Home) currently contains 1,876 prokaryotic genomes encoding ECF-transporters with a variety of different substrate specificities (**Table 1**) (44). This number reduces to 1,445 representative organisms upon removal of sub-strains of the same species. Of these 717 are Firmicutes, 378 Proteobacteria, 175 Actinobacteria, 51 Tenericutes, and 124 belong to other phyla or Archaea.

The dedicated group I transporters are defined as ECF transporters that have all subunits encoded in a single operon (13, 39). There are 1,927 individual group I ECF-transporters (**Figure 2a**), but the number of organisms containing these transporters is smaller because they can carry more than one group I ECF-transporter, which is most pronounced in archaea and actinobacteria, with for example six group I transporters

present in *Thermofilum pendens* (13, 27, 39). While they are most prevalent in Firmicutes, group I systems are present in a wider range of organisms than group II ECF transporters (**Figure 2a**).

Box B2: Difficulties in ECF-type ABC transporter nomenclature

- Many databases wrongly annotate the ECF-T and ECF-A subunits of ECF-transporters as CbiQ or CbiO, respectively, although these terms are specific for the cobalt ECF-transporter CbiMNQO.
- The name of the S-component HmpT has changed to PdxU2, because genome context analysis showed that the protein is specific for pyridoxin (13, 27). The most prominent example of the use of the name HmpT is the ECF-HmpT full complex structure from 2013 (42).
- No uniform naming rules have been adapted because many gene and protein names were assigned before the discovery of ECF-transporters leading to situations where CbiM or BioM are S-component or ATPase, respectively. We advise to use the unique names of all subunits for group I transporters, for instance CbrTUV for the vitamin B12 specific transporter. For group II transporters we propose to use the name 'ECF' for the ECF module, followed by the name of the S-component. For example, the name ECF-CbrT for the vitamin B12 specific group II transporter.

Group II transporters are defined as ECF transporters that have the ECF module subunits encoded in one operon, and have one or multiple S-component genes scattered over the genome (13, 27, 39). There are 787 group II ECF-modules that collectively are predicted to interact with 4,387 S-components to allow for transport of different substrates (**Figure 2b**). Almost all group II transporters are found in Firmicutes (**Figure 2b**). The number of S-components and group II ECF modules per organism is highly variable. For example, *Enterococcus Faecium* DO carries as many as 21 S-components and three ECF-modules. It is unknown if the different modules in one organism interact with specific subsets of S-components. Both group I and group II ECF-transporters may be present within a given organism, e.g. *Lactobacillus delbrueckii* carries the thiamine-specific group I ECF-transporter YkoEDC as well as a group II ECF module that can interact with seven different S-components. Finally, apart from the transition metal ion importers that exclusively belong to group I, there seems to be no apparent linkage between the nature of the transported

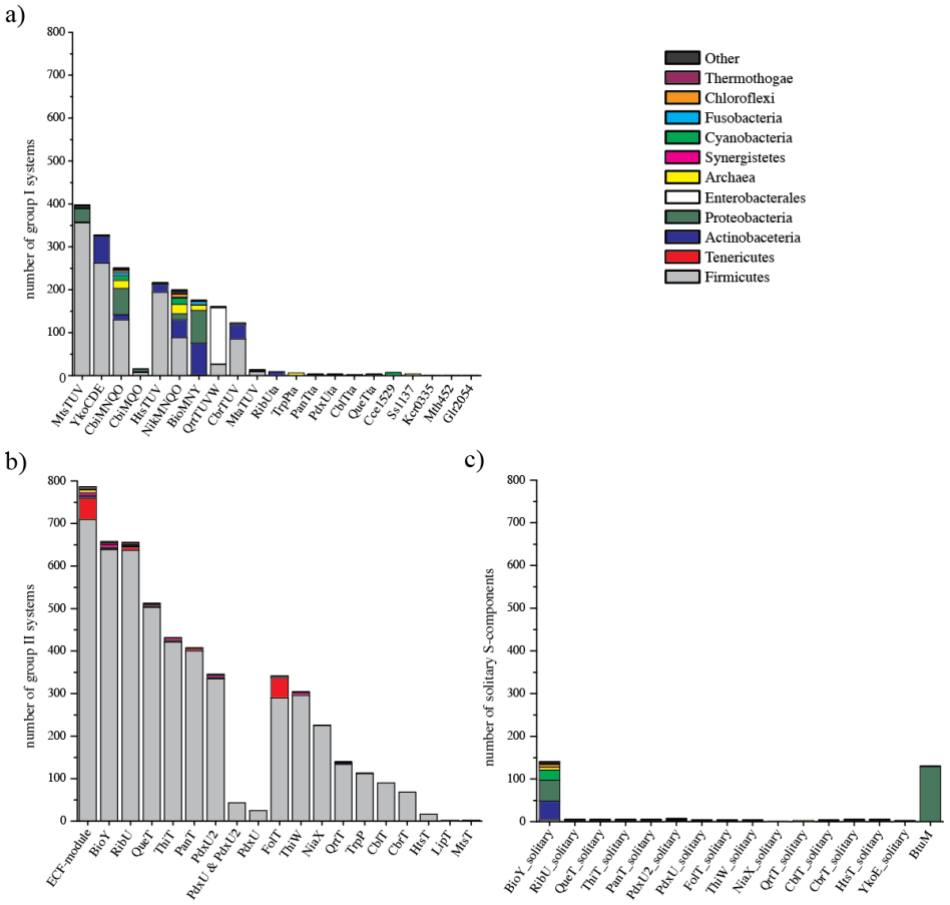

Figure 2: Phylogeny of ECF-type ABC transporters based on the SEED database. The color coding for the different genera in all panels can be found in the inset and the phylogeny was generated using PhyloT (https://phylot.biobyte.de). a) Phylogeny of group I and b) group II transporters. c) Phylogeny of solitary S-components (BtuM not annotated in the SEED database, taken from (30)).

substrate and grouping into I or II. For example, group I CbrTUV and group II ECF-CbrT are both specific for vitamin B12 (**Table 1**) (45).

Solitary S-components are defined as S-components present in organisms that do not encode an ECF module (30, 39, 43). The absence of an ECF module can be deduced from failure to identify a T-component, or from analysis of the ABC-type ATPases. In organisms with solitary S-components, the latter are all associated with ABC transporters from different types than ECF transporters (30). In contrast to full ECF-transporters, solitary S-components are not widespread in Firmicutes. There are 304 solitary S-components, which are distributed mainly over

two families (**Figure 2c**). 141 solitary BioY proteins (specific for biotin) are most prevalent in Proteobacteria, Actinobacteria, and Cyanobacteria. The 131 solitary S-components that belong to the BtuM family, which is specific for Vitamin B12, are almost exclusively found in Proteobacteria (30). Sequence analysis failed to recognize that BtuM is an S-component, but a recent crystal structure showed that it have the S-component fold. It is not yet annotated as S-component in the SEED database (21, 30).

There are currently 27 families of S-components, predicted or confirmed to be specific for different substrates (**Table 1**). S-components that are specific for different substrates often share very little sequence identity (~15%), which raises the possibility that families of S-components, possibly for novel substrates, have escaped detection. This makes identification of new S-components difficult, as exemplified by the characterization of BtuM (13, 27, 30, 39).

Some cyanobacteria (**Table 1**) and plants encode and ECF-T protein, but carry genes for neither ECF-A nor S-components. These ECF-T proteins, called cyano_T, are either non-functional, broken ECF-transporters or have acquired a new function, which may be unrelated to nutrient transport (27).

Besides the differences in genetic organization, also regulation of expression differs between group I and II transporters. Group I ECF-transporter levels are often regulated by the intracellular substrate concentration, most commonly by riboswitches (13, 39). Likewise, levels of S-components from group II ECF transporters are strongly regulated by the cellular needs, with more protein produced when the substrates are scarce (13, 39). In contrast, the expression of the group II ECF-module is constitutive giving rise to a constant pool of units, available to interact with substrate-bound S-components (13, 39). The differentially regulated expression of the group II ECF module and associated S-components can lead to an imbalance, where a great surplus of S-components exists. These excess S-components may act as substrate scavengers remaining bound to their substrate until an ECF-module becomes available (39).

Table 1: Diversity of ECF-type ABC-transporters based on (13).

System	ECF-T	ECF-A	S-component	Add. component	Group[a]	Substrate[b]	Notes	Ref.[c]
BioMNY	BioN	BioM	BioY		I & II	**Biotin**		(14, 16)
BioY			BioY		solitary	**Biotin**		(43)
BtuM			BtuM		solitary	**Cobalamin**		(30)
CbiMNQO	CbiQ	CbiO	CbiM	CbiN	I	**Cobalt**		(15, 32)
CblT	CblTt	CblTa	CblT		I & II	Cobalamin precursor	[d]	
CbrTUV	CbrV	CbrU	CbrT		I & II	**Cobalamin**		(45)
Cce1529	Cce1531	Cce1530	Cce1529		I	Unknown	not in (13), archaeal	
Cyano_T	Cyano_T				?	Unknown	not in (13)	(27)
FolT			FolT		II	**Folate**		(26)
Glr2054	Glr2053	Glr2054	Glr2052		I	Unknown	not in (13), cyanobacterial	
HtsTUV	HtsU	HtsV	HtsT		I & II	Unknown		
Kcr335	Kcr0337	Kcr0336	Kcr0335		I	Unknown	not in (13), archaeal	
LipT			LipT		II	Lipoate		
MtaTUV	MtaV	MtaU	MtaT		I	Methylthio-adenosine		
MTH452	MTH453	MTH454	MTH452		I	Unknown	not in (13), archaeal	
MtsTUV	MtsV	MtsU	MtsT		I & II	Methionine precursors		
NiaX			NiaX		II	**Niacin**		(46)
NikMNQO	NikQ	NikO	NikM	NikN	I	**Nickel**		(15)
PanT	PanTt	PanTa	PanT		I & II	**Pantothenate**	[d]	(47, 48)
PdxU	PdxUt	PdxUa	PdxU		I & II	Pyridoxine	[d]	
PdxU2			PdxU2		II	**Pyridoxine** (27)	formerly HmpT (27)	(42)[d]
QrtTUVW	QrtU	QrtV, QrtW	QrtT		I	Queuosine precursor		
QueT	QueTt	QueTa	QueT		I & II	Queuosine precursor	[d]	
RibU	RibUt	RibUa	RibU		I & II	**Riboflavin**	[d], group I in Bifidobacteria	(22, 23)
Ss1137	Ss1135	Ss1136	St1137		I	*Unknown*	not in (13), archaeal	
ThiT			ThiT		II	**Thiamine**		(26, 49)
ThiW	?	?	ThiW		(I) & II	Thiazole		
TrpP	TrpPt	TrpPa	TrpP		I & II	Tryptophan	[d]	
YkoEDC	YkoC	YkoD	YkoE		I	**Thiamine**		(50)

[a]All names are given for the group I transporters, the naming for the corresponding group II transporters is ECF- followed by the name of the S-component, e.g. the vitamin B12 specific ECF-transporter is termed CbrTUV for group I and ECF-CbrT for group II (45). Grouping was derived from entries in the SEED database and my differ from (39) and does not include solitary S-components (same substrate specificity assumed).

[b]Highlighted substrates are experimentally confirmed.

[c]Referenced are the relevant *experimental* studies that show the substrate specificity of the respective transport systems. If no reference is given the substrate specificity is taken from predictions from (13).

[d]In (13) these S-components were identified as exclusively occurring in group II ECF-transporters, but group I examples can now be found in the SEED database.

[e]Only the structure of the *apo* complex is reported; no functional data proving substrate-specificity is given.

Crystal structures of ECF-transporters

Currently, five crystal structures of complete group II complexes, and one structure of a group I transporter are available (31, 32, 42, 45, 48, 51). Additionally, structures of isolated S-components (group I, II, and solitary) and of the ATPase subunits have been reported (**Suppl. Table 1**) (25, 30, 32, 50, 52–58).

Collectively, the structures support the notion that the S-component, ECF-T, and two homologous or identical ATPases are present in a 1:1:1:1 stoichiometry for both group I and II transporters (13, 39, 46). In some cases, two or three subunits of the transporters may be fused in various combinations, resulting in multiple-domain proteins with fusion of the two ATPases being most common (13, 39). S-components from group II ECF-transporters can dissociate from the complex dynamically and exist most likely as monomers until they association again with an ECF-module (25, 49, 53, 54). The group I ECF transporters for Ni^{2+} and Co^{2+} appear to require one or two additional small integral membrane subunits for transport (CbiN, NikN, or NikKL) but the exact role of these subunits is unclear (13, 15, 32).

Deviations from the generic 1:1:1:1 subunit stoichiometry in ECF-transporter and monomeric S-components have been postulated for BioMNY and ECF-RibU, based on *in vivo* analyses and cross-linking studies (58–61). It is difficult to reconcile these data with the crystal structures and other biochemical data (39, 46, 62). It is possible that supramolecular complexes of different subunit stoichiometry are formed in some conditions, for example *in vivo*, but the apparent differences in stoichiometry could also stem from experimental artefacts (58–61). In our discussion of the proposed transport mechanism, we will adhere to the 1:1:1:1 subunit stoichiometry.

Powering transport by ATP hydrolysis

ATP hydrolysis is essential for substrate transport by ECF transporters (46). The ATPases of ECF-transporters have all the hallmarks of ABC transporter ATPases (**Figure 1**) that have been extensively reviewed elsewhere (17, 40, 63). The ~31 kDa proteins form dimeric assemblies with (pseudo) two-fold symmetry. Two catalytic sites for ATP hydrolysis

are located at the dimer interface (27, 42, 51, 58). The ATPase dimer consists either of two identical (homodimer, ECF-AA) or homologous (heterodimer, ECF-AA') ATPases (13). ECF transporters ATPases do not contain degenerate sites, a feature that is sometimes observed with heterodimeric ATPases of ABC transporters (33, 64–70). Structurally, each ATPase is a three-domain protein consisting of a RecA-like domain, an α-helical domain and a C-terminal extension (58). The RecA-like and α-helical domain are universal to all ABC-transporter ATPases (27, 63).

Structural and biochemical studies indicate that the ATPases of ECF-transporters function in a similar manner as those of other ABC-transporters (17, 27, 32, 39, 52, 58, 71, 72). In the absence of ATP the two subunits are separated from each other and adopt an 'open' conformation (58, 63). ATP binding leads to tight association of the dimer by bringing the RecA domain from one subunit in close contact with the α-helical domain of the other. In the resulting 'closed' conformation, the catalytic sites are now complete, ready for ATP hydrolysis to proceed (32, 63). Upon ATP hydrolysis and release of ADP and orthophosphate the dimer opens again. The 'open' and 'closed' conformations have been observed structurally in isolated ATPase dimers in the absence of the membrane subunits (32, 58). For the complete group I transporter BioMNY, it has also been shown that 'open' and 'closed' states are visited by EPR-experiments (71). In addition, intermediate states may also exist (71). In all crystal structures of complete ECF transporter complexes determined to date, the ATPases are in the 'open' conformation, which limits our understanding on how conformational changes in the ATPases are propagated to the membrane subunits (31, 32, 42, 45, 48, 51). A structure of ECF-FolT2 from *L. delbrueckii* in complex with the slowly hydrolysable ATP analogue AMP-PNP has been solved (31), but the ATPases remained in an 'open' conformation, with the nucleotides contacting exclusively the RecA domains (**Figure 3**). In other ABC transporter systems non-hydrolysable ATP analogues can lead to closure but sometimes fail to do so (33, 70, 73). In BioMNY, the ATPase activity is only moderately affected by inhibitors such as AMP-PNP or orthovanadate. Taken together, ECF-transporters may be less sensitive compared to other ABC-transporters to ATPase inhibitors (71).

Within each ATPase subunit there is a groove between the two domains where interaction with the ECF-T subunit takes place. Specific for the ATPases of ECF-transporters, the groove between the domains contains a

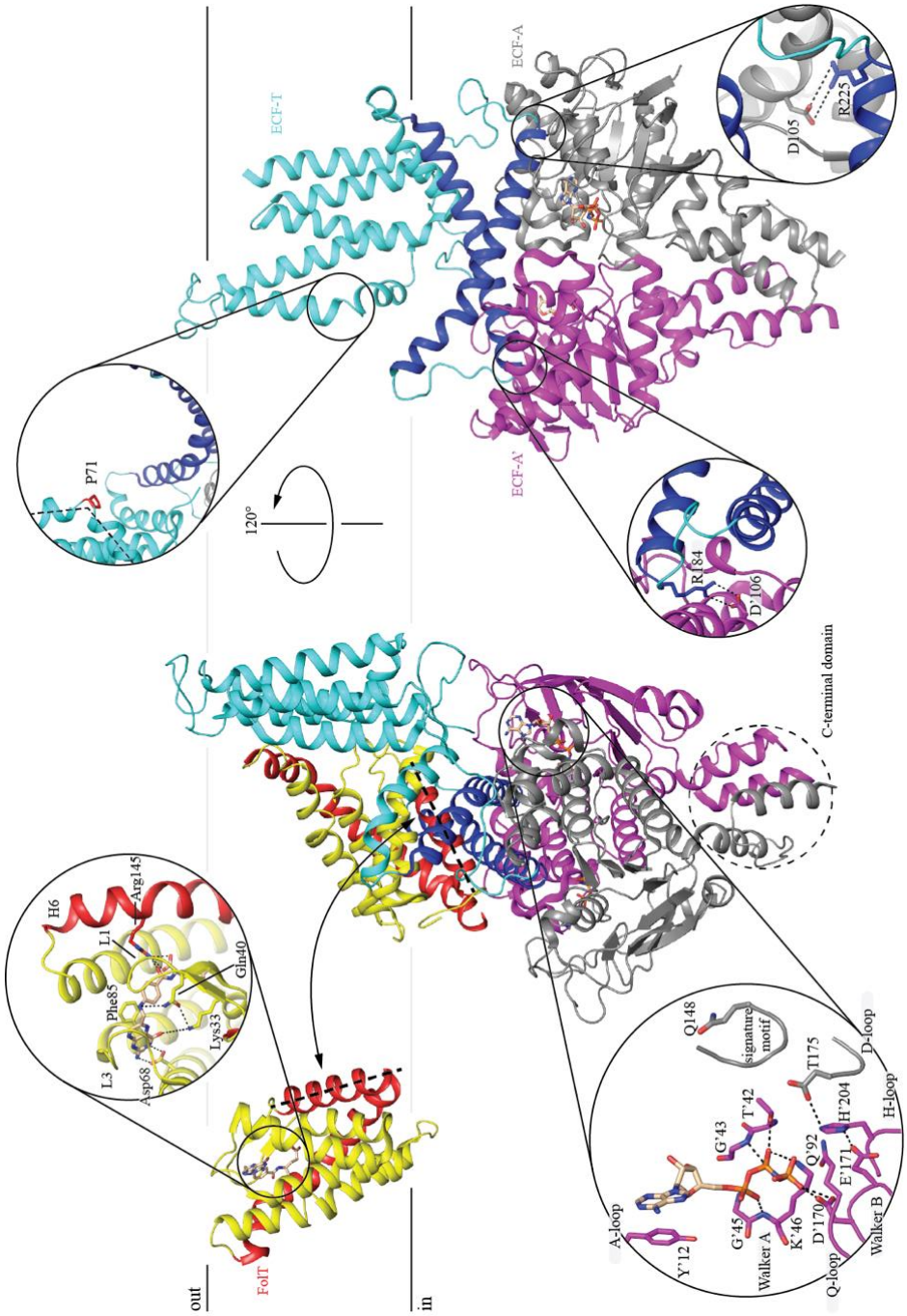

conserved acidic residue that makes contact with a conserved arginine residue in ECF-T (see below, **Figure 3**) (47, 58, 59). The groove of the ATPases from ECF transporters also contains a specific element, called

Q-helix, comprised of six residues with sequence X-P-D/E-X-Q-ϕ (X is any and ϕ is a hydrophobic residue). The Q-helix is located toward the dimer interface and essential for transport activity, although it is neither directly involved in ATP binding nor hydrolysis (58).

The group II ECF-transporter ATPases possess an additional C-terminal helical extension (**Figure 3**) that is absent in many group I ECF-transporter ATPases (13). It likely mediates dimer formation in the absence of nucleotides (58). C-terminal extensions at the NBDs can also be found in type I ABC-importers (**Figure 1**), where they usually have regulatory functions (74–76). Whether the C-terminal domain in the ATPases of ECF-transporters also exerts regulatory function over transport activity remains to be shown.

Biochemical characterization of the ATPase activity has been carried out for ECF-transporters from various organisms. **Suppl. Table 2** summarizes data on ATPase activity that has been determined for ECF-transporters. The K_M values for ATP hydrolysis range from ~0.1 mM up to ~16 mM (**Suppl. Table 2**). In the full complexes, ATP hydrolysis is not stimulated by the presence of the transported substrate, which contrasts with other ABC transporters (17, 31, 71). In the group I cobalt transporter CbiMNQO, ATPase activity is dependent on the presence of the S-component, but it is not clear whether this is a generic property of ECF transporters (32). Comparisons of transport kinetics (**Suppl. Table 3**) and ATPase activity have revealed ECF-type ABC transporters, like group II ABC transporters, exhibit ATPase activity without coupling to transport events (31, 77). Whether the futile ATPase activity is an artefact or mechanistically relevant is unclear (see mechanistic discussion below).

Figure 3: Overview of structural features in ECF-type ABC transporters. From left to right, viewed from the plane of the membrane: the folate-bound S-component FolT (pdb: 5D0Y), the ECF-transporter ECF-FolT2 (pdb: 5D3M), and the ECF module of ECF-FolT2 rotated 120° relative to the middle panel. FolT and FolT2 are colored yellow, ECF-T cyan, and the ATPases magenta (ECF-A') or grey (ECF-A). Coupling helices are dark blue, helix 1 and 6 in FolT/FolT2 are red, and substrates (folate in FolT and AMP-PNP in ECF-AA') are wheat. Helix 1 in FolT and FolT2 is highlighted with a dashed line and shows the ~90° toppling between the upright and toppled states. The top-left blow-up shows the folate-bound substrate binding pocket in FolT. Highlighted are residues that are involved in substrate binding, which are located in loop1 and 3 and helix 6. The bottom-left blow-up highlights one of the two ATP-binding sites, occupied with an AMP-PNP molecule. Highlighted are all residues involved in nucleotide binding and all motifs present in canonical ABC-transporter ATPases. In the top-right blow-up helix 3 of ECF-T is highlighted by a dashed line. The kink in the helix at Pro71 is the hinge point for conformational flexibility of the

The scaffold subunit ECF-T

The integral membrane subunit ECF-T is the scaffold of the complex. It has an L-shape with a peripheral coupling domain on the cytoplasmic side of the membrane that binds to the ATPase subunits, and an integral membrane domain that keeps the ECF module associated with the lipid bilayer (**Figure 3**).

The transmembrane domain is poorly conserved and can vary in the number of transmembrane helices ranging from four (e.g. in BioN QrtU), five (most ECF-Ts), six (YkoC, CbrV, and some QrtU), seven (ECF-T in *Thermotogales* and some BioN), to eight (some CbrV) (27). In contrast, the coupling domain is better conserved, and contains two long α-helices that are arranged in an 'X' shape (**Figure 3**). These α-helices form the main interaction site for ATPases and are hence called coupling-helices, with each coupling helix making tight contact with a single ATPase (59). Both coupling helices contain a conserved arginine residue at their carboxy-terminal end, which binds in the deep groove of the ATPase subunit near the Q-helix and anchors the subunits together (**Figure 3**). The conserved arginine residue is part of a short motif, X-Arg-X (most often Ala-Arg-Gly) (47). Because of the tight interaction between the C-terminal ends of the coupling helices and the ATPase subunits, it is expected that the coupling helices are forced to move jointly with the ATPases when the latter switch between 'open' and 'closed' conformations upon nucleotide binding and release, thereby transferring conformational changes in the ATPases fueled by ATP hydrolysis to the membrane subunit of ECF-T (27, 32, 39, 52).

Coupling helices are a common structural feature of ABC transporters used to propagate conformational changes from the ATPases to the membrane domains (78). The main difference to ECF-transporters is that other ABC transporters have one coupling helix per membrane domain, each interacting with one ATPase, whereas ECF-T harbors both helices and thus contacts two ATPases. Further, the coupling helices in other ABC-transporters are much shorter than the ones in ECF transporters, and are well separated from each other instead of forming an interacting X-shaped structure (**Figure 1 and 3**) (63, 78).

While the surface of the coupling domain of ECF-T that faces the cytoplasm interacts with the ATPases, the opposite side of the domain,

exposed toward the membrane interior, allows for the interaction with the S-component (**Figure 3**). The interacting surfaces of ECF-T and the S-component are hydrophobic and highly complementary in shape. They are also extensive, covering about one third of the surface of the S-component explaining the tight interaction between the membrane subunits observed in the nucleotide-free complexes (31, 42, 51). The coupling domain is located between the S-component and the ATPase subunits, and prevents the S-component from interacting directly with the ATPases (42, 51). Nonetheless, movement of the coupling helices upon closing and opening of the ATPase dimer will also affect the of of the coupling helices upon closing and opening of the ATPase dimer will also affect the interaction interface of ECF-T with the S-component (31, 42). This may cause dissociation of the S-component (at least in group II transporters) and reorientation of the substrate binding site leading to alternating access (31, 52).

In all crystal structures of ECF transporters, the coupling domains of ECF-T, the ATPase subunits, and the S-components have very similar conformations, regardless of the nature of the S-component in the complex (FolT, FolT2, PanT, CbrT, PdxU2, or CbiM), or the presence or absence of the nucleotide analogue AMP-PNP (31, 32, 42, 45, 48, 51). In contrast, the membrane domains of ECF-T adopt different conformations in the various crystal structures. They pivot to different extents relative to the scaffold domain, indicating that they can display considerable conformational flexibility, even in complexes trapped in the same state (**Figure 3**). Such conformational differences are observed in structures of the identical ECF modules complexes with different S-components (ECF-PanT, ECF-FolT and ECF-PdxU2 from *L. brevis*, and ECF-FolT2 and ECF-CbrT from *L. delbrueckii*) (31, 42, 45, 48, 51). In these cases, the flexibility may be required to accommodate specific structural features of the S-components, which are poorly related in sequence (13). The conformational differences are also observed in two crystal structures of the same ECF transporter (ECF-FolT2), suggesting that the flexibility may be an inherent feature of ECF-T proteins (31), which could be relevant for the mechanism of transport (see mechanistic discussion below). Regardless of the conformational differences observed in the membrane domains of ECF-T in the various structures, they all are in contact with the bound S-component, and may act as a flexible and 'greasy' sliding surface to allow movements of the S-components during transport (see below) (42).

Membrane embedded substrate binding proteins – S-components

S-components are the substrate binding proteins of ECF-transporters. S-components are integral membrane proteins of ~20-25 kDa and not related to soluble, periplasmic or extracellular binding proteins in type I and type II ABC importers (**Figure 1 and Box B1**) (63). Crystal structures have been determined of isolated S-components from group I (NikM, YkoE) and group II transporters (BioY, FolT, RibU, ThiT), and of solitary BtuM, all in substrate-bound states (**Suppl. Table 1**) (25, 30, 50, 53–57). The core structure of all S-components is a bundle of six α-helices arranged like a cylinder. Some group I S-components have additional N- or C-terminal extensions (32, 50, 55). Even though S-component families for different substrates do not share significant sequence similarity, their structures are well conserved. For example, the interface consisting mostly of α-helices H1, H2, and H3 of S-components that interacts with the ECF-T subunit is well conserved (31, 53).

The orientation of the isolated S-components in the membrane has been deduced from the positive inside rule and molecular dynamics simulations, indicating that the N- and C-termini of the 6-helix bundles are located in the cytoplasm, and the six helices are membrane-spanning (50, 79). In this orientation the binding site is located close to the extracellular side of the membrane in a deep pocket (30, 50, 53). Substrates are bound with high affinity, often in the low or sub-nanomolar range (**Suppl. Table 4**), which can be explained from the structures, since in many cases every possible hydrogen bond interaction between substrate and protein is satisfied (57, 80–82). The group I S-components NikM and CbiM (specific for nickel and cobalt ion, respectively) contain an additional N-terminal α-helix and have their N-terminus located on the extracellular side of the membrane. The first two amino acids of the extra helices participate in substrate binding (32, 55).

In all isolated S-components from group II transporters as well as in the group I S-component NikM, the binding pocket is occluded by extracellular loops (25, 53–57). Structures of isolated S-components in the *apo* state have not been determined, but in the structures of the full complexes the S-components are in *apo*-states (31, 32, 42, 45, 48, 51). Comparison of the *apo* and substrate-bound structures suggests that loops L1 (connecting transmembrane helices H1 and H2) and L3 (connecting

helices H3 and H4) act as the extracellular gate for substrate access (31, 53, 54, 57, 79, 83). Other conformational changes do not appear to occur upon substrate binding in S-components, and thus the helical core of S-components appears rigid. This conclusion is consistent with EPR experiments showing that only changes in the conformation of loop L1 occur upon thiamine binding to isolated ThiT (79). Differently from this gating mechanism, the group I S-component YkoE from *Bacillus subtilis* does not possess such gating loops. Although the substrate thiamine is deeply buried inside the protein, it is not occluded from the environment. Also in the solitary S-component BtuM, the binding site is not occluded (30, 50).

An unprecedented structural feature of the S-components became apparent when the first structures of full complexes of ECF-transporters were solved (42, 51): the S-components are toppled in the complex by almost 90° compared to the predicted orientation of the isolated S-components. The transmembrane helices H1-H4 lay parallel to the membrane, close to the cytoplasmic side, instead of traversing the bilayer. In the toppled state, the substrate binding site is accessible from the cytoplasm (**Figure 3**). It is noteworthy that the positively charged cytoplasmic loops remain located on the cytoplasmic side of the membrane in the toppled state, and may prevent toppling to greater extent, or full rotation of the protein. Loops L1 and L3, which are predicted to be located extracellularly in the isolated S-components, are also located close to the cytoplasmic side of the membrane in the toppled state. These loops generally do not contain charged residues, which may facilitate the adoption of the toppled state (31). Loop L5 remains close to the extracellular side of the membrane in both states (**Figure 3**).

Toppling may be a new mechanism of transport, which allows alternate exposure of the binding site to either side of the membrane, thus following the generic alternating access model of membrane transport (84, 85). In the proposed toppling mechanism, the substrate binding pocket travels through the membrane, but remains confined to the S-component (**Figure 3**). It has been hypothesized that ECF-T plays a key role in aiding with the toppling of the S-component by offering a surface for the S-component to glide along, although solitary S-components like BioY and BtuM may achieve transport also by a toppling-type mechanism without an ECF-module (30, 31, 42, 43). The toppling mechanism of transport resembles the elevator mechanism found in secondary transporters (86). In

transporters using the elevator mechanism, the transport domain (equivalent to the S-component) moves through the membrane to carry the substrate from one side to the other, and a scaffold domain (equivalent to ECF-T) provides a stable scaffold along which the movement can take place. In the glutamate transporter family, the transport domains occlude the substrate completely (like in S-components belonging to group II), whereas in other cases (such as in CitS or vcINDY) the substrates are not completely occluded by the transport domain and face the scaffold domain during transport (as may be the case in YkoE) (50, 86, 89–92). A difference between the elevator mechanisms and the toppling mechanism is, that toppling involves mostly rotation of the S-component, with a minor translational component, whereas the converse takes place in elevator-like movements (86, 89, 93, 94). A structural feature common to all S-components that may be facilitate toppling, is the long helix H6 that in both the upright and toppled state is tilted relative to the membrane by ± 45°. This tilt is likely required to match the width of the lipid bilayer meaning that it would stick out of it in a perpendicular orientation. Thus, this helix might act as a switch locking the S-component in either state (**Figure 3**).

Box B3. Power Stroke and Thermal Ratchet mechanism (87, 88)

The coupling between the chemical reaction of ATP hydrolysis and the vectoral process of substrate translocation is poorly understood in ABC transporters. ATP hydrolysis is often assumed to drive a Power Stroke that forces the substrate to move from one side of the membrane to the other via a series of conformational changes. These conformational changes would be highly unfavorable without the free energy released by interactions of the protein with ATP, ADP or inorganic phosphate. 'Coupling' is achieved if the conformational changes can take place only if the transported substrate is bound.

The Thermal Ratchet provides an alternative conceptual framework to describe ATP-coupled substrate transport. In a thermal ratchet model the substrate movement step across the membrane takes place by thermal motions (like in facilitated diffusion mechanisms), but interactions of the transport protein with another component stabilize the inward facing conformation. The bias comes at a price: free energy from ATP hydrolysis is needed to reset the transporter for a next round of transport. In a ratchet mechanism, the resetting of the substrate-free transporter is coupled to ATP hydrolysis, instead of substrate movement across the membrane.

Although S-components for different substrates do not share significant sequence identity, in the transmembrane helix H1 of group II transporters a A-X-X-X-A motif is found, which is essential for the tight interaction with the coupling domains in the ECF-module and activity of the transporter (39, 53, 95). This motif does not seem to be conserved in solitary S-components, which do not interact with an ECF module, at least for BtuM (30). For dedicated group I transporters, there are variations of the motif, like A-A-X-X-X-A for BioMNY or S/A-X-X-X-I/V-V for YkoEDC (50, 71). Therefore, the motif appears to be critical for non-solitary S-components to interact with the ECF module, but given the more extensive interaction surface, the motif alone is unlikely to be sufficient to mediate specificity of complex assembly. Structural data provides a clue as to that large hydrophobic patches are involved in mediating protein-protein interactions (31, 42, 51), but how they achieve specificity that, at the same time, is promiscuous with different affinities in group II transporters remains unclear (39).

Transport mechanisms

Two mechanistic interpretations of the structural and biochemical data are currently prevalent, which can be classified roughly as Thermal Ratchet and Power Stroke models (**Box B3**) (31, 52). We will discuss the mechanistic models using **Figure 4**.

State one is the only conformation, in which the full complexes have been structurally resolved to date (**Suppl. Table 1**). The ATPases are in the open conformation and the *apo* S-component is toppled over with its binding pocket exposed to the cytosol. The side-chains that constitute the high-affinity substrate binding site in the isolated S-components are displaced in this state, which suggests that substrate affinity is lost. This notion is consistent with the observation that binding of the transported substrate to the full complexes in the nucleotide-free state has not been observed (45, 52). Apparently, the free energy released by the interaction between the S-component and ECF-T is used to destroy the binding site. The mechanism, by which this disruption occurs may differ. In group II transporters the binding site destruction is mostly allosteric, with the gating loops L1 and L3 pried apart as a result of the association of the S-component with the ECF module (31, 45, 48, 51). In the group I

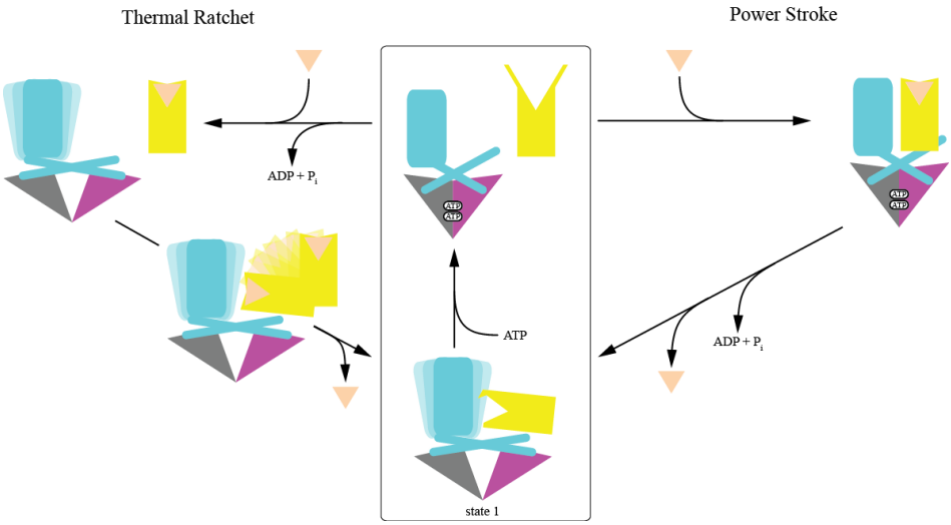

Figure 4: Proposed transport mechanisms for ECF-type ABC transporters. ATPases are shown as grey and magenta triangles, ECF-T in cyan with its transmembrane domain as box and the two coupling helices as bars, and an S-component is depicted in yellow. In the ground state of the transporter (center bottom, state 1), where the ATPases are nucleotide-free and separated, the S-component is in its toppled state and the binding site is disrupted and exposed to the cytoplasmic side. The membrane domain of ECF-T is flexible as indicated. Upon binding of ATP molecules (middle top) the ATPases move toward each other, which also results in a different conformation of the coupling helices potentially disrupting the interaction interface with the S-component, leading to dissociation of the S-component, and toppling to the upright conformation with the binding site exposed to the exterior. In this conformation the S-component can tightly bind the transported substrate. These steps are common to both proposed mechanisms. In the Thermal Ratchet model (left side), ATP is hydrolyzed and ADP+P_i are released, which results in separated ATPases. The substrate-bound S-component can now associate with the complex and flexibility in the membrane domain of ECF-T allows for interaction with different S-components. The S-component topples and clicks onto the coupling domain, thereby disrupting its substrate-binding site and releasing the substrate in the cytosol. In case of the Power Stroke mechanism (right side), the substrate-bound S-component can only associate with the nucleotide-bound ECF-module and hydrolysis of ATP triggers toppling. This results in binding-site disruption and substrate release.

transporter CbiMNQO, direct competition also pays a role, with a phenylalanine sidechain of ECF-T entering the binding pocket (**Figure 5**) (32, 55). This competition resembles the 'scoop-loop' mechanism used by the type I ABC transporter for maltose, and a similar mechanism is proposed for the Type II ABC transporter for vitamin B12, even though their transport mechanisms are unrelated to that of ECF transporters (77, 96).

Both the Power Stroke and Thermal Ratchet models postulate that Mg-ATP binding leads to reorientation of the *apo* S-component to an upright conformation, with the empty binding site exposed to the outside, ready to

bind a substrate molecule from the environment. ATP binding to the ATPase subunits likely leads to repositioning of the coupling helices in ECF-T, which would modify the tight interface with the S-component, located on the opposite face of the coupling helices, and thus can lead to reorientation of the S-component (31, 52).

The most direct evidence for this step comes from monitoring substrate binding and S-component release in detergent solution upon Mg-ATP binding (52). Release of the S-component is a prerequisite for the observed competition of different S-components for the same ECF module (see section on competition below). Whether release also occurs in group I transporters is not clear. The group I transporter BioMNY does not release the S-component BioY when reconstituted in nanodiscs, whereas in detergent solution they do dissociate. In the former case, possible release may have been obscured by the belt protein, which creates a confined bilayer patch. In the latter case, the authors state that the observation is irrelevant because conditions were non-physiological (43, 71).

Once the S-component has bound the transported substrate from the outside, the two models start deviating (**Figure 4**). In the Power Stroke model (52), the substrate translocation step is deterministic: the substrate-loaded S-component binds to the ATP-bound ECF module, which triggers ATP hydrolysis, thereby opening of the ATPase subunits with concomitant rearrangement of the coupling helices of ECF-T, essentially pulling the S-component to the inward facing toppled state observed in the crystal structures of the full complexes (**Figure 3**). This inward state has the disrupted substrate binding site, facilitating the release of the transported cargo, and leading to accumulation of the substrate in the cytosol.

In the Thermal Ratchet model (31), the ECF module hydrolyses ATP regardless of the presence of a substrate-loaded S-component. The substrate-loaded S-component can topple over spontaneously. It can then reach the toppled state by clicking into the interaction surface of ECF-T, again leading to disruption of the binding site and release of the substrate. In this mechanism ATP hydrolysis is not required to translocate the substrate, but to reset the ECF-module and regenerate the binding interface for the S-component (**Figure 4**).

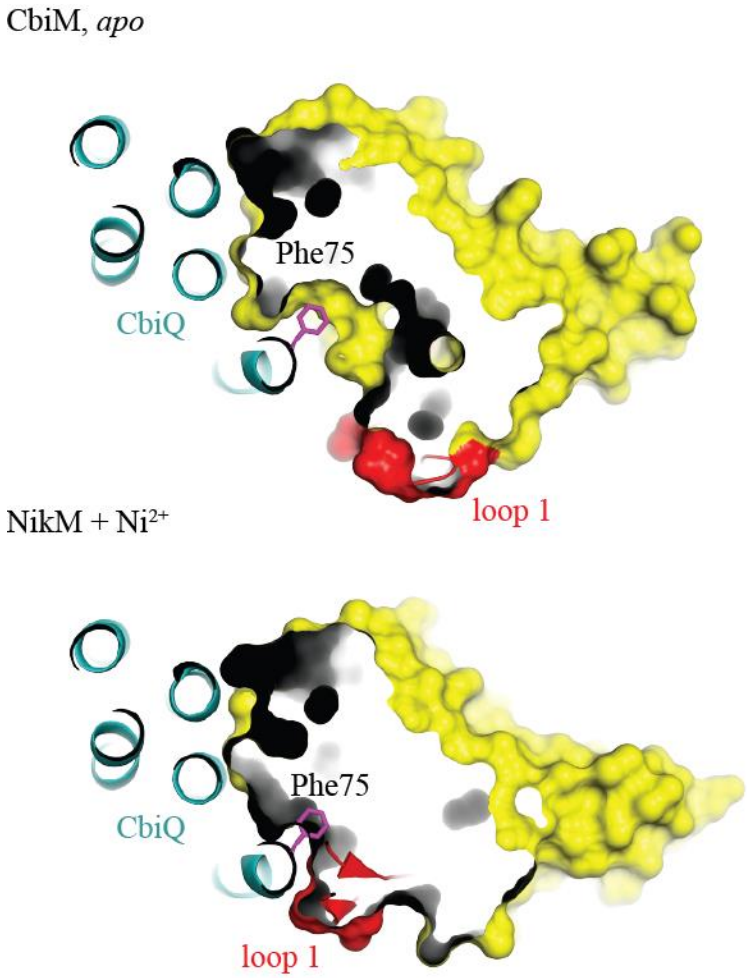

Figure 5: Mechanisms of substrate release by binding site disruption by ECF-T. In the *apo* complex of CbiMQO (top), loop 1 (red) of the S-component CbiM (yellow) has moved away from the binding pocket, effectively disrupting it, and the position has been overtaken by Phe75 located in helix 3 of ECF-T (cyan). Bottom: When the Ni^{2+}-bound S-component NikM is structurally aligned with CbiM, Phe75 would clash with the surface of the S-component and therefore, a substrate-bound state in the full complex is not possible. The S-component either binds the substrate or the ECF module, but not both.

The Thermal Ratchet model postulates that S-components can topple over spontaneously, once substrate is bound. Although substrate binding leads to burying of exposed hydrophilic and charged residues in the S-components, which might make toppling possible, it has been questioned if such toppling can occur. Molecular dynamics simulations seem to argue against it, but it is noteworthy that such simulations were done in non-natural, homogeneous bilayers (50). It is possible that bilayer

imperfections *in vivo* facilitate toppling. In addition, the ECF module itself may cause bilayer wobbles, allowing the substrate loaded S-component to topple over only in the vicinity of the ECF module. Indeed, the full ECF transporter complexes appear to wobble and twist the bilayer (**Figure 6**). In addition, the conformational flexibility of the membrane domain of ECF-T, as observed in the crystal structures (see above), may also aid to reshape the membrane and hence facilitate toppling.

Arguing against the Thermal Ratchet model is data form Karpowich, *et al.* (52), showing that the substrate-bound S-component in detergent solution interacts with a hydrolysis-inactive mutant of the ECF module in the Mg-ATP-bound state with an affinity of K_D ~8 μM. However, it was not shown if the S-component still had substrate bound in the complex, what orientation the S-component adopted, and whether nucleotide was still bound (52). Further testing is required to show if this interaction is relevant in the wild-type protein, and if it occurs in lipid bilayers. Future experiments should preferentially be done in as native conditions as possible, because the use of mutant proteins, detergent micelles, lipid nanodiscs and proteoliposomes of unnatural lipid composition may obscure essential steps.

The Power Stroke model postulates, that specific interaction of the substrate-bound S-component with ECF-T triggers ATP hydrolysis. ECF-T must therefore recognize structural differences between substrate-free and substrate-bound S-components, which are small, and confined largely to differences in the position of the loops L1, located extracellularly (see above) (79). Such discriminative interaction has not yet been observed. For group II transporters this mechanism implies that S-components for different substrates all can induce ATP hydrolysis. However, loop L1 is not conserved between different S-components, neither in length, conformation, nor sequence (13, 25, 53, 54, 56, 57).

Possibly, the Power Stoke and Thermal Ratchet mechanism are not as different as they seem. The observed futile ATPase activity of ECF transporters may lead to continuous remodeling and wobbling of the bilayer, which would facilitate toppling in the Thermal Ratchet model (31). In that case, ATP hydrolysis would facilitate toppling, without necessarily being deterministic. Both models differ from proposed mechanisms for Type I and Type II ABC importers, where the binding of

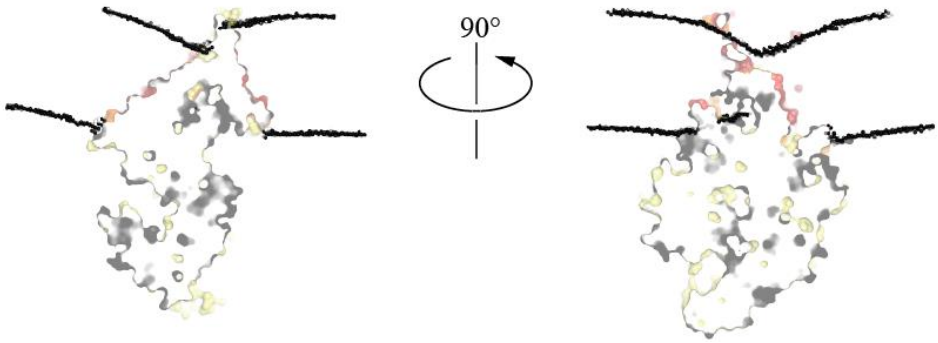

Figure 6: Membrane distortions caused by ECF-type ABC-transporters. The membrane conformation around ECF-PdxU2 was simulated and taken from the MembProtMD database (http://memprotmd.bioch.ox.ac.uk/home/). Shown is a slice through from two angles through ECF-PdxU2 (surface representation, coloring for surface exposure to acyl-chains from yellow to red, not exposed to exposed) and the surrounding membrane boundaries (black dots). The transporter distorts, bends, and thins the membrane.

ATP is associated with substrate release from the soluble binding protein (63).

Much less is known about the transport mechanism used by solitary S-components. So far, transport of biotin and cobalamin by members of the two largest families of solitary S-components, BioY and BtuM, respectively, has been assayed *in vivo*, by complementation studies of specifically engineered, recombinant *Escherichia coli* strains that are auxotrophic for the respective substrates (30, 43, 97). Although such *in vivo* transport assays can be regarded as physiologically relevant, further testing is required to corroborate the transport claims (30).

Mechanistically it is unclear how solitary transporters work. Although it cannot be excluded that solitary S-components interact with a yet to be identified protein, it is unlikely that the BioY and BtuM encounter a specific partner in the heterologous *E. coli* expression host used for the complementation assays (30, 43). Based on the predicament that S-components can topple spontaneously, a facilitated diffusion mechanism with intracellular trapping was suggested for BtuM, where transport of cobalamin through the membrane could be achieved by toppling (30). For BioY the possibility of S-component dimerization as part of the transport mechanism has been proposed, but conclusive data to support this hypothesis is lacking (61). It is noteworthy, that cobalamin and biotin are required only in minute quantities by the cell, and thus a slow transport rate might be acceptable (98, 99).

Whether solitary BioY and BtuM have acquired a transport function that is absent from the S-components in group I and II transporters needs to be established. It appears that most group I and II S-component cannot support transport in similar complementation assays without the expression of an ECF-module (45, 48, 53, 54). For instance, whereas solitary BtuM does support transport of cobalamin, the isolated group II S-component CbrT for the same substrate does not. Only when the ECF module is expressed simultaneously, complementation occurs (45). BioY from the group I transporter BioMNY from *Rhodobacter capsulatus* was initially thought to be able to transport biotin, but later complementation studies with engineered *E. coli* strains showed that only real solitary BioY proteins can transport the substrate (16, 43, 54, 61). The cobalt specific S-component CbiM together with auxiliary protein CbiN and the nickel-specific counterparts NikMN may display solitary transport activity. The additional components CbiN and NikN, were required for this transport to occur (32, 100). It is possible that these components facilitate toppling. Notably, it is unlikely that potential transport by isolated S-components form group I ECF transporters is physiologically relevant, because these transporters form dedicated complexes, from which the S-components may not dissociate (71, 72).

Competition between different S-components for the ECF-module

The structures of the group II ECF-transporters containing identical ECF modules but different S-components have revealed how different S-components can interact with the same ECF module (see above). The shapes of the interaction surfaces of the S-components are well conserved despite lack of sequence similarity (31, 42, 51, 54). Intriguingly, S-components compete more effectively for the same ECF module during transport catalysis in the presence of the transported substrate than in the *apo* state. This observation was made originally by Henderson *et al.* and later confirmed in recombinantly expressed ECF transporters (7, 101). Thus, during turnover ECF-transporters must be able to distinguish between the *apo* and substrate bound states of the different S-components (101). In the Power Stroke model, such distinction is direct, as only the interaction with the substrate bound S-components leads to ATP hydrolysis. In the Thermal Ratchet model the distinction is indirect.

Toppling of the S-component is more efficient in the bound state than in the *apo* state, likely because hydrophilic loops L1 and L3 are exposed in the *apo* state, making toppling energetically highly unfavorable (31). In either case, dissociation of the S-component from the ECF module is required to explain competition, something that was demonstrated directly for Group II ECF transporters (52).

Not all S-components are equally good competitors for the ECF module. In Henderson's work, biotin had only minor effect on transport of folate or thiamin, whereas biotin uptake was greatly affected by the addition of both of the other vitamins. Thus, it appeared that transport of different substrates follows different kinetics although the ECF module is the same (7). In more recent studies, these findings were corroborated in a recombinant system (101). The group II ECF-transporter from *L. lactis* catalyzes import of thiamin and niacin (S-components ThiT and NiaX, respectively). When expressed in *E. coli*, niacin transport was approximately 100-fold faster than thiamine transport (53, 101), indicating that transport kinetics are strongly dependent on the nature of the S-component, even if the ECF module is the same. (7, 101). This difference in transport rate points toward the fact, that the two S-components have different modes of interactions with the same ECF-module although other factors may come into play, such as propensity to topple, ability to diffuse away from the ECF module, ease by which the gates can be pried open by the coupling domain.

There are also examples from type I ABC transporters that can interact with different SBPs. For example, in *Salmonella typhimurium* two SBPs, HisJ and ArgT, share one ABC-importer for the uptake of histidine and arginine, respectively (102). The glutamine and asparagine ABC-transporter GlnPQ, uses two different SBPs that are fused to the transmembrane part in a tandem configuration and, hence, compete for the same translocation channel for their substrates (103). This system was used to elucidate in detail dynamics and kinetics of the interaction between the SBPs and the transmembrane part on the single molecule level, a technique that will be useful to also investigate ECF-transporter assembly in the future (104). In another example, in the *Thermotoga maritima* mannose ABC transporter, variants of the same SBP with different affinities but the same substrate specificity interact with the transporter increasing its dynamic range for substrate recognition. This allows the organism to optimally react to changing environmental concentrations of

the substrate (105). Because the various substrates of ECF transporters are required in different quantities, the apparent difference in competition kinetics could mirror the requirements of different substrates of the cell.

Concluding remarks

The relation between ECF-type ABC transporters and 'conventional' ABC transporters and the mechanism of the latter has been reviewed extensively in the past (17, 27, 39, 40, 63, 106–108). In this section we will place focus on two aspects of ECF transporters.

First, ECF-transporter most likely function by dynamic toppling of S-components. α-helical segments H1-H4 in the S-components can therefore be oriented membrane-spanning (upright) or horizontal (parallel to the membrane plane). Horizontal helices have recently also been found in unrelated membrane proteins. Two prominent examples are the eukaryotic retinol transporter STRA6 and the rotary ATP synthases (109, 110). A single particle cryo-EM structure of STRA6 showed that the dimer forms a large outer cleft that is shielded at the bottom by two layers of horizontal α-helices. It is likely the location of the substrate binding site. In contrast to ECF transporters, the translocation path of the substrate would not require rearrangement of these helices and thus they can be considered static (109). The ATP synthase uses two long horizontal helices in the A-subunit in interaction with the c-ring, for separating entry and exit pathways for the protons. Also this structural feature is static (110, 111). In contrast, the horizontal helices in the S-component are predicted to undergo dynamic transitions between horizontal and transmembrane (39). Reorientation of helices may also occur occasionally in membrane proteins during biogenesis and folding, but in these cases it happens only once, whereas in ECF transporters the transitions are expected to occur during each turnover (112). Dynamic transitions of the orientation of α-helices occur frequently in e.g. transporters albeit to a lesser extent than in ECF transporters, e.g. in the domain movements during elevator-like transport (86, 89, 93). Hence, ECF transporters may be on the extreme end of the scale, but it appears that horizontal helices *and* dynamic transitions in the orientation of membrane spanning α-helices are more general (112, 113).

Second, ECF-transporters may be a suitable systems to study integral membrane protein-protein interactions (114, 115). To study such interactions, membrane protein model systems have been established that vary in complexity. Association in dimerization was studied using glycophorin A, which consists of a single α-helix. A common membrane protein interaction motif was identified, the G/S/A-X-X-X- G/S/A (X mostly hydrophobic in nature) motif and multiples thereof (95, 116–118). A more complex model system is the exceptional stable dimer of the *E. coli* chloride transporter ClC-ec1. Mutations allowed for destabilization of the interface, yielding monomeric protein, which makes this protein suitable to study the interface of a dimeric polytopic membrane protein (119, 120). However, because ClC-ec1 has a single interface, this system does not allow for the study of dynamic reorientation of membrane protein interfaces. These frequently occur in transport proteins, e.g. in the glutamate transporter homolog Glt_{Tk}, the citrate transporter CitS, and the succinate transporter vcINDY, where a transport domain slides along a static scaffold domain (89–92, 121). Glt_{Ph} has been used to study the kinetics of intra-protein movement by a single molecule fluorescence approach, but the molecular determinants that allow these dynamic transitions are not understood (122). ECF-transporters may be a suitable system to address questions on kinetics of dynamic assembly of a complex in lipid environment (S-component association/dissociation), structure function relation ('greasy' van der Waals surface provided by ECF-T (42)), and molecular determinants of dynamic membrane protein interactions. The latter may be of a more general interest since it would show how a natural modular system achieves tight interaction and poly-specificity at the same time.

Acknowledgments

This work was supported by grants from the Netherlands Organisation for Scientific Research (NWO Vici grant 865.11.001 to D.J. Slotboom) and the European Research Council (ERC; ERC Starting Grant 282083 to D.J. Slotboom).

References

1. Henderson GB, Huennekens FM. 1974. Transport of folate compounds into Lactobacillus casei. *Arch. Biochem. Biophys.* 164(2):722–28
2. Henderson GB, Zevely EM, Huennekens FM. 1976. Folate transport in Lactobacillus casei: Solubilization and general properties of the binding protein. *Biochem. Biophys. Res. Commun.* 68(3):712–17
3. Henderson GB, Zevely EM. 1977. Purification and Properties of a Membrane-associated, Protein from Lactobacillus casei. *J. Biol. Chem.* 252:3760–65
4. Henderson GB, Zevely EM, Kadner RJ, Huennekens FM. 1977. The folate and thiamine transport proteins of lactobacillus casei. *J. Supramol. Struct.* 6(2):239–47
5. Henderson GB, Zevely EM. 1978. Binding and transport of thiamine by Lactobacillus casei. *J. Bacteriol.* 133(3):1190–96
6. Henderson GB, Zevely EM, Huennekens FM. 1979. Coupling of energy to folate transport in Lactobacillus casei. *J. Bacteriol.* 139(2):552–59
7. Henderson GB, Zevely EM, Huennekens FM. 1979. Mechanism of folate transport in Lactobacillus casei: Evidence for a component shared with the thiamine and biotin transport systems. *J. Bacteriol.* 137(3):1308–14
8. Henderson GB, Potuznik S. 1982. Cation-Dependent Binding of Substrate to the Folate Transport Protein of Lactobacillus casei Cation-Dependent Binding of Substrate to the Folate Transport Protein of Lactobacillus casei. *J. BACTEIOLOGY.* 150(3):1098–1102
9. Henderson GB, Kojima JM, Kumar HP. 1985. Differential interaction of cations with the thiamine and biotin transport proteins of Lactobacillus casei. *BBA - Biomembr.* 813(2):201–6
10. Henderson GB, Kojima JM, Kumar HP. 1985. Kinetic evidence for two interconvertible forms of the folate transport protein from Lactobacillus casei. *J. Bacteriol.* 163(3):1147–52
11. Ames GF-L, Lever J. 1970. Components of histidine transport: histidine-binding proteins and hisP protein. *Proc. Natl. Acad. Sci. U. S. A.* 66(4):1096–1103
12. Ferro-Luzzi Ames G, Mimura CS, Shyamala V. 1990. Bacterial periplasmic permeases belong to a family of transport proteins operating from Escherichia coli to human: Traffic ATPases. *FEMS*

Microbiol. Lett. 75(4):429–46
13. Rodionov DA, Hebbeln P, Eudes A, Ter Beek J, Rodionova IA, et al. 2009. A novel class of modular transporters for vitamins in prokaryotes. *J. Bacteriol.* 91(1):42–51
14. Entcheva P, Phillips DA, Streit WR. 2002. Functional analysis of Sinorhizobium meliloti genes involved in biotin synthesis and transport. *Appl. Environ. Microbiol.* 68(6):2843–48
15. Rodionov D, Hebbeln P. 2006. Comparative and functional genomic analysis of prokaryotic nickel and cobalt uptake transporters: evidence for a novel group of ATP-binding cassette transporters. *J. Bacteriol.* 188(1):317–27
16. Hebbeln P, Rodionov DA, Alfandega A, Eitinger T. 2007. Biotin uptake in prokaryotes by solute transporters with an optional ATP-binding cassette-containing module. *Proc. Natl. Acad. Sci.* 104(8):2909–14
17. Davidson AL, Dassa E, Orelle C, Chen J. 2008. Structure, Function, and Evolution of Bacterial ATP-Binding Cassette Systems. *Microbiol. Mol. Biol. Rev.* 72(2):317–64
18. Gelfand MS, Mironov AA, Jomantas J, Kozlov YI, Perumov DA. 1999. A conserved RNA structure element involved in the regulation of bacterial riboflavin synthesis genes
19. Kreneva RA, Gel'fand MS, Mironov AA, Yomantas YA, Kozlov YI, et al. 2000. Inactivation of the ypaA gene in Bacillus subtilis; analysis of the resulting phenotypic expression. *Russ. J. Genet. C/C Genet.* 36(8):972–74
20. Rodionov DA, Vitreschak AG, Mironov AA, Gelfand MS. 2002. Comparative genomics of thiamin biosynthesis in procaryotes. New genes and regulatory mechanisms. *J. Biol. Chem.* 277(50):48949–59
21. Rodionov DA, Vitreschak AG, Mironov AA, Gelfand MS. 2003. Comparative Genomics of the Vitamin B12 Metabolism and Regulation in Prokaryotes. *J. Biol. Chem.* 278(42):41148–59
22. Burgess CM, Slotboom DJ, Eric R, Duurkens RH, Poolman B, et al. 2006. The riboflavin transporter RibU in Lactococcus lactis : molecular characterization of gene expression and the transport mechanism. *J. Bacteriol.* 188(8):2752–60
23. Duurkens RH, Tol MB, Geertsma ER, Permentier HP, Slotboom DJ. 2007. Flavin binding to the high affinity riboflavin transporter RibU. *J. Biol. Chem.* 282(14):10380–86
24. Vogl C, Grill S, Schilling O, Stülke J, Mack M, Stolz J. 2007.

Characterization of riboflavin (vitamin B2) transport proteins from Bacillus subtilis and Corynebacterium glutamicum. *J. Bacteriol.* 189(20):7367–75

25. Zhang P, Wang J, Shi Y. 2010. Structure and mechanism of the S component of a bacterial ECF transporter. *Nature*. 468(7324):717–20
26. Eudes A, Erkens GB, Slotboom DJ, Rodionov DA, Naponelli V, Hanson AD. 2008. Identification of genes encoding the folate- and thiamine-binding membrane proteins in firmicutes. *J. Bacteriol.* 190(22):7591–94
27. Eitinger T, Rodionov DA, Grote M, Schneider E. 2011. Canonical and ECF-type ATP-binding cassette importers in prokaryotes: Diversity in modular organization and cellular functions
28. Maruyama Y, Itoh T, Kaneko A, Nishitani Y, Mikami B, et al. 2015. Structure of a Bacterial ABC Transporter Involved in the Import of an Acidic Polysaccharide Alginate. *Structure*. 23(9):1643–54
29. Hvorup RN, Goetz BA, Niederer M, Hollenstein K, Perozo E, Locher KP. 2007. Asymmetry in the Structure of the ABC Transporter-Binding Protein Complex BtuCD-BtuF. *Science* 317(5843):1387–90
30. Rempel, S., Colucci, E., de Gier, J.W., Guskov, A., Slotboom DJ. 2018. Cysteine-mediated decyanation of vitamin B12 by the predicted membrane transporter BtuM. *Nat. Commun.*, pp. 1–8
31. Swier LJYM, Guskov A, Slotboom DJ. 2016. Structural insight in the toppling mechanism of an energy-coupling factor transporter. *Nat. Commun.* 7:11072
32. Bao Z, Qi X, Hong S, Xu K, He F, et al. 2017. Structure and mechanism of a group-I cobalt energy coupling factor transporter. *Cell Res.* 27(5):675–87
33. Hohl M, Briand C, Grütter MG, Seeger MA. 2012. Crystal structure of a heterodimeric ABC transporter in its inward-facing conformation. *Nat. Struct. Mol. Biol.* 19(4):395–402
34. Dawson RJP, Locher KP. 2006. Structure of a bacterial multidrug ABC transporter. *Nature*. 443(7108):180–85
35. Lee J-Y, Kinch LN, Borek DM, Wang J, Wang J, et al. 2016. Crystal structure of the human sterol transporter ABCG5/ABCG8. *Nature*, pp. 1–17
36. Luo Q, Yang X, Yu S, Shi H, Wang K, et al. 2017. Structural basis for lipopolysaccharide extraction by ABC transporter LptB2FG. *Nat. Struct. Mol. Biol.* 24(5):469–74

37. Crow A, Greene NP, Kaplan E, Koronakis V. 2017. Structure and mechanotransmission mechanism of the MacB ABC transporter superfamily. *Proc. Natl. Acad. Sci.*, p. 201712153
38. Greene NP, Kaplan E, Crow A, Koronakis V. 2018. Antibiotic resistance mediated by the MacB ABC transporter family: A structural and functional perspective
39. Slotboom DJ. 2014. Structural and mechanistic insights into prokaryotic energy-coupling factor transporters. *Nat. Rev. Microbiol.* 12(2):79–87
40. Rees DC, Johnson E, Lewinson O. 2009. ABC transporters: The power to change
41. Higgins CF. 1992. ABC Transporters: From Microorganisms to Man. *Annu. Rev. Cell Biol.* 8(1):67–113
42. Wang T, Fu G, Pan X, Wu J, Gong X, et al. 2013. Structure of a bacterial energy-coupling factor transporter. *Nature*. 497(7448):272–76
43. Finkenwirth F, Kirsch F, Eitinger T. 2013. Solitary bio Y proteins mediate biotin transport into recombinant Escherichia coli. *J. Bacteriol.* 195(18):4105–11
44. Overbeek R, Begley T, Butler RM, Choudhuri J V, Chuang HY, et al. 2005. The subsystems approach to genome annotation and its use in the project to annotate 1000 genomes. *Nucleic Acids Res.* 33(17):5691–5702
45. Santos JA, Rempel S, Mous ST, Pereira CT, ter Beek J, et al. 2018. Functional and structural characterization of an ECF-type ABC transporter for vitamin B12. *Elife*. 7:e35828
46. Ter Beek J, Duurkens RH, Erkens GB, Slotboom DJ. 2011. Quaternary structure and functional unit of Energy Coupling Factor (ECF)-type transporters. *J. Biol. Chem.* 286(7):5471–75
47. Neubauer O, Alfandega A, Schoknecht J, Sternberg U, Pohlmann A, Eitinger T. 2009. Two essential arginine residues in the T components of energy-coupling factor transporters. *J. Bacteriol.* 191(21):6482–88
48. Zhang M, Bao Z, Zhao Q, Guo H, Xu K, et al. 2014. Structure of a pantothenate transporter and implications for ECF module sharing and energy coupling of group II ECF transporters. *Proc. Natl. Acad. Sci. U. S. A.* 111(52):18560–65
49. Erkens GB, Slotboom DJ. 2010. Biochemical characterization of ThiT from lactococcus lactis: A thiamin transporter with picomolar substrate binding affinity. *Biochemistry*. 49(14):3203–12

50. Josts I, Almeida Hernandez Y, Andreeva A, Tidow H. 2016. Crystal Structure of a Group I Energy Coupling Factor Vitamin Transporter S Component in Complex with Its Cognate Substrate. *Cell Chem. Biol.* 23(7):827–36
51. Xu K, Zhang M, Zhao Q, Yu F, Guo H, et al. 2013. Crystal structure of a folate energy-coupling factor transporter from Lactobacillus brevis. *Nature*. 497(7448):268–71
52. Karpowich NK, Song JM, Cocco N, Wang DN. 2015. ATP binding drives substrate capture in an ECF transporter by a release-and-catch mechanism. *Nat. Struct. Mol. Biol.* 22(7):565–71
53. Erkens GB, Berntsson RPA, Fulyani F, Majsnerowska M, Vujičić-Žagar A, et al. 2011. The structural basis of modularity in ECF-type ABC transporters. *Nat. Struct. Mol. Biol.* 18(7):755–60
54. Berntsson RP-A, ter Beek J, Majsnerowska M, Duurkens RH, Puri P, et al. 2012. Structural divergence of paralogous S components from ECF-type ABC transporters. *Proc. Natl. Acad. Sci.* 109(35):13990–95
55. Yu Y, Zhou M, Kirsch F, Xu C, Zhang L, et al. 2014. Planar substrate-binding site dictates the specificity of ECF-type nickel/cobalt transporters. *Cell Res.* 24(3):267–77
56. Zhao Q, Wang C, Wang C, Guo H, Bao Z, et al. 2015. Structures of FolT in substrate-bound and substrate-released conformations reveal a gating mechanism for ECF transporters. *Nat. Commun.* 6:
57. Karpowich NK, Song J, Wang DN. 2016. An Aromatic Cap Seals the Substrate Binding Site in an ECF-Type S Subunit for Riboflavin. *J. Mol. Biol.* 428(15):3118–30
58. Karpowich NK, Wang D-N. 2013. Assembly and mechanism of a group II ECF transporter. *Proc. Natl. Acad. Sci. U. S. A.* 110(7):2534–39
59. Neubauer O, Reiffler C, Behrendt L, Eitinger T. 2011. Interactions among the A and T units of an ECF-type biotin transporter analyzed by site-specific crosslinking. *PLoS One*. 6(12):
60. Finkenwirth F, Neubauer O, Gunzenhäuser J, Schoknecht J, Scolari S, et al. 2010. Subunit composition of an energy-coupling-factor-type biotin transporter analysed in living bacteria. *Biochem. J.* 431(3):373–80
61. Kirsch F, Frielingsdorf S, Pohlmann A, Eitinger T, Ziomkowska J, Herrmann A. 2012. Essential amino acid residues of BioY reveal that dimers are the functional S unit of the Rhodobacter capsulatus biotin transporter. *J. Bacteriol.* 194(17):4505–12

62. Erkens GB, Majsnerowska M, Ter Beek J, Slotboom DJ. 2012. Energy coupling factor-type ABC transporters for vitamin uptake in prokaryotes. *Biochemistry*. 51(22):4390–96
63. ter Beek J, Guskov A, Slotboom DJ. 2014. Structural diversity of ABC transporters. *J. Gen. Physiol.* 143(4):419–35
64. Procko E, O'Mara ML, Bennett WFD, Tieleman DP, Gaudet R. 2009. The mechanism of ABC transporters: general lessons from structural and functional studies of an antigenic peptide transporter. *FASEB J.* 23(5):1287–1302
65. Lubelski J, Van Merkerk R, Konings WN, Driessen AJM. 2006. Nucleotide-binding sites of the heterodimeric LmrCD ABC-multidrag transporter of Lactococcus lactis are asymmetric. *Biochemistry*. 45(2):648–56
66. Tsai M-F, Li M, Hwang T-C. 2010. Stable ATP binding mediated by a partial NBD dimer of the CFTR chloride channel. *J. Gen. Physiol.* 135(5):399–414
67. Csanády L. 2010. Degenerate ABC composite site is stably glued together by trapped ATP. *J. Gen. Physiol*. 135(5):395–98
68. Basso C, Vergani P, Nairn AC, Gadsby DC. 2003. Prolonged Nonhydrolytic Interaction of Nucleotide with CFTR's NH 2 - terminal Nucleotide Binding Domain and its Role in Channel Gating. *J. Gen. Physiol.* 122(3):333–48
69. Perria CL, Rajamanickam V, Lapinski PE, Raghavan M. 2006. Catalytic site modifications of TAP1 and TAP2 and their functional consequences. *J. Biol. Chem.* 281(52):39839–51
70. Oldham ML, Chen J. 2011. Snapshots of the maltose transporter during ATP hydrolysis. *Proc. Natl. Acad. Sci.* 108(37):15152–56
71. Finkenwirth F, Sippach M, Landmesser H, Kirsch F, Ogienko A, et al. 2015. ATP-dependent conformational changes trigger substrate capture and release by an ECF-type biotin transporter. *J. Biol. Chem.* 290(27):16929–42
72. Finkenwirth F, Kirsch F, Eitinger T. 2017. Complex Stability during the Transport Cycle of a Subclass i ECF Transporter. *Biochemistry*. 56(34):4578–83
73. Oldham ML, Chen J. 2011. Crystal structure of the maltose transporter in a pretranslocation intermediate state. *Science* 332(6034):1202–5
74. Chen S, Oldham ML, Davidson AL, Chen J. 2013. Carbon catabolite repression of the maltose transporter revealed by X-ray crystallography. *Nature*. 499(7458):364–68

75. Böhm A, Diez J, Diederichs K, Welte W, Boos W. 2002. Structural model of MalK, the ABC subunit of the maltose transporter of Escherichia coli: Implications for mal gene regulation, inducer exclusion, and subunit assembly. *J. Biol. Chem.* 277(5):3708–17
76. Yu J, Ge J, Heuveling J, Schneider E, Yang M. 2015. Structural basis for substrate specificity of an amino acid ABC transporter. *Proc. Natl. Acad. Sci. U. S. A.* 112(16):5243–48
77. Lewinson O, Lee AT, Locher KP, Rees DC. 2010. A distinct mechanism for the ABC transporter BtuCD-F revealed by the dynamics of complex formation. *Nat. Struct. Mol. Biol.* 17(3):332–38
78. Dawson RJP, Hollenstein K, Locher KP. 2007. Uptake or extrusion: Crystal structures of full ABC transporters suggest a common mechanism
79. Majsnerowska M, Hänelt I, Wunnicke D, Schäfer L V., Steinhoff HJ, Slotboom DJ. 2013. Substrate-induced conformational changes in the S-component ThiT from an energy coupling factor transporter. *Structure*. 21(5):861–67
80. Swier LJYM, Monjas L, Guskov A, De Voogd AR, Erkens GB, et al. 2015. Structure-based design of potent small-molecule binders to the S-component of the ECF transporter for thiamine. *ChemBioChem*. 16(5):819–26
81. Monjas L, Swier LJYM, Setyawati I, Slotboom DJ, Hirsch AKH. 2017. Dynamic Combinatorial Chemistry to Identify Binders of ThiT, an S-Component of the Energy-Coupling Factor Transporter for Thiamine. *ChemMedChem*. 12(20):1693–96
82. Lohse J, Swier LJYM, Oudshoorn RC, Médard G, Kuster B, et al. 2017. Targeted Diazotransfer Reagents Enable Selective Modification of Proteins with Azides. *Bioconjug. Chem.* 28(4):913–17
83. Zhao H, Piszczek G, Schuck P. 2015. SEDPHAT - A platform for global ITC analysis and global multi-method analysis of molecular interactions. *Methods*. 76:137–48
84. Jardetzky O. 1966. Simple allosteric model for membrane pumps [27]
85. Drew D, Boudker O. 2016. Shared Molecular Mechanisms of Membrane Transporters. *Annu. Rev. Biochem.* 85(1):543–72
86. Reyes N, Ginter C, Boudker O. 2009. Transport mechanism of a bacterial homologue of glutamate transporters. *Nature*. 462(7275):880–85

87. Wang H, Oster G. 2002. Ratchets, power strokes, and molecular motors. *Appl. Phys. A Mater. Sci. Process.* 75(2):315–23
88. Wagoner JA, Dill KA. 2016. Molecular Motors: Power Strokes Outperform Brownian Ratchets. *J. Phys. Chem. B.* 120(26):6327–36
89. Jensen S, Guskov A, Rempel S, Hänelt I, Slotboom DJ. 2013. Crystal structure of a substrate-free aspartate transporter. *Nat. Struct. Mol. Biol.* 20(10):1224–27
90. Wöhlert D, Grötzinger MJ, Kühlbrandt W, Yildiz Ö. 2015. Mechanism of Na+-dependent citrate transport from the structure of an asymmetrical CitS dimer. *Elife*. 4(December2015):e09375
91. Lolkema JS, Slotboom DJ. 2017. Structure and elevator mechanism of the Na+-citrate transporter CitS
92. Mulligan C, Fenollar-Ferrer C, Fitzgerald GA, Vergara-Jaque A, Kaufmann D, et al. 2016. The bacterial dicarboxylate transporter VcINDY uses a two-domain elevator-type mechanism. *Nat. Struct. Mol. Biol.* 23(3):256–63
93. Garaeva AA, Oostergetel GT, Gati C, Guskov A, Paulino C, Slotboom DJ. Cryo-EM structure of the human neutral amino acid transporter ASCT2. *Nat. Struct. Mol. Biol.*
94. Lee C, Kang HJ, von Ballmoos C, Newstead S, Uzdavinys P, et al. 2013. A two-domain elevator mechanism for sodium/proton antiport. *Nature*. 501(7468):573–77
95. Kleiger G, Grothe R, Mallick P, Eisenberg D. 2002. GXXXG and AXXXA: Common α-helical interaction motifs in proteins, particularly in extremophiles. *Biochemistry*. 41(19):5990–97
96. Chen J. 2013. Molecular mechanism of the Escherichia coli maltose transporter. *Curr. Opin. Struct. Biol.* 23(4):492–98
97. Fisher DJ, Fernández RE, Adams NE, Maurelli AT. 2012. Uptake of Biotin by Chlamydia Spp. through the Use of a Bacterial Transporter (BioY) and a Host-Cell Transporter (SMVT). *PLoS One*. 7(9):
98. Di Girolamo PM, Kadner RJ, Bradbeer C. 1971. Isolation of vitamin B 12 transport mutants of Escherichia coli. *J. Bacteriol.* 106(3):751–57
99. Choi-Rhee E, Cronan JE. 2005. Biotin synthase is catalytic in vivo, but catalysis engenders destruction of the protein. *Chem. Biol.* 12(4):461–68
100. Kirsch F, Eitinger T. 2014. Transport of nickel and cobalt ions into bacterial cells by S components of ECF transporters. *BioMetals*. 27(4):653–60

101. Majsnerowska M, Ter Beek J, Stanek WK, Duurkens RH, Slotboom DJ. 2015. Competition between Different S-Components for the Shared Energy Coupling Factor Module in Energy Coupling Factor Transporters. *Biochemistry*. 54(31):4763–66
102. Higgins CF, Ames GF. 1981. Two periplasmic transport proteins which interact with a common membrane receptor show extensive homology: complete nucleotide sequences. *Proc. Natl. Acad. Sci. U. S. A.* 78(10):6038–42
103. Fulyani F, Schuurman-Wolters GK, Žagar AV, Guskov A, Slotboom DJ, Poolman B. 2013. Functional diversity of tandem substrate-binding domains in ABC transporters from pathogenic bacteria. *Structure*. 21(10):1879–88
104. Gouridis G, Schuurman-Wolters GK, Ploetz E, Husada F, Vietrov R, et al. 2015. Conformational dynamics in substrate-binding domains influences transport in the ABC importer GlnPQ. *Nat. Struct. Mol. Biol.* 22(1):57–64
105. Ghimire-Rijal S, Lu X, Myles DA, Cuneo MJ. 2014. Duplication of genes in an ATP-binding cassette transport system increases dynamic range while maintaining ligand specificity. *J. Biol. Chem.* 289(43):30090–100
106. Parcej D, Tampé R. 2010. ABC proteins in antigen translocation and viral inhibition
107. George AM, Jones PM. 2012. Perspectives on the structure-function of ABC transporters: The Switch and Constant Contact Models
108. Lewis VG, Ween MP, McDevitt CA. 2012. The role of ATP-binding cassette transporters in bacterial pathogenicity
109. Chen Y, Clarke OB, Kim J, Stowe S, Kim YK, et al. 2016. Structure of the STRA6 receptor for retinol uptake. *Science* 353(6302):
110. Allegretti M, Klusch N, Mills DJ, Vonck J, Kühlbrandt W, Davies KM. 2015. Horizontal membrane-intrinsic α-helices in the stator a-subunit of an F-type ATP synthase. *Nature*. 521(7551):237–40
111. Hahn A, Vonck J, Mills DJ, Meier T, Kuhlbrandt W. 2018. Structure, mechanism, and regulation of the chloroplast ATP synthase. *Science* 360(6389):eaat4318
112. Bowie JU. 2013. Membrane protein twists and turns
113. Von Heijne G. 2006. Membrane-protein topology
114. Nooren IMA, Thornton JM. 2003. Diversity of protein-protein interactions
115. Perkins JR, Diboun I, Dessailly BH, Lees JG, Orengo C. 2010. Transient Protein-Protein Interactions: Structural, Functional, and

Network Properties
116. Lemmon MA, Flanagan JM, Hunt JF, Adair BD, Bormann BJ, et al. 1992. Glycophorin A dimerization is driven by specific interactions between transmembrane α-helices. *J. Biol. Chem.* 267(11):7683–89
117. Brosig B, Langosch D. 2008. The dimerization motif of the glycophorin A transmembrane segment in membranes: Importance of glycine residues. *Protein Sci.* 7(4):1052–56
118. Senes A, Engel DE, Degrado WF. 2004. Folding of helical membrane proteins: The role of polar, GxxxG-like and proline motifs
119. Robertson JL, Kolmakova-Partensky L, Miller C. 2010. Design, function and structure of a monomeric ClC transporter. *Nature*. 468(7325):844–47
120. Last NB, Miller C. 2015. Functional Monomerization of a ClC-Type Fluoride Transporter. *J. Mol. Biol.* 427(22):3607–12
121. Kebbel F, Kurz M, Arheit M, Grütter MG, Stahlberg H. 2013. Structure and substrate-induced conformational changes of the secondary citrate/sodium symporter CitS revealed by electron crystallography. *Structure*. 21(7):1243–50
122. Erkens GB, Hänelt I, Goudsmits JMH, Slotboom DJ, van Oijen AM. 2013. Unsynchronised subunit motion in single trimeric sodium-coupled aspartate transporters. *Nature*. 502:119–23

Supplementary Information

Supplementary tables

Suppl. Table 1: Available crystal structures for the ECF-type ABC transporter family.

Name	Host organism	Ligands	Resolution in Å	Accession number
Group I S-components				
NikM	*Thermoanaerobacter tengcongensis*	Ni^{2+}, Co^{2+}	3.2, 1.83, 2.5	4M58, 4M5B, 4M5C
YkoE	*Bacillus subtilis*	Thiamin	1.5	5EDL[a]
Group II S-components				
BioY	*Lactococcus lactis*	Biotin	2.1	4DVE
FolT	*Lactobacillus delbrueckii*	Folate	3.01	5D0Y
FolT	*Enterococcus faecalis*	Folate	3.19	4Z7F
RibU	*Staphylococcus aureus*	Riboflavin	3.6	3P5N
RibU (modified)	*Thermotoga maritima*	Riboflavin	2.61, 3.2, 3.4	5KBW[a], 5KC0, 5KC4
ThiT	*Lactococcus lactis*	Thiamin	2.0	3RLB
ThiT	*Lactococcus lactis*	BAT-25, Pyrithiamin, AV-38, LMG139, LMG135	2.5, 2.1, 2.4, 2.2, 2.2	4MHW, 4MUU, 4N4D, 4POP, 4POV
Solitary S-component				
BtuM	*Thiobacillus denitrificans*	Cobalamin	2.01	6FFV
Group I ATPases				
CbiO	*Rhodobacter capsulatus*		2.3	4MKI
CbiO_E166Q	*Rhodobacter capsulatus*	AMP-PCP, Mg^{2+}	1.45	5X40
Group II ATPases				
ECF-AA'	*Thermotoga maritima*	ADP	2.7	4HLU
ECF-AA'	*Thermotoga maritima*	AMP-PNP, Mg^{2+}	3.0	4ZIR
Group I ECF-transporter				
CbiMQO	*Rhodobacter capsulatus*		2.79, 3.47	5X3X, 5X41[a]
Group II ECF-transporter				
ECF-CbrT	*Lactobacillus delbrueckii*		3.4	6FNP
ECF-FolT	*Lactobacillus brevis*		3.0	4HUQ
ECF-FolT2	*Lactobacillus delbrueckii*		3.0	5JSZ
ECF-FolT2	*Lactobacillus delbrueckii*	AMP-PNP	3.3	5D3M
ECF-PanT	*Lactobacillus brevis*		3.25	4RFS
ECF-PdxU2	*Lactobacillus brevis*		3.5	4HZU

[a] Lipidic cubic phase (LCP) crystallization.

Suppl. Table 2: List of determined parameters of ATPase activity in ECF-type ABC transporters.

Transporter & organism	ECF-group	Substrates	Experimental methods	Sample types	Kinetic parameters[a]	References
BioMNY (*Rhodobacter capsulatus*)	I	Varying ATP concentrations	Free phosphate colorimetric determination	Purified	v_{max} = 390 nmol P_i/min/mg	(60)
ECF-RibU (*Streptococcus thermophilus*)	II	5 mM ATP	Free phosphate colorimetric determination	Purified	v_{max} = 47.9 mol/min/mol (v_{max} = 0.8 ATP/sec/ECF-RibU)	(58)
BioMNY (*Rhodobacter capsulatus*)	I	2 mM ATP	Free phosphate colorimetric determination	Nanodiscs	v_{max} = 0.73 ± 0.01 µmol P_i/min/mg K_m = 0.14 ± 0.02 mM k_{cat} = 1.27 s^{-1}	(71)
BioMNY (*Rhodobacter capsulatus*)	I	2 mM ATP	Free phosphate colorimetric determination	Purified	v_{max} = 0.53 ± 0.04 µmol P_i/min/mg	(71)
CbiMNQO (*Rhodobacter capsulatus*)	I	Varying ATP concentrations	Free phosphate colorimetric determination	Purified	k_{cat} = 29.7 min^{-1} K_m = 153.8 µM	(32)
CbiMQO (*Rhodobacter capsulatus*)	I	Varying ATP concentrations	Free phosphate colorimetric determination	Purified	k_{cat} = 33.9 min^{-1} K_m = 150.7 µM	(32)
CbiQO (*Rhodobacter capsulatus*)	I	Varying ATP concentrations	Free phosphate colorimetric determination	Purified	k_{cat} = 2.5 min^{-1} K_m = 277.3 µM	(32)
ECF-RibU (*Lysteria monocytogenes*)	II	Varying ATP concentrations	Free phosphate colorimetric determination	Proteoliposomes	v_{max} = 488 ± 67 nmol/min/mg (v_{max} = 56.12 nmol/min/nmol)	(52)
ECF-RibU (*Lysteria monocytogenes*)	II	Varying ATP concentrations	Free phosphate colorimetric determination	Purified	v_{max} = 1150 ± 28 nmol/min/mg K_m = 165 ± 16 µM	(52)
ECF-RibU (*Listeria monocytogenes*)	II	Varying ATP concentrations	SEC, preincubated with ATP concentrations	Purified (H-loop mutations)	K_D = 101 ± 19 µM	(52)
ECF-FolT2 (*Lactobacillus delbrueckii*)	II	Varying ATP concentrations, 100 nM folate	Radiolabeled substrate uptake assay	Proteoliposomes	K_m = 5.54 mM n_H = 1.75	Unpublisded (Stanek, W., *et al.*)

ECF-PanT (*Lactobacillus delbrueckii*)	II	Varying ATP concentrations, 100 nM pantothenate	Radiolabeled substrate uptake assay	Proteoliposomes	K_m = 5.61 mM n_H = 1.74	Unpublisded (Stanek, W., *et al.*)
ECF-PanT (*Lactobacillus delbrueckii*)	II	Varying ATP concentrations, 500 nM pantothenate	Coupled enzyme assay	Proteoliposomes	K_m = 16.38 mM v_{max} = 200.23 pmol/min/pmol, n_H = 1.83	Unpublisded (Stanek, W., *et al.*)

[a]Kinetics given in commonly used units with the parameters as stated in the original publications in parentheses, where applicable.

Suppl. Table 3: Representative transport kinetics of ECF-type ABC transporters.

Transporter & organism	Substrates	Sample types	Kinetic parameters of transport	References
ECF-FolT (*Lactobacillus casei*)	[G-^{3}H]Folate	Whole cells	K_m = 0.35 µM v_{max} = 0.44 nmol/min/10^{10} cells	(1)
	[$^{14}CH_3$]Amethopterin		K_m = 0.21 µM, v_{max} = 0.44 nmol/min/10^{10} cells	
	[3',5'-^{3}H]5-methyl tetrahydrofolate		K_m = 0.90 µM v_{max} = 0.56 nmol/min/10^{10} cells	
ECF-FolT (*Lactobacillus casei*)	[3',5',9(n)-^{3}H]folate	Whole cells, energized	v_{max} = 0.35 nmol/min/10^{10} cells	(6)
ECF-ThiT (*Lactobacillus casei*)	[thiazole-2-^{4}C]thiamine	Whole cells, energized	K_m < 10 nM v_{max} = 0.6 nmol/min/10^{10} cells	(5)
BioY (*Rhodobacter capsulatus*)	D-[8,9-^{3}H]biotin	Whole cells, energized	K_m = 250 nM v_{max} = 60 pmol/mg/min	(16)
BioMNY (*Rhodobacter capsulatus*)	D-[8,9-^{3}H]biotin	Whole cells, energized	K_m = 5 nM v_{max} = 6 pmol/mg/min	(16)
BioY (*Chlamydia trachomatis*)	D-[8,9-^{3}H(N)] biotin	Whole cells	K_m = 3.35 nM v_{max} = 55.1 pmol/mg/min	(97)
ECF-FolT2 (*Lactobacillus delbrueckii*)	[3,5,7,9-^{3}H]folate	Proteoliposomes	K_m = 58.8 nM v_{max} = 0.771 pmol/min/µg, k_{cat} = 0.00148 s^{-1}	Unpublisded data (Stanek, W., *et al.*)
ECF-PanT (*Lactobacillus delbrueckii*)	D-[2,3-^{3}H]pantothenate concentrations	Proteoliposomes	K_m = 46.1 nM v_{max} = 2.2 pmol/min/µg, k_{cat} = 0.00429 s^{-1}	Unpublisded data (Stanek, W., *et al.*)
ECF-CbrT (*Lactobacillus delbrueckii*)	[^{57}Co]cyano-cobalamin	Proteoliposomes	K_m = 2.1 ± 0.4 nM v_{max} = 0.06 ± 0.01 nmol/mg/s	(45)

Suppl. Table 4: List of determined substrate binding affinities for S-components of ECF-transporters.

Transporter & organism	Substrates	Experimental methods	Sample types	Affinity values	Reference
FolT (*Lactobacillus casei*)	[^{3}H]folate	Radiolabeled substrate binding	Whole cells at 4°C	K_D = 36 nM 0.35 nmol/10^{10} cells	(2)
ThiT (*Lactobacillus casei*)	[thiazole-2-^{14}C]thiamin	Radiolabeled substrate binding	Whole cells, glucose and iodoacetate	K_D < 10 nM	(5)
ECF-FolT (*Lactobacillus casei*)	[3',5',9(n)-^{3}H]folate	Radiolabeled substrate binding	Whole cells, not energized	0.45 nmol/10^{10} cells	(7)
ECF-ThiT (*Lactobacillus casei*)	[thiazole-2-^{14}C]thiamin	Radiolabeled substrate binding	Whole cells, not energized	0.70 nmol/10^{10} cells	(7)
ECF-FolT (*Lactobacillus casei*)	[3',5',7,9-^{3}H]folate	Radiolabeled substrate binding, various conditions	Whole cells and membrane vesicles	K_D = 0.1 – 0.42 nM	(10)
ECF-ThiT (*Lactobacillus casei*)	[^{35}S]thiamin	Radiolabeled substrate binding to cells	Whole cells, deenergized	K_D = 0.03 nM	(9)
ECF-BioY (*Lactobacillus casei*)	[^{3}H]biotin	Radiolabeled substrate binding to cells	Whole cells, deenergized	K_D = 0.15 nM	(9)
RibU (*Lactococcus lactis*)	Riboflavin	ITC	Purified	K_D = 1.8 ± 0.7 nM	(23)
	Riboflavin	ITC	Membrane vesicles	K_D = 5.0 ± 1.0 nM	
	Riboflavin	Trp-fluorescence quenching	Purified	K_D = 0.6 ± 0.2 nM	
	Roseoflavin			K_D = 2.5 ± 1.2 nM	
	FMN			K_D = 36 ± 6 nM	
	FAD			K_D = no binding	
	Riboflavin	Flow dialysis		K_D = 1.7 ± 3.2 nM	
FolT (*Lactobacillus casei*)	Folate	Trp-fluorescence quenching	Purified	K_D = 9 nM	(26)
ThiT (*Lactobacillus casei*)	Thiamin	Trp-fluorescence quenching	Purified	K_D = 0.5 nM	(26)
ThiT (*Lactococcus lactis*)	Thiamin	Trp-fluorescence quenching	Purified	K_D = 0.122 ± 0.13 nM	(49)
	Thiamin-monophosphate			K_D = 1.01 ± 0.14 nM	
	Thiamin-pyrophosphate			K_D = 1.60 ± 0.00nM	
	Pyrithiamin			K_D = 0.18 ± 0.7 nM	
BioY (*Lactococcus lactis*)	D-biotin	Trp-fluorescence quenching	Purified	K_D = 0.3 nM	(54)

BioY (*Rhodobacter capsulatus*)	D-biotin	Trp-fluorescence quenching	Purified	Too high to determine	(54)
ThiT (*Lactococcus lactis*)	Thiamin	Trp-fluorescence quenching	Purified	k_{on} 3.4×10^8 M^{-1} s^{-1} $k_{off,\ calculated}$ 0.004 s^{-1} (K_D = 11 pM)	(79)
FolT (*Enterococcus faecalis*)	Folate	ITC	Purified	K_D = 29.8 ± 4.7 nM	(56)
FolT (*Lactobacillus delbrueckii*)	Folate	Trp-fluorescence quenching	Purified	K_D = 1.0 ± 0.24 nM	(31)
FolT2 (*Lactobacillus delbrueckii*)	Folate	Trp-fluorescence quenching	Purified	K_D = 20 ± 2.19 nM	(31)
FolT2 (*Lactobacillus delbrueckii*)	Folate	ITC	Membrane vesicles	K_D = 14.4 ± 9.3 nM	Unpublisded data (Stanek, W., *et al.*)
YkoE (*Bacillus subtilis*	Thiamin	Trp-fluorescence quenching	Purified	K_D = 4.5 nM	(50)
RibU (*Listeria monocytogenes*)	Riboflavin	FSEC	Purified, released from whole complex	K_D = 526 ± 74 nM	(57)
CbrT (*Lactobacillus delbrueckii*)	Cyano-cobalamin Hydroxycobalamin Methylcobalamin	ITC	Membrane vesicles	K_D = 9.2 ± 4.5 nM K_D = 9.6 ± 6.9 nM K_D = 4.5 ± 0.3 nM	(45)
CbrT (*Lactobacillus delbrueckii*)	Cobinamide	ITC	Membrane vesicles	K_D = 36 ±15 nM	(45)
BtuM (*Thiobacillus denitrificans*)	Cobinamide	ITC	Purified (His- or EPEA-affinity tag)	K_D = 0.65 ± 0.27 μM K_D = 0.58 ± 0.13 μM	(30)
PanT (*Lactobacillus delbrueckii*)	Pantothenate	ITC	Membrane vesicles	K_D =21.4 ± 22.9 nM	Unpublisded data (Stanek, W., *et al.*)

Chapter 2

Functional and structural characterization of an ECF-type ABC transporter for vitamin B12

Santos, J.A.[†1], **Rempel, S.[†1]**, Mous, S.T.M.[1], Pereira, C.T.[2], ter Beek, J.[1], de Gier, J.W.[3], Guskov, A.[1], and Slotboom, D.J.[1,4]

[1]*Groningen Biomolecular and Biotechnology Institute (GBB), University of Groningen, The Netherlands*

[2]*Institute of Biology, University of Campinas (UNICAMP), Brazil*

[3]*Department of Biochemistry and Biophysics, Stockholm University, Sweden*

[4]*Zernike Institute for Advanced Materials, University of Groningen, The Netherlands*

† equal contribution, adapted from the manuscript published in *eLife*, **7**, 2018

Abstract

Vitamin B12 (cobalamin) is the most complex of the B-type vitamins and is synthetized *via* an intricate pathway exclusive to a limited number of prokaryotes. Its biological active variants methyl- and adenosyl-cobalamin contain rare organometallic bonds, which are exploited by enzymes in a variety of central metabolic pathways such as L-methionine synthesis and ribonucleotide reduction. Although its biosynthesis and role as co-factor are well understood, knowledge about uptake of cobalamin by prokaryotic Vitamin B12 auxotrophs is scarce. Here, we characterize a cobalamin-specific ECF-type ABC transporter from *Lactobacillus delbrueckii*, ECF-CbrT, and demonstrate that it mediates the specific, ATP-dependent uptake of cobalamin. We solved the crystal structure of the ECF-CbrT complex in an *apo* inward-facing conformation to 3.4 Å resolution. Comparison with the ECF transporter for folate (ECF-FolT2) from the same organism reveals how the identical ECF module adjusts to interact with the different substrate binding proteins FolT2 and CbrT. Although ECF-CbrT is unrelated to the well-characterized vitamin B12 transporter BtuCDF, their biochemical features indicate functional convergence.

Introduction

Vitamin B12 or cobalamin (Cbl) is regarded as the largest and most complex biological 'small molecule'. The molecule consists of a corrin ring chelating a cobalt ion using four equatorial coordinating nitrogen atoms (**Figure 1 and Suppl. Figure 1**). At the α-axial position the cobalt ion is coordinated by the 5,6-dimethylbenzimidazole (DMBI) base that is linked covalently to the corrin ring. Located at the β-axial position is the sixth coordinating moiety (1, 2). This ligand can vary among cobalamin derivatives and forms a rare organometallic covalent bond, which offers unique catalytic properties to enzymes that use Cbl as co-factor. The two most common biological active variants have a methyl- or 5'-deoxyadenosyl group resulting in methyl- and adenosyl-cobalamin (Met-Cbl and Ado-Cbl, respectively) at this position. In the industrially produced variant a cyano-group (CN-Cbl) binds at the β-axial position, and a hydroxy group (OH-Cbl) is present in the degradation product (1).

Enzymes that use Cbl as their co-factor catalyze mostly methyl group transfer reactions, or a variety of different radical-mediated reactions (1, 3). The most prominent example for methyl group transfer is MetE, the Cbl-dependent L-methionine synthase, which uses Met-Cbl to transfer a methyl group onto L-homocysteine to produce L-methionine. The methyl group on Cbl is subsequently restored from methyl-folate (1, 4).

The ability to synthesize Cbl *de novo* is restricted to prokaryotic species in only ~20 genera. Two routes for *de novo* synthesis have been established (aerobic or anaerobic), each requiring approximately 30 different enzymes, which makes *de novo* synthesis a very energy consuming process, and could explain why roughly two thirds of prokaryotes that require Cbl cannot synthesize the molecule and hence depend on uptake (1, 2). For some microbial communities, for instance in the Ross Sea, it has been shown that Cbl production is the limiting factor for biomass production, which generates a demand for Cbl uptake systems among Cbl auxotrophs (5).

In contrast to the well-characterized chemical properties of Cbl, as well as its biosynthesis and role in many enzymatic reactions, the uptake of the vitamin by bacteria is poorly understood. The only characterized Cbl uptake system is the *Escherichia coli* BtuCDF ATP binding cassette (ABC) transporter, which was first described in 1980 (6). Substantial

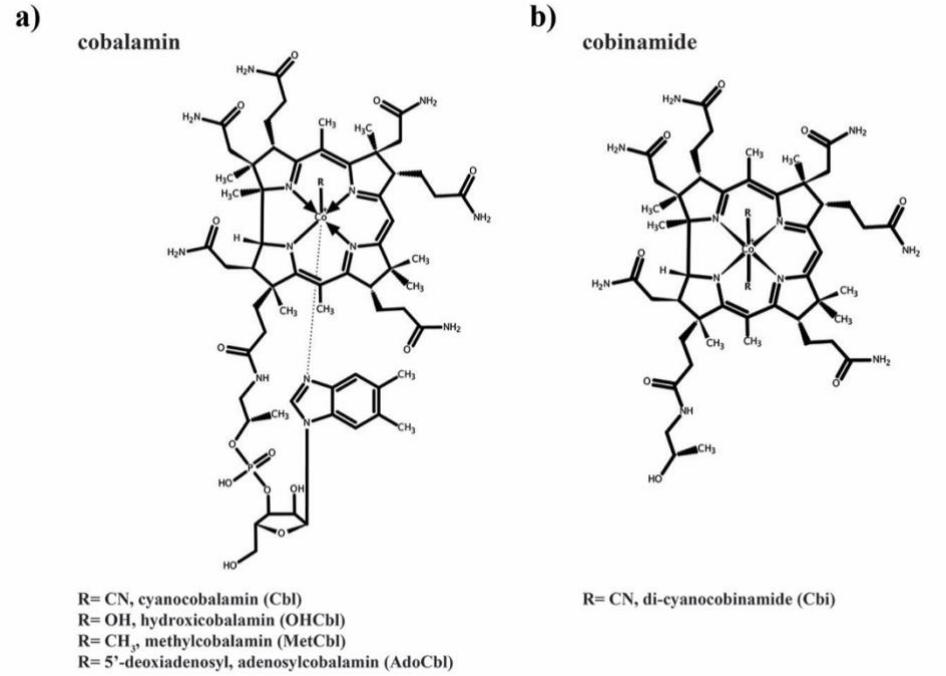

Figure 1: Structures of cobalamin and cobinamide. a) Cobalamin structure, represented in the base-on conformation with the 5',6'-dimethyl-benzimidazole ribonucleotide moiety (α-ligand) coordinating the central cobalt ion. The variable β-ligands are denoted as R in the lower left corner. b) Structure of cobinamide, which lacks the DMBI moiety and has two cyano groups coordinating the cobalt ion from each side of the corrin ring.

understanding of the system has been obtained through a combination of biochemical and structural studies (7–11). The importer uses the periplasmic substrate-binding protein BtuF to capture Cbl or its precursor cobinamide (Cbi) with high affinity (K_D values of ~10 nM and ~40 nM, respectively) (12, 13). Transport is powered by hydrolysis of ATP by the two BtuD subunits located on the cytoplasmic side of the membrane (14). The substrate passes through the membrane at the interface between two copies of the transmembrane protein, BtuC (7, 9). BtuCDF homologs are found widely in prokaryotes, but they are absent from a subset of bacteria that require uptake of the vitamin (15).

An *in silico* study by Rodionov *et al.* in 2009 (15) predicted that the energy coupling factor (ECF-) type ABC transporter ECF-CbrT might be a Cbl transporter (15). ECF-transporters are multi-subunit membrane complexes that consist of two ATPases, similar to the ATPases of ABC transporters, and two membrane embedded proteins, not related to any other protein

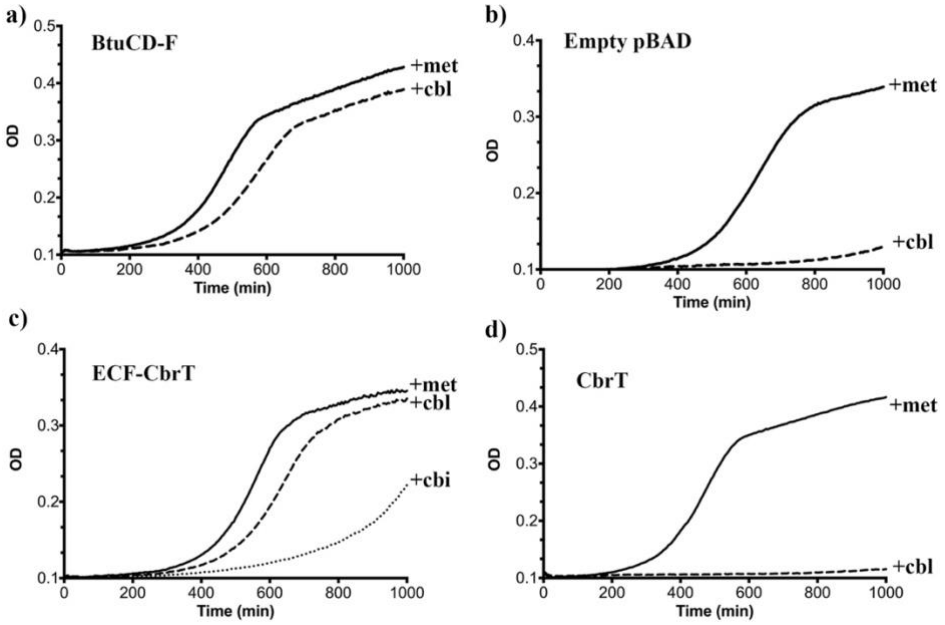

Figure 2: ECF-CbrT supports cobalamin-dependent growth of an *E. coli* deletion strain. a) The triple knock out strain *E. coli* ΔFEC expressing the BtuCDF ABC-transporter (positive control) grows in the presence of 50 µg ml^{-1} L-methionine or 1 nM CN-Cbl with lag-times of 300 minutes or 380 minutes, respectively, b) *E. coli* ΔFEC carrying only the empty expression vector (negative control) grows only in the presence of 50 µg ml^{-1} L-methionine but not with 1 nM CN-Cbl. The lag-times of the negative control is 450 minutes or >1000 minutes, respectively. c) *E. coli* ΔFEC expressing the entire ECF-CbrT transporter supports growth in the presence of either 1 nM Cbl or 1 nM Cbi with a lag-time of 470 minutes or 730 minutes, respectively. The lag-time in the presence of 50 µg ml^{-1} L-methionine is 410 minutes. d) Expression of the isolated S-component CbrT without its cognate ECF-module is not able to support growth of *E. coli* ΔFEC in the presence of 1 nM CN-Cbl.

family (16). The two ATPases and one of the transmembrane proteins, EcfT, form the ‘energizing unit’ or ’ECF-module’. The other membrane protein termed S-component acts as the substrate binding protein and dynamically associates with the ECF-module to allow for substrate translocation. In so-called group II ECF transporters multiple S-components specific for different substrates interact with the same ECF module (17–21). For instance, in *Lactobacillus delbrueckii* eight different S-components are predicted to share a single ECF module, one of which, CbrT, was predicted to be specific for Cbl (15, 22).

In this work, we biochemically and structurally characterize the ECF-CbrT complex from *L. delbrueckii*. We demonstrate that ECF-CbrT is a Cbl transporter that catalyzes ATP-dependent uptake of Cbl and its

precursor Cbi. We show that the S-component CbrT mediates high affinity substrate-specificity for Cbl and Cbi, and we report the crystal structure of ECF-CbrT from *L. delbrueckii* at 3.4 Å resolution in its *apo* inward-facing state. Although ECF-CbrT is structurally and mechanistically unrelated to BtuCDF, the kinetic parameters of the two transporters are very similar, suggestive of functional convergence.

Results

Expression of ECF-CbrT complements an Escherichia coli *strain lacking its endogenous vitamin B12 transporter*

To demonstrate that ECF-CbrT is a vitamin B12 transporter we constructed an *Escherichia coli* knock-out strain with three genomic deletions: Δ*btuF*, Δ*metE*, and Δ*btuC::Km*^{R} (*E. coli* ΔFEC) (23–25). A similar strain was previously used by Cadieux *et al.* (13) to identify the substrate binding protein BtuF. The knock-out strain lacks the L-methionine synthase MetE (26). *E. coli* possesses two L-methionine synthases, MetE and MetH. MetH uses Cbl as cofactor, whereas MetE is not dependent on the vitamin (26, 27). Thus, deletion of *metE* makes *E. coli* dependent on Cbl for the synthesis of L-methionine. Because *btuF* and *btuC* are also deleted in *E. coli* ΔFEC, endogenous Cbl-uptake mediated by BtuCDF is abolished (13), and (heterologous) expression of an active Cbl transporter is required to synthesize methionine.

We studied the growth of the deletion strain transformed with an expression plasmid for either BtuCDF (positive control), or an empty plasmid (negative control), or CbrT with or without the ECF module. We grew cells in 96-well plates using minimal medium supplemented with L-methionine or Cbl and monitored the optical density at 600 nm (OD_{600}). In the presence of L-methionine, all strains grew readily, with a lag phase of 300 – 450 minutes (**Figure 2a-d**) (28). The strains expressing BtuCDF or ECF-CbrT showed similar growth characteristics (lag time of 380 minutes and 470 minutes, respectively) in medium containing Cbl instead of methionine (**Figure 2a and 2c**, respectively), whereas the deletion strain expressing isolated CbrT (without its cognate ECF-module) did not show substantial growth in the absence of L-methionine when supplemented with Cbl (**Figure 2d**). The results demonstrate that the full

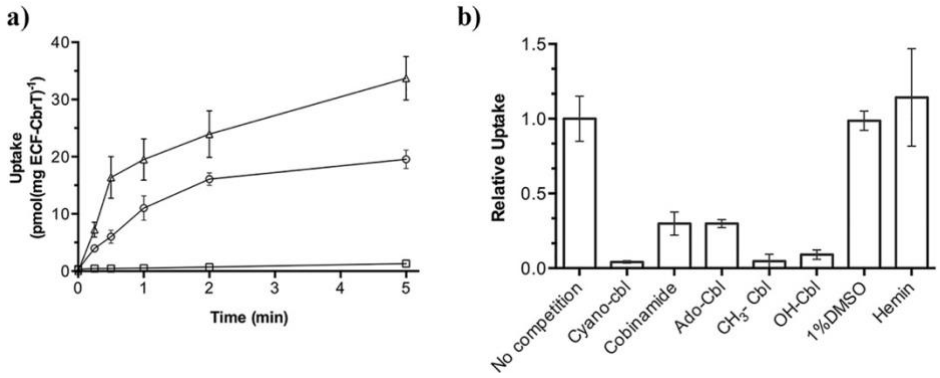

Figure 3: ^{57}Co-cyanocobalamin (cyano-Cbl) and ^{57}Co-cobinamide (Cbi) transport by purified and reconstituted ECF-CbrT. a) ATP-dependent uptake of radiolabeled CN-Cbl and Cbi by ECF-CbrT in proteoliposomes. Proteoliposomes were loaded with either 5 mM Mg-ATP (circles for CN-Cbl, triangles for Cbi) or 5 mM Mg-ADP (CN-Cbl, squares). b) Competition assay using Cbl-analogs. The initial uptake rate at 1 nM ^{57}Co-cyanocobalamin was measured. Competing compounds (adenosyl-cobalamin (Ado-Cbl), methyl-cobalamin (CH_3-Cbl), hydroxyl-cobalamin (OH-Cbl), cobinamide or hemin) were added at a concentration of 250 nM. The uptake was normalized to a condition without competitor (10 pmol mg^{-1} min^{-1}). Since hemin is not readily soluble in an aqueous solution, we added 1 % (v/v) DMSO during the assay, which did not affect the transporter activity. All competition experiments were performed in triplicate and the error bars indicate the standard deviation of the mean.

ECF-CbrT complex constitutes a new Cbl transporter. ECF-CbrT also supported growth of *E. coli* ΔFEC in the presence of Cbi instead of Cbl, albeit with a longer lag-time (730 minutes, **Figure 2c**), indicating that Cbi is a transported substrate of ECF-CbrT. We hypothesize that the longer lag time is due to the extra time required to express the necessary enzymes for Cbl synthesis from Cbi (29). Our further *in vitro* work shows that ECF-CbrT indeed supports efficient Cbi transport (see below).

ECF-CbrT catalyzes ATP-dependent transport of cobalamin and cobinamide

We purified ECF-CbrT, reconstituted the complex in liposomes and assayed for the uptake of radiolabeled Cbl (^{57}Co-cyanocobalamin). Uptake of radiolabeled Cbl into the proteoliposomes was observed only when the proteoliposomes were loaded with Mg-ATP and not when Mg-ADP was incorporated (**Figure 3a**). While this experiment shows that transport is strictly ATP-dependent, similar to what was found for other ECF transporters (20, 22), the ratio between ATP molecules hydrolyzed and Cbl molecules transported cannot be derived from this data. To obtain this ratio, simultaneous measurements of Cbl uptake and ATP hydrolysis rates

are needed, which is technically difficult. Additionally, the related ECF transporter for folate displays are large extent of futile ATP hydrolysis (not coupled to transport (22), which further complicates the determination of the coupling ratio. Nonetheless, the EcfA and EcfA' subunits contain all the motifs to form functional ATPases, and therefore we speculate that transport of Cbl is coupled to the hydrolysis of two ATP molecules. Using an ATP concentration of 5 mM, the apparent K_M for Cbl uptake was 2.1 ± 0.4 nM and the v_{max} = 0.06 ± 0.01 nmol mg^{-1} s^{-1} (**Figure 3 and Suppl. Figure 2**). To test the substrate specificity of the new vitamin B12 transporter, we conducted uptake experiments with a variety of competing compounds that are structurally similar to Cbl (**Figure 3b**). Addition of a 250-fold excess of unlabeled CN-Cbl inhibited the uptake of the radiolabeled substrate almost completely. Met-Cbl and OH-Cbl inhibited uptake to a similar extent as CN-Cbl, whereas Ado-Cbl was less effective (inhibition to ~25%). Addition of a 250-fold excess of Cbi also decreased the uptake of radiolabeled Cbl to ~25% (**Figure 3b**). To test whether Cbi is a transported substrate (that competitively inhibits transport of Cbl) or a non-transported compound that can only bind to the transporter, we directly measured uptake of Cbi (**Figure 3a**). Radiolabeled Cbi is not commercially available and, therefore, we synthesized the compound by treating ^{57}Co-cyanocobalamin with perchloric acid (30). The complete conversion of Cbl into Cbi was confirmed by mass spectrometry. Cbi was transported into liposomes containing ECF-CbrT, and transport required luminal Mg-ATP, confirming that Cbi is a transported substrate (**Figure 3a**). Finally, we tested whether hemin inhibits Cbl transport (**Figure 3b**). Hemin and Cbl are structurally related and share the same precursor uroporphyrinogen-III (31), but unlike Cbl, hemin consists of a flat porphyrin ring with a chelated iron ion, and has a chloride ion as one of the axial ligands. Hemin did not compete with Cbl-uptake (**Figure 3b**), showing that, although promiscuous among Cbl variants and Cbl-precursors, ECF-CbrT is a dedicated vitamin B12 transporter.

We aimed to obtain further biochemical information on the isolated S-component CbrT. We could purify CbrT only in the substrate-bound state (**Figure 4a**) The protein without substrate was unstable in detergent solution and prone to aggregation. Apparently, substrate binding had a stabilizing effect on CbrT, an observation that has been made more often for membrane proteins (20, 21).

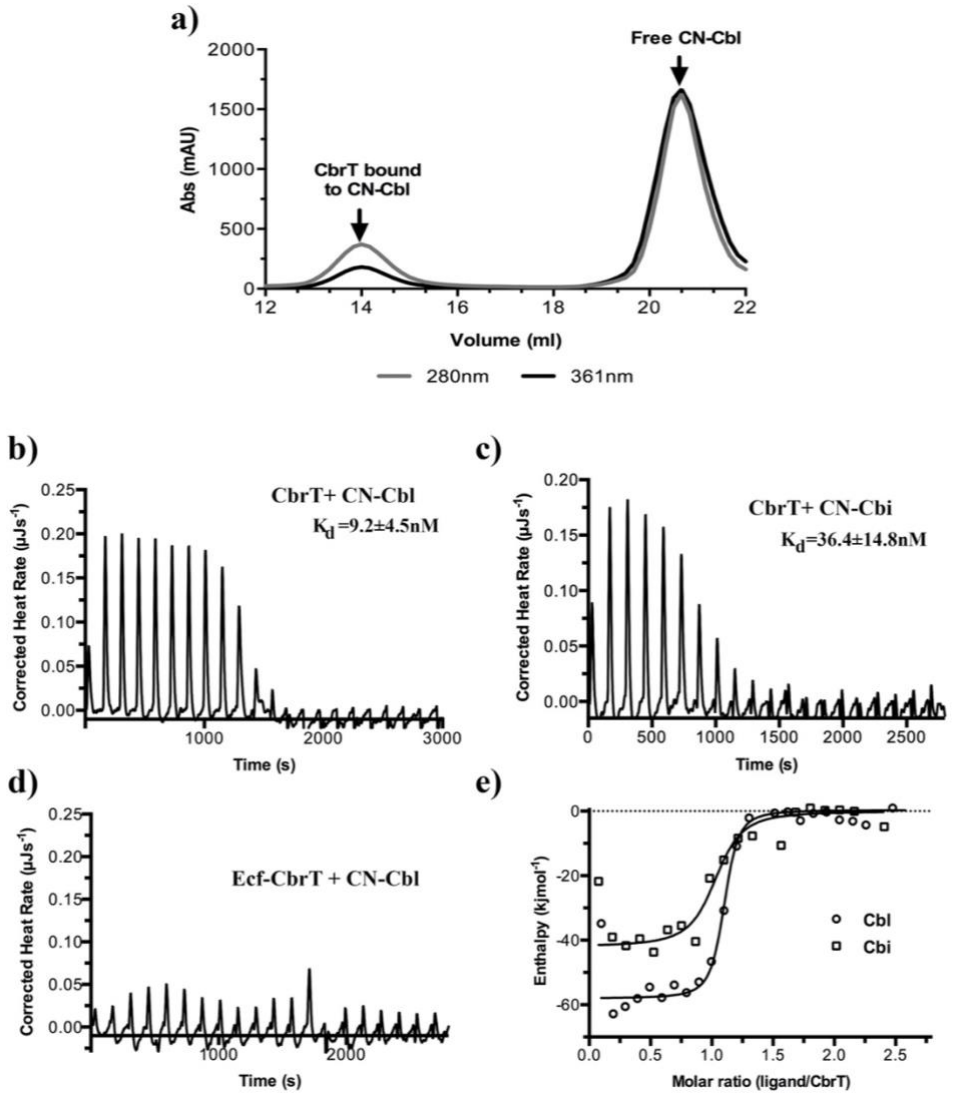

Figure 4: Cobalamin and cobinamide binding to CbrT. a) Co-purification of CN-Cbl with CbrT. The elution peak of the size exclusion column at a volume of 14 ml contains purified CbrT. The protein absorbs light at 280 nm and CN-Cbl at 361nm, showing that CbrT elutes bound to CN-Cbl. b) and c) ITC measurements of Cbl and Cbi binding to CbrT. The determined K_D values for Cbl and Cbi were averaged from triplicate measurements and the error is the standard deviation of the mean. d) ITC measurement showing lack of cobalamin binding to the full ECF-CbrT complex. Fitting of single binding site models to the data is shown in panel e).

From the spectral properties of Cbl that was co-purified with CbrT, we conclude that CbrT binds Cbl in a ~1:1 ratio in detergent solution (**Figure 4a**), which reflects the common substrate to protein stoichiometry for S-

components (21, 22, 32). Because we could not obtain purified *apo* CbrT, we studied the substrate-binding affinity using *E. coli* crude membrane vesicles (CMVs) containing overexpressed *apo* CbrT. Isothermal titration calorimetry (ITC) revealed binding of both CN-Cbl and Cbi with dissociation constants of 9.2 ± 4.5 nM and 36 ± 15 nM, respectively (**Figure 4b, c and e**). As a negative control, CMVs without CbrT were used to exclude unspecific binding of CN-Cbl or Cbi (**Figure 4d**). Cbl analogues, OH-Cbl and Met-Cbl, were also probed with ITC and found to bind to CbrT with similar binding affinities like CN-Cbl (K_D values of 9.6 ± 6.9 nM or 4.5 ± 0.3 nM respectively, **Figure 4 and Suppl. Figure 3**), supporting the notion that CbrT is promiscuous towards the β-axial ligand of Cbl and corroborating the findings of the competition assay.

Although the use of CMVs precluded the determination of the number of binding sites (the concentration of CbrT in the CMVs is unknown), the thermodynamic values (K_D, ΔH, and ΔS) derived from the ITC measurements do not depend on this number. Assuming that CbrT has a single substrate binding site (consistent with the spectral properties, **Figure 4a**), the expression level of CbrT in the membranes could be calculated and we found that CbrT accounted for ~0.9% (w/w) of the protein content in the membrane.

Structure of the vitamin B12-specific ECF transporter in its apo and post substrate-release state

We crystallized the ECF-CbrT complex in detergent (n-Dodecyl-β-D-maltopyranoside, DDM) solution and solved a crystal structure to 3.4 Å (**Figure 5a**) using molecular replacement with the structure of the folate transporter, ECF-FolT2, from *L. delbrueckii* as a search model (22). Statistics of data collection and structure refinement are summarized in **Suppl. Table 1**. There are two copies of ECF-CbrT in the asymmetric unit, corresponding to molecules A and B, each of them comprising CbrT, EcfT, EcfA, and EcfA'.

The identical ECF modules of the ECF-FolT2 and ECF-CbrT complexes have very similar overall structures, with a few notable conformational differences (**Figure 5b**). In both complexes, the two nucleotide-binding domains (NBDs, called EcfA and EcfA') are in a nucleotide-free state, adopting an open conformation with two incomplete ATP-binding sites. With the NBDs of ECF-FolT and ECF-CbrT aligned structurally (rmsd

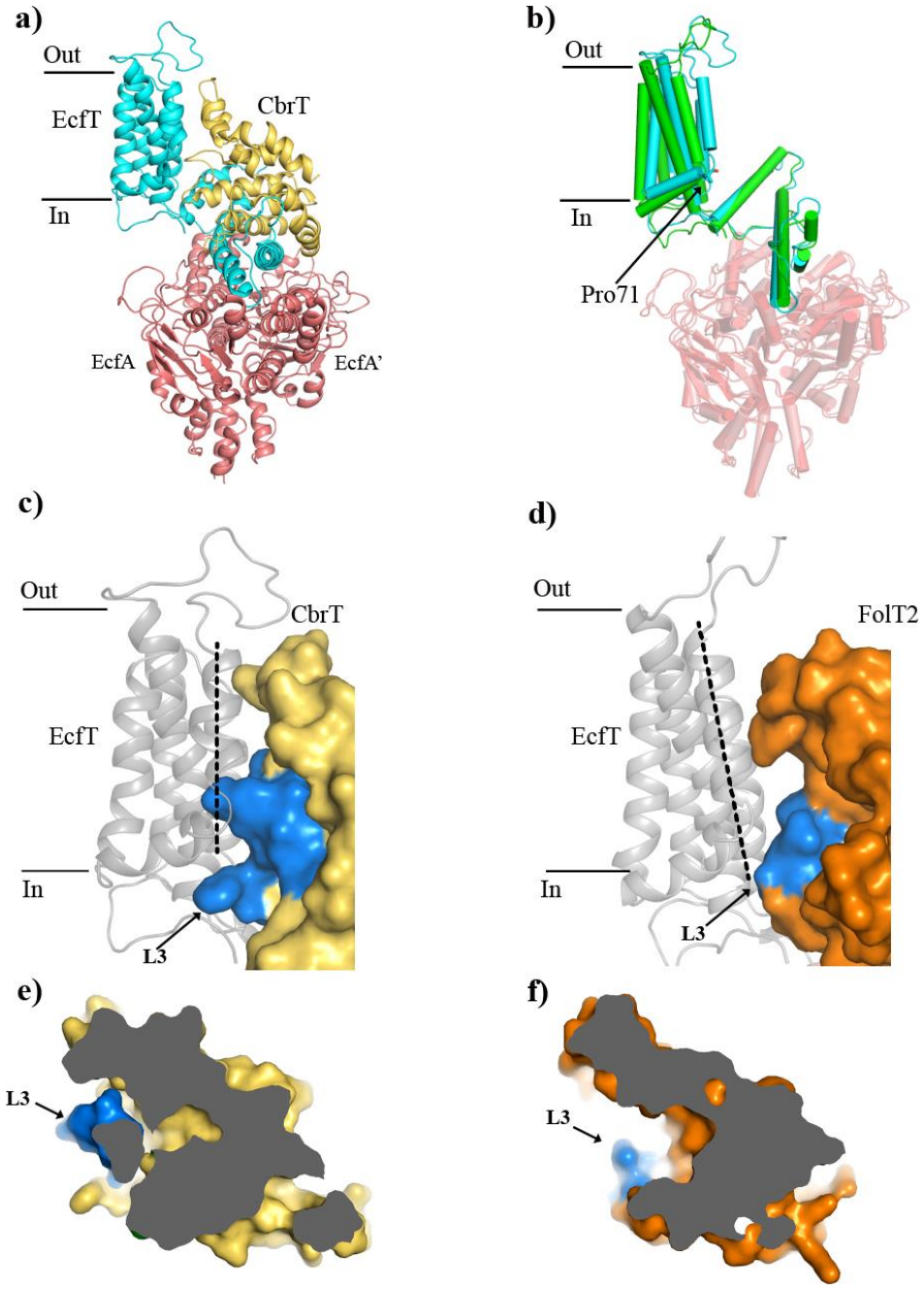

1.8Å), the coupling helices of EcfT, which transmit the conformational changes in the NBDs upon ATP-hydrolysis to the membrane domains, also superimpose well between the two complexes (rmsd 1,5Å). However,

the transmembrane-helices of EcfT adopt different conformations (rmsd 4.4Å). They are offset like rigid bodies, hinging approximately around Pro71 (**Figure 5b**). Structural flexibility of the membrane domain has been observed before (22, 33) and is likely necessary to accommodate different S-components, and may facilitate toppling of the S-components during the catalytic cycle (22).

The S-components CbrT and FolT2, which interact with the same ECF module in *L. delbrueckii*, do not share significant sequence similarity (16% identical residues). Accordingly, the structures show pronounced differences (rmsd 3.1 Å), although the overall folds are the same. Particularly, differences in loop 3 and loop 5 cause alterations of the protein surfaces that interact with the membrane domain of EcfT (**Figure 5c and d**). Therefore, tight association of the different S-components with the same ECF module requires the conformational adaptations in the membrane domain of the interacting EcfT subunits (**Figure 5c and d**).

CbrT is in a 'toppled' orientation in the ECF-CbrT complex with TMS 1, 2, 3, and 4 oriented almost parallel to the membrane plane. Although OH-Cbl was added in excess to the crystallization condition, the substrate was not bound. The *apo* state of the toppled S-component was observed before in other ECF-type transporters and likely represents the inward state after substrate release (22, 33–35). The absence of substrate is in agreement with the proposed transport model, in that the inward oriented *apo* protein is a low affinity state (22). It has been hypothesized that this state precedes ATP hydrolysis, which leads to release of the S-component component from the ECF module, and reorientation of the S-component in the membrane, which brings the substrate binding site to the extracellular side (22).

Figure 5: Comparison of the structures of ECF-CbrT and ECF-FolT from *Lactobacillus delbrueckii*. a) Cartoon representation of ECF-CbrT from the perspective of the plane of the membrane. Cytoplasmic ATPases, EcfA and EcfA', are colored in red, EcfT in cyan and CbrT in yellow. b) Structural differences between the membrane domains of EcfT. The structures of ECF-CbrT (cyan) and ECF-FolT2 (green) from *L. delbrueckii* were superimposed by structural alignment of the ATPase units. Pro71 of EcfT is represented in sticks. c) and d) Surface representation of CbrT (c, yellow) and FolT (d, orange) interacting with EcfT (cartoon representation colored in grey) with loop 3 of the S-components colored in blue. A dashed line highlights the movement of the transmembrane helix 3 of EcfT. e) and f) Loop 3 obstructs access to the substrate binding cavity in CbrT but not in FolT2. e) Slice-through of CbrT in surface representation, viewed from the plane of the membrane. Loop 3 is colored in blue. The ECF module has been omitted for clarity. f) Same slice through representation like in e) but for FolT2.

We hypothesize that the binding site for Cbl is located in a large cavity observed in the CbrT structure. The location of the cavity matches the position of the substrate-binding sites in the structurally characterized S-components in the substrate-bound state (21, 22, 32). In contrast to ECF-FolT2 (22), and structurally characterized ECF complexes from other organisms (33–35), the binding cavity in ECF-CbrT is largely occluded, and not accessible from the cytosol (**Figure 5e and f**). The occlusion is caused mainly by the position of loop 3, which obstructs access to the cavity in ECF-CbrT. We speculate that occlusion of the empty binding site after cytoplasmic release of the substrate may be required for the subsequent reorientation of the S-component, upon release from the ECF module.

Discussion

Comparative genomics studies have identified a wide range of ECF transporter families along with their putative substrate specificities mediated by their S-components (15). Based on its genetic organization and the lack of a BtuCD-F transporter homolog in the *Lactobacillales* genomes, CbrT was predicted to be a vitamin B12-specific S-component (15). In *L. delbrueckii*, which was shown to be auxotrophic for vitamin B12 (36), CbrT occurs within the *nrdJ–cbrS–cbrT–pduO* gene cluster. This genetic organization strongly implies an involvement of the substrate binding protein CbrT in Cbl uptake: First, *nrdJ* is annotated as an Ado-Cbl dependent ribonucleotide reductase requiring the vitamin as a co-factor. Second, PduO is a cobalamin adenosyltransferase, which converts Cbl into Ado-Cbl making it accessible for NrdJ. We showed that ECF-CbrT not only transport Cbl but also mediates uptake of Cbi (**Figure 3a**). Therefore, *L. delbrueckii* is expected to have the genetic repertoire to synthesize Cbl using Cbi as a precursor. However, we could not find homologs of the enzymes CobS, CobU and CobT, which are known to convert Cbi into cobalamin in *E. coli* (29). Possibly other proteins might functionally compensate for their absence, which was shown for thiamin kinase YcfN, which could replace CobU in *Salmonella typhimurium* (37). However, it is also possible that *L. delbrueckii* CbrT binds Cbi in a futile manner, in which case Cbi would be transported but not used as a substrate for any enzyme. Finally, predicted CbrT homologs in *Lactobacillales* display a high degree of sequence identity, ranging from 25% to 60%

compared to *L. delbrueckii* CbrT. Thus, we hypothesize that these CbrT homologs share the same function and represent substrate binding proteins for both Cbl and Cbi.

Our results show that ECF-CbrT is a new vitamin B12 transporter that is able to restore Cbl-Our results show that ECF-CbrT is a new vitamin B12 transporter that is able to restore Cbl- and Cbi-dependent growth in *E. coli* ΔFEC (**Figure 2c**). Further characterization using uptake experiments with the purified ECF-CbrT complex (**Figure 3a**) and binding studies on CbrT (**Figure 4**) show that the transporter is promiscuous towards the β-ligand of Cbl and also accepts Cbi as substrate (**Figure 3b**). A similar behavior has also been observed for BtuCDF (12).

All three naturally occurring Cbl variants, OH-Cbl, Ado-Cbl and Met-Cbl, inhibit uptake of radiolabeld CN-Cbl (**Figure 3b**). Whereas almost full inhibition was observed by a 250-fold excess of OH-Cbl, CN-Cbl and Met-Cbl, Ado-Cbl inhibited only to 25%. This might be due to its bulkier β-ligand and a consequent steric hindrance. Nonetheless, the assay shows that ECF-CbrT is promiscuous towards the β-axial ligand of vitamin B12. Generally, poly-specificity to Cbl (and Cbl-derivatives, see below) and Cbi seems to be an inherent feature of vitamin B12 binding proteins, which is the case for BtuF, human Cbl-carriers and also CbrT (12, 38). In the human Cbl-carriers that share a similar promiscuity, the β-ligand side of the bound substrate is partially solvent exposed (39–41). In CbrT, the broader substrate specificity might be related to flexibility of loops 1 and 3 that are the gates of CbrT and would make contact with the varying β-axial ligands.

In other ECF-transporters, the S-components exhibit remarkable high affinities toward their respective substrates with K_D values in the low nanomolar range (16). ITC measurements with CbrT in the absence of the ECF module also show high affinity binding with CN-Cbl, OH-Cbl, Met-Cbl, and Cbi (**Figure 4b, c, and e**). The slightly lower affinity for Cbi (4-fold) is probably due to the lack of the α-ligand (**Figure 1 and Suppl. Figure 1**) that leads to fewer possible protein-substrate interactions.

Strikingly, the affinity binding constants for CN-Cbl and Cbi are in the same range as the respective affinities determined for BtuF (Cbl 9.1 nM and Cbi of 40 nM) (12), which might imply that Cbl-transporters evolved to acquire the substrates with similar efficiency. Together with our v_{max}

and K_M (**Suppl. Figure 2**) determination, we additionally show that the rate limiting step is substrate translocation, which means that the observed affinities are probably optimized for efficient substrate scavenging, followed by a slow translocation step. Human carriers achieve even higher affinities for Cbl (in the sub-picomolar range (38), but in these cases the *off* rate is practically zero and substrate release requires proteolysis, which is not the mechanism of (ABC) transporters.

Although it was already known for a long time that a plethora of prokaryotic vitamin B12 uptake systems must exist, only the BtuCDF complex had been extensively characterized. This is somewhat surprising, considering the potential relevance of bacterial vitamin B12 transport for pharmaceutical applications. For instance, given the increase in antibiotic resistance and its serious threat to public health (42), it is imperative to find and characterize novel protein targets for drug design. Several pathogenic bacteria, such as *Streptoccoccus pyogenes* and *Clostridium tetani*, carry a *cbrT* gene, lack a BtuCDF homolog, and are Cbl-auxotrophs, which makes them strictly dependent on dedicated transporters to scavenge either vitamin B12 or its precursors from the environment. Because humans use endocytosis to take up Cbl (43), Cbl-specific prokaryotic transporters are potential drug targets for vitamin B12 auxotrophic pathogens.

Materials and Methods

Molecular Methods

For expression, CbrT (LDB_RS00385) was amplified by means of polymerase chain reaction (PCR) using *L. delbrueckii* subsp. *bulgaricus* genomic DNA as a template. For expression of the entire complex, CbrT was inserted into the second multiple cloning site of p2BAD_ECF with *XbaI* and *XhoI* restriction sites (22). For expression of solitary CbrT, the gene was inserted with a C-terminal 8His-tag into pBAD24 using *NcoI* and *HindIII* restriction sites (44). A single glycine (Gly2) was introduced to be in frame with the start-codon of the *NcoI* restriction site, which is not present in the full complex. All primers used are listed in **Suppl. Table 2** and all sequences were checked for correctness by sequencing.

Expression and membrane vesicle preparation

ECF-CbrT was expressed as described previously (22) with the following adaptations: Plain Luria Miller broth (LB) medium was used and the growth temperature was kept constant at 37°C throughout. After three hours of expression, the cells were harvested by centrifugation (20 min, 7,446×g, 4°C), and resuspended in 50 mM KPi, pH 7.5. Cells were either immediately used for membrane vesicles preparation or the resuspended cells were flash frozen in liquid nitrogen and stored at -80°C until use. Membrane vesicles were prepared as previously described (22).

ECF-CbrT Purification

Crude membrane vesicles containing ECF-CbrT were solubilized in buffer A (50 mM KPi, pH 7.5, 300 mM NaCl, 10%glycerol, 1% (w/v) n-dodecyl-β-D-maltopyranoside (DDM, Anatrace) for 45 min at 4°C under constant shaking. Insolubilized material was removed by centrifugation (35min, 287 000 × g, 4°C), the supernatant was loaded on a BioRad PolyPrep column containing 0.5 mL Ni^{2+}-sepharose bed volume (GE healthcare), pre-equilibrated with 20 column volumes (CV) buffer B (50 mM KPi, pH 7.5, 300 mM NaCl, 10% glycerol) and allowed to incubate for one hour at 4°C under constant movement. Unbound protein was allowed to flow through and the column was washed with 20 CV of buffer C (50 mM KPi, pH 7.5, 300 mM NaCl, 10% glycerol, 50mM imidazole, 0.05% DDM). ECF–CbrT was eluted with buffer D (50 mM KPi, pH 7.5, 300mM NaCl, 10% glycerol, 500mM imidazole, 0.05% (w/v) DDM) in three fractions of 0.4 ml, 0.75 ml and 0.5 ml, respectively. ECF-CbrT eluted mostly in the second elution fraction that was loaded on a Superdex 200 Increase 10/300 gel filtration column (GE Healthcare) that was equilibrated with buffer E (50mM HEPES pH 8.0, 150 mM NaCl, 0.05% DDM). For crystallization, ECF-CbrT was purified following the same protocol but buffers A to D contained 1% DDM. Buffers A to D were supplemented with 0.5 mM hydroxyl-cobalamin (OH-Cbl, Sigma Aldrich) and buffer E contained 10 μM OH-Cbl. For all experiments, the peak fractions were collected, combined and either used directly for reconstitution or concentrated in a Vivaspin disposable ultrafiltration device with a molecular weight cut-off of 30 kDa (Sartorius Stedim Biotech SA) to a final concentration of 6 mg ml^{-1}.

Construction of the E. coli *ΔFEC strain*

The E. coli strains JW0154 (*ΔbtuF::Km^R*), JW3805(*ΔmetE::Km^R*) and JW1701*(ΔbtuC::Km^R*) from the Keio collection (23) were purchased from the Coli Genetic Stock Center, Yale. *E. coli* JW0154 (*ΔbtuF::Km^R*) was used as the basis for constructing *E. coli* ΔFEC. The kanamycin resistance cassette of JW0154 was removed using the FLP recombinase as described before (24), resulting in *E. coli* ΔF. The *metE::Km^R* locus from JW3805 was introduced in *E. coli* ΔF using P1-mediated generalized transduction as described (25, 45), resulting in *E. coli* ΔFE*::Km^R*. The kanamycin cassette was removed using the FLP recombinase, resulting in *E. coli* ΔFE. The *ΔbtuC::Km^R* locus of JW1701 was introduced in *E. coli* ΔFE using P1-mediated generalized transduction, resulting in *E. coli* ΔFEC. Colony PCRs based on three primer pairs (*buF*-locus, 5'-atggctaagtcactgttcagg-3' & 5'-ctaatctacctgtgaaagcgc-3'; *butC*-locus, 5'-atgctgacacttgcccgc-3' & 5'-ctaacgtcctgcttttaacaataacc-3'; *metE*-locus, 5'-atgacaatattgaatcacaccctcg-3' & 5'-ttacccccgacgcaagttc-3') were used to verify *Km^R*-insertions, the FLP-recombinase-mediated removal of Km^R-markers and the absence of any genomic duplications resulting in the presence of any wild-type *metE*, *btuC* and *btuF* loci.

Growth assay with E. coli *ΔFEC strains*

The strains carrying various expression vectors were grown overnight at 37°C on LB-agar plates supplemented with 25 μg ml^{-1} kanamycin and 100 μg ml^{-1} ampicillin. The composition of the M9-based (47.7 mM Na_2HPO_4*$12H_2O$, 17.2 mM KH_2PO_4, 18.7 mM NH_4Cl, 8.6 mM NaCl) minimal medium was supplemented with 0.4% glycerol, 2 mM $MgSO_4$, 0.1 mM $CaCl_2$, 100 μg ml^{-1} L-arginine, 25 μg ml^{-1} kanamycin and 100 μg ml^{-1} ampicillin. A single colony was picked and used to inoculate a 3 ml to 6 ml liquid pre-culture supplemented with 50 μg ml^{-1} L-methionine (Sigma-Aldrich). The pre-culture was grown ~24 hours at 37°C, shaking in tubes with gas-permeable lids (Cellstar). The main cultures were inoculated in a 1:500 inoculation ratio. The main culture had a volume of 200 μl and was supplemented with 0.00001% L-arabinose (Sigma-Aldrich) and either 50 μg ml^{-1} L-methionine, 1 nM dicyano-cobinamide (Sigma Aldrich), or 1 nM cyano-cobalamin (Acros Organics). The medium was added to a sterile 96 well-plate (Cellstar). The 96-well plate was sealed with a sterile and gas-permeable foil (BreatheEasy, Diversified

Biotech). The cultures were grown for 1000 minutes in a BioTek Power Wave 340 plate reader at 37°C, shaking. The OD_{600} was measured every five minutes at 600 nm. All experiments were conducted as technical triplicates from biological triplicate. To obtain lag-times the averaged growth curves were fitted with the Gompertz-fit in Origin 8 and further analyzed as described (28).

Crystallization and structure determination

Initial crystallization conditions for ECF-CbrT were screened at 4 °C using commercial sparse-matrix crystallization screens in a sitting-drop setup and a Mosquito robot (TTP Labtech, UK). Initial crystals were found in the B11 condition (0.2 M KCl, 0.1 M Sodium citrate pH 5.5, 37% (v/v) Pentaerythritol propoxylate (5/4 PO/OH) of the MemGold1 HT-96 screen (Molecular Dimensions, UK) that diffracted up to 7.5 Å resolution. Using this condition as a starting point and the detergent (HR2-408) screen (Hampton Research, USA), an optimized condition could be found and contained the detergent ANAPOE®-$C_{12}E_{10}$ (Polyoxyethylene(10)dodecyl ether, Hampton Research) as an additive, which yielded crystals diffracting up to 3.4 Å resolution.

X-ray diffraction data was collected from cooled (100 K) single crystals at synchrotron beam lines at the Swiss Light Source (SLS, beamline PX1), Switzerland. The crystals of *apo* ECF–CbrT belong to space group P1 (unit cell parameters: a=85.47, b=92.86, c=105.51, α=72.568, β=66.274, γ=62.893).

To correct for anisotropy, the dataset was treated with the diffraction anisotropy server prior to further processing (46). Data were processed with XDS (47) and scaled with Xscale (48). Data collection statistics are summarized in **Suppl. Table 1**. The structure of the ECF-CbrT complex was solved by molecular replacement with PHASER MR (49) using the *apo* ECF-FolT2 structure of *L. delbrueckii* (22) (PDB code 5JSZ) as a search model. For model completion, several cycles of model building with COOT (50) and refinement with PHENIX (51) were performed. The Ramachandran statistics are 72,32% for favored regions, 26,64% for allowed regions and 1,05% for outliers. All structural figures in the main text were prepared with open-source version of pymol (https://sourceforge.net/projects/pymol/).

Preparation of radiolabeled cobinamide from radiolabeled cobalamin

The required amount of cyano-cobalamin (radiolabeled and unlabeled) was mixed in a 1:1 (v/v) ratio with 70% perchloric acid (Sigma-Aldrich) and incubated for ten minutes at 70°C. To quench the reaction and prevent damage to the substrate, the resulting cobinamide substrate was added to buffer G (as described above), which was additionally supplemented with 5 M NaOH to restore the pH back to 7.5.

Radiolabeled vitamin B12 transport assay

Purified ECF-CbrT was reconstituted in proteoliposomes as described previously (52). Proteoliposomes were thawed and loaded with 5 mM $MgSO_4$ or $MgCl_2$ and 5 mM Na_2-ATP or Na_2-ADP through three freeze-thaw cycles. Loaded proteoliposomes were extruded nine times through a polycarbonate filter with a 400 nm pore-size (Avestin), pelleted by centrifugation (267,008 g, 35 minutes, 4°C) and resuspended in buffer F (50 mM KPi pH 7.5) to 2 µl/mg lipids. The uptake reaction was started by addition of concentrated and loaded proteoliposomes to buffer G (50 mM KPi pH 7.5, varying concentrations of ^{57}Co-cyanocobalamin (150 to 300 µCi/mg, in 0,9% benzylalcohol, MP Biomedicals) in a 1:100 ratio. At elsewhere specified time points 200 µl samples were taken transferred into 2 ml ice cold buffer F and filtered over OE67 cellulose acetate filters (GE Healthcare) soaked in Buffer F supplemented with cyanocobalamin (Acros chemicals). The filter was washed with 2 ml ice cold buffer F and transport of radiolabeled substrate was counted in Perkin Elmer Packard Cobra II gamma counter. All uptake assays were performed at 30°C while stirring.

Substrate-binding assay

ITC measurements were performed using a NanoITC calorimeter (TA Instruments) at 25 °C. Membrane vesicles containing CbrT (200µl, 10 mg/ml in 50 mM Kpi, pH 7.5) were added to the NanoITC cell. Ligands were prepared in 50 mM KPi, pH 7.5 and titrated into the cell in 1ul injections with 140s between each injection. Membrane vesicles containing the full-complex ECF-CbrT that does not bind CN-Cbl (10 mg/ml in 50 mM Kpi, pH 7.5) were used as a negative control. Data were analyzed with the Nano Analyze Software.

Data deposition

The atomic coordinates and structure factors have been deposited in the Protein Data Bank, www.pdb.org (PDB ID code 6FNP).

Acknowledgments

We thank Prof. Dr. A.J.M. Driessen for the use of the setup in the isotope lab and the beamline personnel of PXI at SLS for their technical support. This work was supported by grants from the Netherlands Organisation for Scientific Research (NWO Vici grant 865.11.001 to D.-J.S. and NWO Vidi grant 723.014.002 to A.G.), the São Paulo Research Foundation (BEPE fellowship 2015/26203-0 to C.T.P), the European Research Council (ERC starting grant 282083 to D.-J.S.), and the European Molecular Biology Organization (EMBO long-term fellowship ALTF 687-2015 to J.A.S. and EMBO short-term fellowship ASTF-382-2015 to S.R.).

References

1. Gruber K, Puffer B, Kräutler B. 2011. Vitamin B12-derivatives—enzyme cofactors and ligands of proteins and nucleic acids. *Chem. Soc. Rev.* 40(8):4346
2. Roth J, Lawrence J, Bobik T. 1996. COBALAMIN (COENZYME B_{12}): Synthesis and Biological Significance. *Annu. Rev. Microbiol.* 50(1):137–81
3. Giedyk M, Goliszewska K, Gryko D. 2015. Vitamin B_{12} catalysed reactions. *Chem. Soc. Rev.* 44(11):3391–3404
4. Banerjee R V, Matthews RG. 1990. Cobalamin-dependent methionine synthase. *FASEB J.* 4(5):1450–59
5. Bertrand EM, Saito MA, Jeon YJ, Neilan BA. 2011. Vitamin B12 biosynthesis gene diversity in the Ross Sea: the identification of a new group of putative polar B12 biosynthesizers. *Environ. Microbiol.* 13(5):1285–98
6. DeVeaux LC, Kadner RJ. 1985. Transport of vitamin B12 in Escherichia coli: cloning of the btuCD region. *J. Bacteriol.*

162(3):888–96
7. Korkhov VM, Mireku SA, Veprintsev DB, Locher KP. 2014. Structure of AMP-PNP–bound BtuCD and mechanism of ATP-powered vitamin B12 transport by BtuCD–F. *Nat. Struct. Mol. Biol.* 21(12):1097–99
8. Goudsmits JMH, Jan Slotboom D, van Oijen AM. 2017. Single-molecule visualization of conformational changes and substrate transport in the vitamin B12 ABC importer BtuCD-F. *Nat. Commun.* 8(1):1652
9. Korkhov VM, Mireku SA, Locher KP. 2012. Structure of AMP-PNP-bound vitamin B12 transporter BtuCD–F. *Nature*. 490(7420):367–72
10. Borths EL, Locher KP, Lee AT, Rees DC. 2002. The structure of Escherichia coli BtuF and binding to its cognate ATP binding cassette transporter. *Proc. Natl. Acad. Sci. U. S. A.* 99(26):16642–47
11. Locher K. P., Lee A. T. RDC. 2002. The E. coli BtuCD Structure: A Framework for ABC Transporter Architecture and Mechanism. *Science* 296(5570):1091–98
12. Mireku SA, Ruetz M, Zhou T, Korkhov VM, Kräutler B, Locher KP. 2017. Conformational Change of a Tryptophan Residue in BtuF Facilitates Binding and Transport of Cobinamide by the Vitamin B12 Transporter BtuCD-F. *Sci. Rep.* 7:41575
13. Cadieux N, Bradbeer C, Reeger-Schneider E, Köster W, Mohanty AK, et al. 2002. Identification of the periplasmic cobalamin-binding protein BtuF of Escherichia coli. *J. Bacteriol.* 184(3):706–17
14. Borths EL, Poolman B, Hvorup RN, Locher KP, Rees DC. 2005. In Vitro Functional Characterization of BtuCD-F, the *Escherichia coli* ABC Transporter for Vitamin B $_{12}$ Uptake †. *Biochemistry*. 44(49):16301–9
15. Rodionov DA, Hebbeln P, Eudes A, Ter Beek J, Rodionova IA, et al. 2009. A novel class of modular transporters for vitamins in prokaryotes. *J. Bacteriol.* 91(1):42–51
16. Slotboom DJ. 2014. Structural and mechanistic insights into prokaryotic energy-coupling factor transporters. *Nat. Rev. Microbiol.* 12(2):79–87
17. Henderson GB, Zevely EM, Huennekens FM. 1979. Mechanism of folate transport in Lactobacillus casei: Evidence for a component shared with the thiamine and biotin transport systems. *J. Bacteriol.*

137(3):1308–14
18. Karpowich NK, Song JM, Cocco N, Wang DN. 2015. ATP binding drives substrate capture in an ECF transporter by a release-and-catch mechanism. *Nat. Struct. Mol. Biol.* 22(7):565–71
19. Majsnerowska M, Ter Beek J, Stanek WK, Duurkens RH, Slotboom DJ. 2015. Competition between Different S-Components for the Shared Energy Coupling Factor Module in Energy Coupling Factor Transporters. *Biochemistry*. 54(31):4763–66
20. Ter Beek J, Duurkens RH, Erkens GB, Slotboom DJ. 2011. Quaternary structure and functional unit of Energy Coupling Factor (ECF)-type transporters. *J. Biol. Chem.* 286(7):5471–75
21. Berntsson RP-A, ter Beek J, Majsnerowska M, Duurkens RH, Puri P, et al. 2012. Structural divergence of paralogous S components from ECF-type ABC transporters. *Proc. Natl. Acad. Sci.* 109(35):13990–95
22. Swier LJYM, Guskov A, Slotboom DJ. 2016. Structural insight in the toppling mechanism of an energy-coupling factor transporter. *Nat. Commun.* 7:11072
23. Baba T, Ara T, Hasegawa M, Takai Y, Okumura Y, et al. 2006. Construction of Escherichia coli K-12 in-frame, single-gene knockout mutants: the Keio collection. *Mol. Syst. Biol.* 2:2006.0008
24. Datsenko KA, Wanner BL. 2000. One-step inactivation of chromosomal genes in Escherichia coli K-12 using PCR products. *Proc. Natl. Acad. Sci.* 97(12):6640–45
25. Thomason LC, Costantino N, Court DL. 2007. *E. coli* Genome Manipulation by P1 Transduction. *Curr. Protoc. Mol. Biol.* 1.17.1-1.17.8
26. DAVIS BD, MINGIOLI ES. 1950. Mutants of Escherichia coli requiring methionine or vitamin B12. *J. Bacteriol.* 60(1):17–28
27. Banerjee R V., Johnston NL, Sobeski JK, Datta P, Matthews RG. 1989. Cloning and sequence analysis of the Escherichia coli metH gene encoding cobalamin-dependent methionine synthase and isolation of a tryptic fragment containing the cobalamin-binding domain. *J. Biol. Chem.* 264(23):13888–95
28. Zwietering MH, Jongenburger I, Rombouts FM, Van't Riet K. 1990. Modeling of the bacterial growth curve. *Appl. Environ. Microbiol.* 56(6):1875–81
29. Lawrence JG, Roth JR. 1995. The cobalamin (coenzyme B12) biosynthetic genes of Escherichia coli. *J. Bacteriol.* 177(22):6371–

80
30. Schneider Z, Stroiński A. 1987. *Comprehensive B12 : chemistry, biochemistry, nutrition, ecology, medicine*. De Gruyter. 409 pp.
31. Roth J, Lawrence J, Bobik T. 1996. COBALAMIN (COENZYME B 12): Synthesis and Biological Significance. *Annu. Rev. Microbiol.* 50(1):137–81
32. Erkens GB, Berntsson RPA, Fulyani F, Majsnerowska M, Vujiĉić-Žagar A, et al. 2011. The structural basis of modularity in ECF-type ABC transporters. *Nat. Struct. Mol. Biol.* 18(7):755–60
33. Zhang M, Bao Z, Zhao Q, Guo H, Xu K, et al. 2014. Structure of a pantothenate transporter and implications for ECF module sharing and energy coupling of group II ECF transporters. *Proc. Natl. Acad. Sci. U. S. A.* 111(52):18560–65
34. Wang T, Fu G, Pan X, Wu J, Gong X, et al. 2013. Structure of a bacterial energy-coupling factor transporter. *Nature*. 497(7448):272–76
35. Xu K, Zhang M, Zhao Q, Yu F, Guo H, et al. 2013. Crystal structure of a folate energy-coupling factor transporter from Lactobacillus brevis. *Nature*. 497(7448):268–71
36. Kusaka I, Kitahara K. 1962. Effect of several vitamins on the cell division and the growth of Lactobacillus delbrueckii. *J. Vitaminol. (Kyoto)*. 8:115–20
37. Otte MM, Woodson JD, Escalante-Semerena JC. 2007. The thiamine kinase (YcfN) enzyme plays a minor but significant role in cobinamide salvaging in Salmonella enterica. *J. Bacteriol.* 189(20):7310–15
38. Fedosov SN, Petersen TE, Nexø E. 1995. Binding of Cobalamin and Cobinamide to Transcobalamin from Bovine Milk. *Biochemistry*. 34(49):16082–87
39. Mathews FS, Gordon MM, Chen Z, Rajashankar KR, Ealick SE, et al. 2007. Crystal structure of human intrinsic factor: cobalamin complex at 2.6-A resolution. *Proc. Natl. Acad. Sci. U. S. A.* 104(44):17311–16
40. Furger E, Frei DC, Schibli R, Fischer E, Prota AE. 2013. Structural basis for universal corrinoid recognition by the cobalamin transport protein haptocorrin. *J. Biol. Chem.* 288(35):25466–76
41. Wuerges J, Geremia S, Fedosov SN, Randaccio L. 2007. Vitamin B12 transport proteins: crystallographic analysis of beta-axial ligand substitutions in cobalamin bound to transcobalamin. *IUBMB Life*.

59(11):722–29
42. Alós JI. 2015. Resistencia bacteriana a los antibióticos: una crisis global
43. Quadros E V. 2010. Advances in the understanding of cobalamin assimilation and metabolism
44. Guzman LM, Belin D, Carson MJ, Beckwith J. 1995. Tight regulation, modulation, and high-level expression by vectors containing the arabinose P(BAD) promoter. *J. Bacteriol.* 177(14):4121–30
45. Miller J. 1972. Experiments in molecular genetics. In *Experiments in molecular genetics*. Cold Spring Harbor, NY: Cold Spring Harbor Laboratory
46. Strong M, Sawaya MR, Wang S, Phillips M, Cascio D, Eisenberg D. 2006. Toward the structural genomics of complexes: Crystal structure of a PE/PPE protein complex from Mycobacterium tuberculosis. *Proc. Natl. Acad. Sci.* 103(21):8060–65
47. Kabsch W, K. W, G. RRB. 2010. XDS. *Acta Crystallogr. Sect. D Biol. Crystallogr.* 66(2):125–32
48. Kabsch W. 2010. Integration, scaling, space-group assignment and post-refinement. *Acta Crystallogr. Sect. D Biol. Crystallogr.* 66(2):133–44
49. McCoy AJ, Grosse-Kunstleve RW, Adams PD, Winn MD, Storoni LC, Read RJ. 2007. Phaser crystallographic software. *J. Appl. Crystallogr.* 40(4):658–74
50. Emsley P, Lohkamp B, Scott WG, Cowtan K. 2010. Features and development of Coot. *Acta Crystallogr. Sect. D Biol. Crystallogr.* 66(4):486–501
51. Adams PD, Afonine P V, Bunkóczi G, Chen VB, Davis IW, et al. 2010. PHENIX: A comprehensive Python-based system for macromolecular structure solution. *Acta Crystallogr. Sect. D Biol. Crystallogr.* 66(2):213–21
52. Geertsma ER, Nik Mahmood NAB, Schuurman-Wolters GK, Poolman B. 2008. Membrane reconstitution of ABC transporters and assays of translocator function. *Nat. Protoc.* 3(2):256–66

Supplementary Information

Supplementary tables

Suppl. table 1: Data collection, phasing and refinement statistics.

	ECF-CbrT
Data collection	
Space group	P 1
Unit cell dimensions	
a, *b*, *c* (Å)	85.47, 92.86, 105.51
α, *β*, *γ* (°)	72.57, 66.27, 62.89
Resolution range (Å)	47.80, 3.40
R_{merge} (%)	17.7 (>100) [a]
$I/\sigma I$	3.82 (0.38) [a]
Completeness (%)	93 (94) [a]
Redundancy	3,68 (3,7) [a]
Refinement	
Resolution (Å)	3.4
No. of reflections	31753
R_{work}/R_{free}	0.238/ 0.293
Total no. of atoms	15083
R.m.s. deviations	
Bond lengths (Å)	0.010
Bond angles (Å)	1.487

[a]Values in parentheses are for the highest-resolution shell.

Suppl. table 2: Primer list used in this study.

Primer name	Sequence (5' – 3')
CbrT_Ld_NcoI_frwd	TAACCATGGGACAGACCAAGGAACGCTAC
CbrT_Ld_cHis8_HindIII_rev	AATAAGCTTTCATTAATGATGATGGTGATGGTGGT GGTGAGCATTTTGCTTCCACCC
CbrT_Ld_XbaI_frwd	CCATCTAGATGCAGACCAAGGAACGCTACCAG
CbrT_Ld_XhoI_rev	AATCTCGAGTCATTAAGCATTTTGCTTCCACCCTGC
Seq_frwd	CTCTACTGTTTCTCCATACCCG
Seq_rev	GCTGAAAATCTTCTCTCATCCG

Supplementary figures

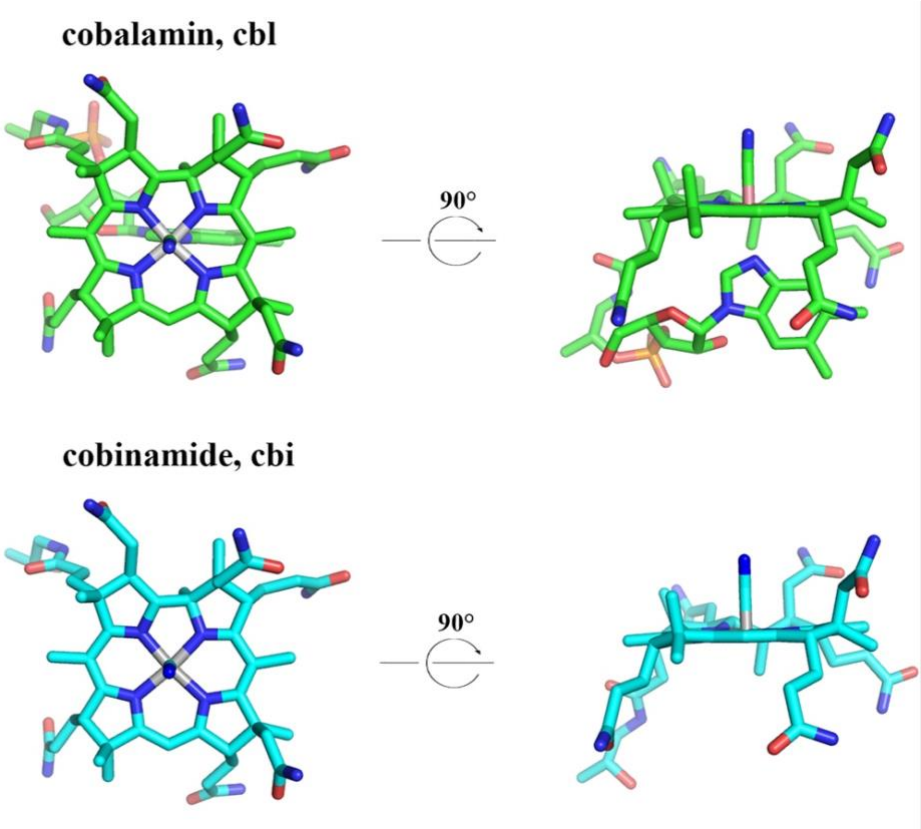

Suppl. Figure 1: 3D structures of cobalamin and cobinamide. Cobalamin (green) and cobinamide (cyan) are shown in stick representation. The central cobalt ion is colored in grey, nitrogen atoms in blue, oxygen atoms in red and phosphate atoms in orange.

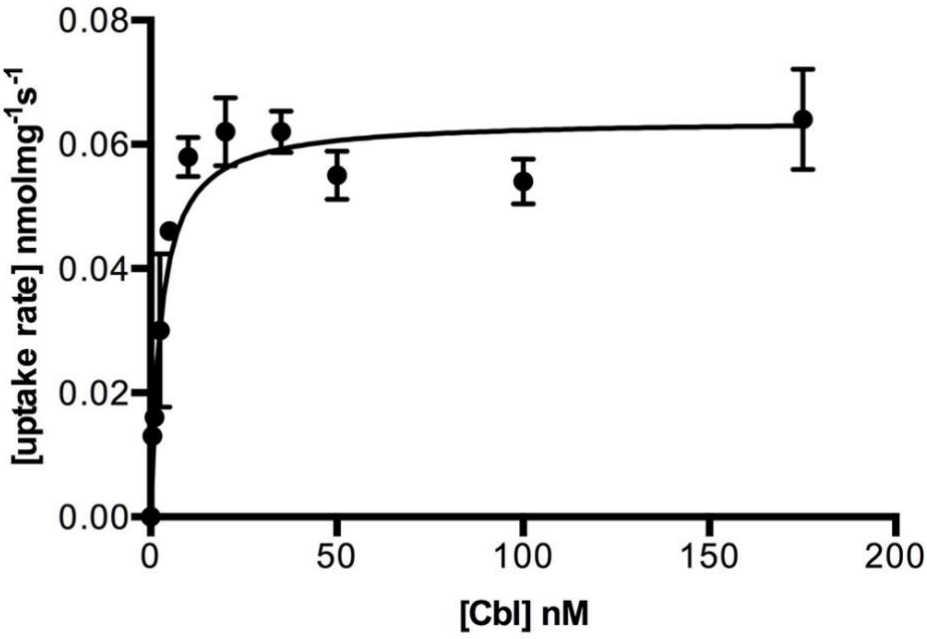

Suppl. Figure 2: Kinetics of cobalamin uptake by ECF-CbrT. Transport rates are shown as a function of the cobalamin concentration. Proteoliposomes were loaded with 5 mM Mg-ATP. Experiments were performed in triplicated and error bars show the standard deviation of the mean. The data was fitted with a Michaelis-Menten function to obtain the K_M value of 2.1 ± 0.4 nM and the V_{max} value of 0.06 ± 0.01 pmol mg^{-1} s^{-1}.

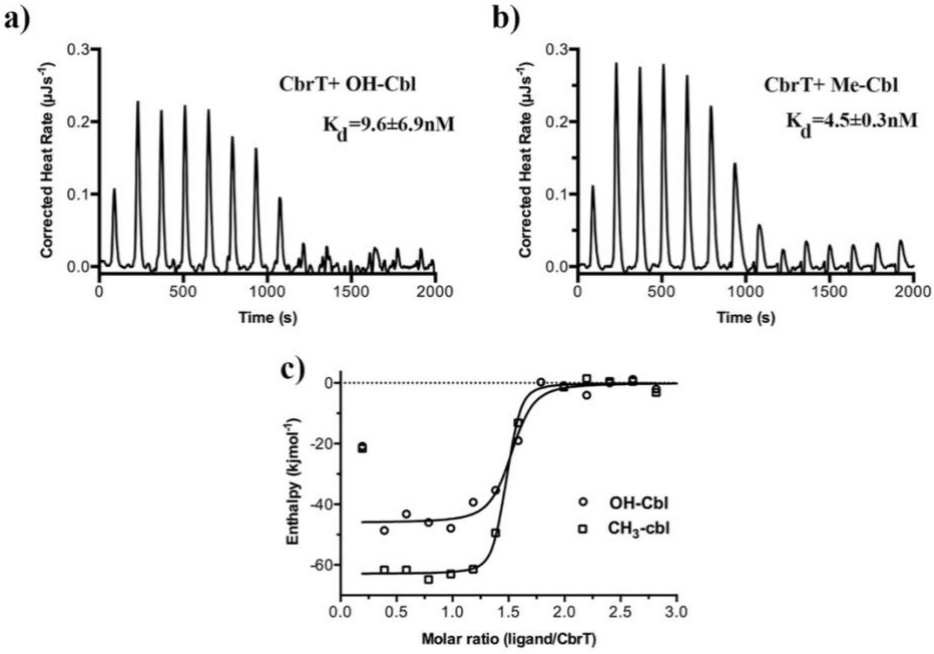

Suppl. Figure 3: Binding of Cbl-analogs to CbrT. ITC measurements of a) OH-Cbl and b) CH_3-Cbl binding to CbrT. The determined K_D values were averaged from duplicate measurements and the error is the standard deviation of the mean. Fitting of single binding site models to the data is shown in c).

Chapter 3

Cysteine-mediated decyanation of vitamin B12 by the predicted membrane transporter BtuM

Rempel, S.[1], Colucci, E.[1], de Gier, J.W.[2], Guskov, A.[1], and Slotboom, D.J.[1,3]

[1]*Groningen Biomolecular and Biotechnology Institute (GBB), University of Groningen, The Netherlands*

[2]*Department of Biochemistry and Biophysics, Stockholm University, Sweden*

[3]*Zernike Institute for Advanced Materials, University of Groningen, The Netherlands*

Adapted from the manuscript published in *Nature Communications*, **9**, 2018.

Abstract

Uptake of vitamin B12 is essential for many prokaryotes, but in most cases the membrane proteins involved are yet to be identified. We present the biochemical characterization and high-resolution crystal structure of BtuM, a predicted bacterial vitamin B12 uptake system. BtuM binds vitamin B12 in its base-off conformation, with a cysteine residue as axial ligand of the corrin cobalt ion. Spectroscopic analysis indicates that the unusual thiolate coordination allows for decyanation of vitamin B12. Chemical modification of the substrate is a property other characterized vitamin B12-transport proteins do not exhibit.

Introduction

Cobalamin (Cbl) is one of the most complex cofactors (**Suppl. Figure 1a**) known, and used by enzymes catalyzing for instance methyl-group transfer and ribonucleotide reduction reactions (1, 2). For example in methionine synthase MetH, the cofactor is used to transfer a methyl moiety onto L-homocysteine to produce L-methionine (1, 3). Many bacteria require Cbl for survival (1, 2, 4, 5), but only a small subset of prokaryotic species can produce this molecule *de novo*, *via* either an aerobic or anaerobic pathway (4, 5). Roughly two thirds of archaea and eubacteria are Cbl-auxotrophs that rely on uptake of either Cbl or its precursor cobinamide (2, 5, 6) (Cbi, **Figure 1a and Suppl. Figure 1b**). Dependence on uptake has probably evolved, because synthesis of Cbl involves roughly 30 different enzymes and is energetically costly. Gram-negative bacteria require the TonB-dependent transporter BtuB (1) to transport Cbl across the outer membrane (**Suppl. Figure 1c**). For subsequent transport of vitamin B12 across the cytoplasmic membrane, the only characterized bacterial uptake system is the ABC transporter BtuCDF, which is predicted to be present in approximately 50% of Cbl-auxotrophic bacteria (5, 7). Many Cbl-auxotrophic Gram-negative bacteria do not encode BtuCDF, whereas they do contain BtuB. Metabolic reconstruction and chromosomal context analyses, e.g. co-localization with the gene for BtuB, have identified potential alternative inner membrane vitamin B12 transporters, one of which is BtuM (5). BtuM homologs are small

Figure 1: Function and structure of $BtuM_{Td}$. a) Schematic representation of Cobalamin (Cbl) showing the corrinoid ring with the central cobalt ion (red). The ligand at the β-axial position is in this case a cyano group, but differs in various Cbl variants (**Suppl. Figure 1a and b**). The ligand at the α-axial position (base-on conformation) is the 5,6-dimethylbenzimidazole base, which is covalently linked to the corrinoid ring. When this coordination is lost, Cbl is termed base-off. Cbi lacks the 5,6-dimethylbenzimidazole base (indicated by the zigzagged red line). b) Growth assays with *E. coli* ΔFEC was conducted in the presence of 50 μg ml^{-1} L-methionine or 1 nM Cbl. Additional experiments in the presence of different Cbl concentration are shown in **Suppl. Figure 2f and g**. All growth curves are averages of nine experiments (three biological triplicates, each with three technical replicates). Top panel: cells containing the empty expression vector (pBAD24) in the presence of methionine (blue line) or Cbl (grey line) and cells expressing the BtuCDF system (black and red lines, respectively). Bottom panel: cells expressing $BtuM_{Td}$ (black and red lines) or mutant $BtuM_{Td}$_C80S (blue and grey) in the presence of L-methionine and Cbl, respectively. The inset displays a western blot showing that the mutant is expressed to wild-type levels (the full length western blot can be found in **Suppl. Figure 2h**). c) The structure of $BtuM_{Td}$ in cartoon representation, colored from blue (N-terminus) to red (C-terminus) and viewed from the membrane plane. α-helices (H1-6) and connecting loops (L1-5) are indicated. Cbl is shown in stick representation with carbon atoms colored wheat, the oxygen and nitrogen atoms in red and blue, respectively, the cobalt ion in pink. Four n-nonyl-β-D-glucopyranoside detergent molecules are also shown in stick representation (carbons in light grey).

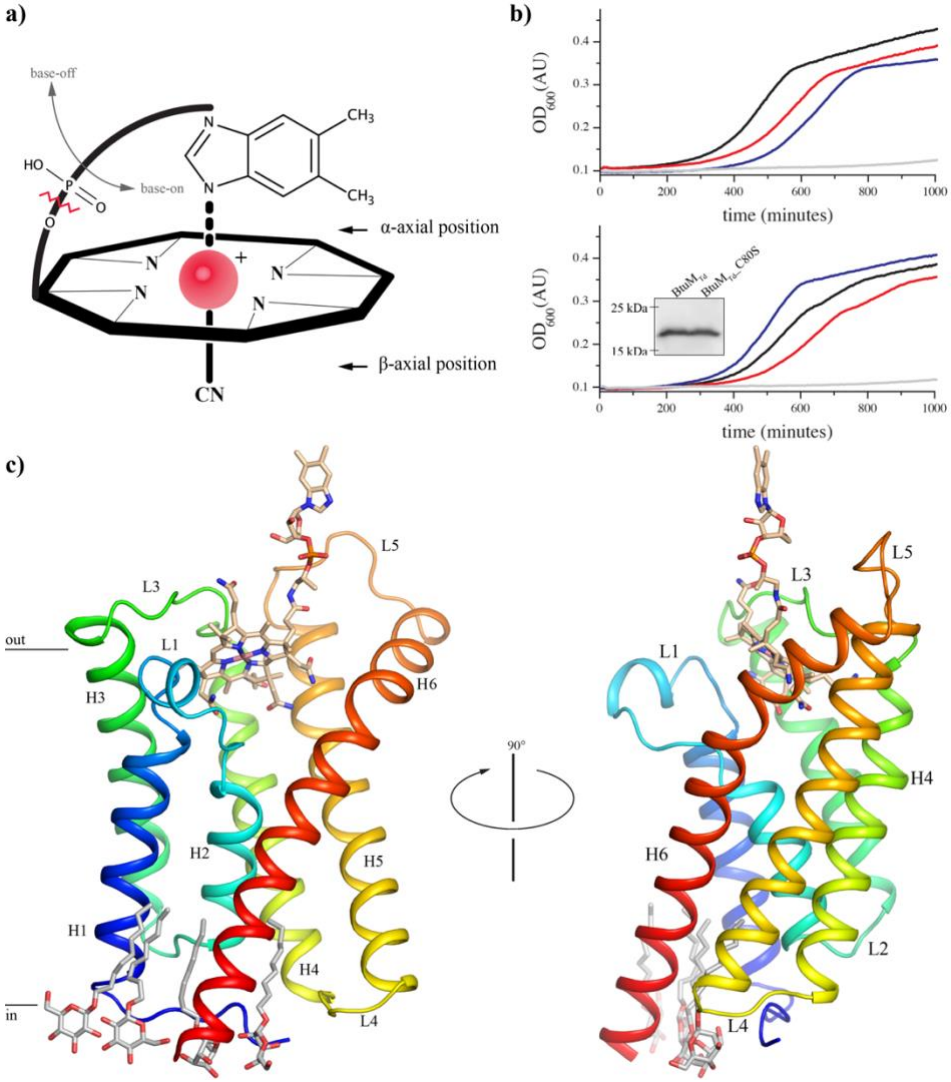

membrane proteins of ~22 kDa, and found predominantly in Gram-negative species, distributed mostly over α-, β-, and γ-proteobacteria (**Suppl. Data 1**).

Here, we sought to characterize the predicted vitamin B12 transporter BtuM from *Thiobacillus denitrificans* ($BtuM_{Td}$). We show that $BtuM_{Td}$ is involved in transport of Cbl *in vivo* and we solved its structure to 2 Å resolution. A cobalt-cysteine interaction allows for chemical modification of the substrate prior to translocation, which is a rare feature among uptake systems.

Results

BtuM$_{Td}$ supports vitamin B12 dependent growth

To test experimentally whether BtuM$_{Td}$ is a potential Cbl-transporter we constructed an *Escherichia coli* triple knockout strain, *E. coli* ΔFEC, based on Cadieux *et al.* (8). In this strain, the gene encoding the Cbl-independent methionine synthase, MetE (9), is deleted. The *metE* deletion makes it impossible for *E. coli* ΔFEC to synthesize methionine, unless it can import Cbl 8, 9). In that case, L-methionine can be synthesized using the Cbl-dependent methionine synthase, MetH (3, 8). *E. coli* ΔFEC has additional deletions in *btuF* and *btuC*, encoding subunits of the endogenous Cbl-transporter BtuCDF (7, 8). Therefore, *E. coli* ΔFEC cannot import Cbl, prohibiting MetH-mediated L-methionine synthesis. Consequently, *E. coli* ΔFEC can grow only if L-methionine is present or if vitamin B12 import is restored by (heterologous) expression of a Cbl-transport system (8). The phenotype of *E. coli* ΔFEC was confirmed in growth assays (**Suppl. Figure 2a**). Cells that are not expressing any Cbl-transporter did not exhibit substantial growth in methionine-free medium, whereas cells complemented with an expression plasmid for BtuCDF grew readily (**Figure 1b**). Cells expressing BtuM$_{Td}$ had a similar growth phenotype, indicating that BtuM$_{Td}$ is a potential transporter for vitamin B12 (**Figure 1b**).

Crystal structure of BtuM$_{Td}$ bound to vitamin B12

The BtuM family contains an invariably conserved cysteine residue (**Suppl. Figure 3a**). In BtuM$_{Td}$ this cysteine is located at position 80, and mutation to serine abolishes the ability of the protein to complement the *E. coli* ΔFEC strain (**Figure 1b**). To investigate the role of the cysteine we solved a crystal structure at 2.0 Å resolution of BtuM$_{Td}$ in complex with Cbl. Data collection as well as refinement statistics are summarized in **Table 1**. BtuM$_{Td}$ consists of six transmembrane helices with both termini located on the predicted cytosolic side (**Figure 1c**). The amino acid sequences of BtuM proteins are not related to any other protein (5) but, surprisingly, BtuM$_{Td}$ resembles the structure of S-components from energy-coupling factor (ECF)-type ABC-transporters (10) (**Suppl. Figure 4 and Suppl. Table 1**). In contrast to BtuM proteins, ECF-type ABC

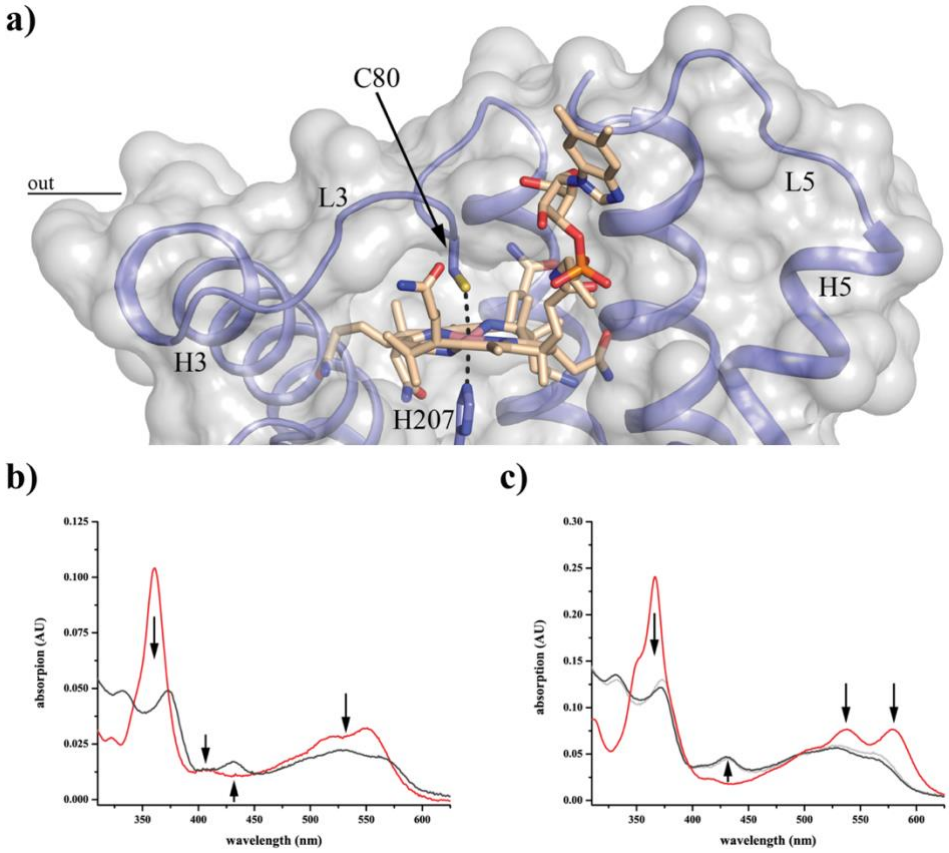

Figure 2: Binding of vitamin B12 by BtuM$_{Td}$. a) Transparent surface representation (light grey) of the binding pocket of BtuM$_{Td}$ with bound Cbl. The protein backbone is shown in blue. The Co-ion is coordinated by Cys80 located in L3 (Co-ion to sulphur distance 2.7 Å) and His207 (Co-ion to nitrogen distance 2.4 Å) from a neighboring symmetry mate (**Suppl. Figure 6**). A complete description of the interactions of BtuM$_{Td}$ with its substrate can be found in **Suppl. Figure 11**. b) The spectrum of BtuM$_{Td}$_cHis8-bound Cbl (4.3 μM, black line) compared to unbound cyano-Cbl (2.4 μM, red line). The regions of the spectrum with major changes are indicated with arrows. c) Same as b) but with Cbi bound to the protein (9.2 μM black line), compared to unbound dicyano-Cbi (9.0 μM, red line). The regions of the spectrum with major changes are indicated with arrows. For comparison, a scaled spectrum of Cbl bound to BtuM$_{Td}$_cHis8 (light grey line) from b) is included showing that the spectrum of both substrates bound to the protein is virtually the same, indicating the same binding mode.

transporters are predominantly found in Gram-Positive bacteria. They are multi-subunit complexes consisting of two peripheral ATPases and two transmembrane components (EcfT and S-component) (10, 11). EcfT and the ATPases together form the so-called ECF-module. S-components bind the transported substrate, and dynamically associate with the ECF module to allow substrate translocation (10, 12–14). Intriguingly, no homologs of

EcfT could be found in *T. denitrificans*. In addition, all ABC-type ATPases encoded by the organism are predicted to be part of classical ABC transporters, and not ECF transporters. Therefore, we conclude that the organism does not encode an ECF-module, and hypothesize that solitary $BtuM_{Td}$ may be responsible for Cbl uptake. This hypothesis is supported by the ability of $BtuM_{Td}$ to potentially transport vitamin B12 when expressed heterologously in *E. coli* ΔFEC. Importantly, *E.coli* also does not encode an ECF module (11), hence $BtuM_{Td}$ cannot interact with a module from the host, and $BtuM_{Td}$ must be able to support Cbl uptake using a different mechanism than that of ECF transporters (10, 11). In a few cases, the biotin-specific S-component BioY (15) has also been found in organisms lacking an ECF module and was shown to mediate transport without the need for an ECF-module (15). However, organisms encoding only BioY without an ECF module are rare (15), and in the large majority of organisms BioY is associated with an ECF module (11). In contrast, BtuM homologs (but one exception) are found exclusively in organisms lacking an ECF-module (**Suppl. Data 1**).

Table 1: Data collection, phasing and refinement statistics.

	Cbl-bound $BtuM_{Td}$ native	**Cbl-bound $BtuM_{Td}$ anomalous**
Data collection		
# crystals/# datasets	1/1	1/2
Space group	P 31 2 1	P 31 2 1
Unit cell dimensions		
a, *b*, *c* (Å)	87.54, 87.54, 97.91	86.60, 86.60, 97.51
α, *β*, *γ* (°)	90.0, 90.0, 120.0	90.0, 90.0, 120.0
Resolution range (Å)	41.13 - 2.01 (2.082 - 2.01) [a]	43.30 - 2.50 (2.5896 - 2.5002) [a]
R_{merge} (%)	5.8 (>100) [a]	10.8(>100) [a]
$cc_{1/2}$	100.0 (14.1) [a]	99.9 (50.8) [a]
$I/\sigma I$	16.24 (0.23) [a]	18.23 (1.53) [a]
Completeness (%)	99.9 (99.8) [a]	93.82 (64.7) [a]
Redundancy	10.5 (9.7) [a]	18.8 (11.0) [a]
Refinement		
Resolution (Å)	41.13 - 2.01	43.30 - 2.50
No. of reflections	28953	14144
R_{work}/R_{free}	0.2121/0.2338	0.2492/0.2854
Number of non-hydrogen atoms	1870	1536
Protein	1640	1359
Ligands	208	177
Water	22	0
***B*-factors**		
Protein	89.0	67.2
Cobalamin	65.4	69.3
PEG	106.2	–
Detergent	107.1	–
Water	69.2	–
R.m.s. deviations		
Bond lengths (Å)	0.009	0.009
Bond angles (°)	1.81	1.916

[a]Values in parentheses are for the highest-resolution shell.

Further experiments, for instance using purified protein reconstituted in proteoliposomes, are required to test whether $BtuM_{Td}$ also catalyzes transport *in vitro* without any additional component involved. However, the *in vivo* assay gives a very strong indication that $BtuM_{Td}$ is a transporter itself, as the protein was expressed in a heterologous host that does not contain any ECF module or S-component. Similar *in vivo* experiments have been used extensively in the past to identify other transporters (for instance ref. (16)) and have the advantage over *in vitro* assays that physiologically relevant conditions are used.

$BtuM_{Td}$ binds cobalamin using cysteine ligation

Close to the predicted periplasmic surface of $BtuM_{Td}$ we found well-defined electron density (**Suppl. Figure 5**) representing a bound Cbl molecule. The binding mode of Cbl in the crystal structure (**Figure 2a**) is striking for two reasons. First, the essential Cys80 is the α-axial ligand of the cobalt ion. To our knowledge, cobalt coordination by cysteine has not been observed in any other Cbl-binding protein of known structure. Binding of cysteine to cobalt in a corrinoid has been hypothesized for the mercury methylating enzyme HgcA (17) and observed in a synthetic cyclo-decapeptide, but in the latter case the residue replaced the β-ligand (18).

Second, Cbl is bound to $BtuM_{Td}$ in the base-off conformation in which the 5,6-dimethylbenzimidazole moiety does not bind to the cobalt ion (**Figure 2a**). In contrast, at physiological pH the conformation of free Cbl in aqueous solution is base-on with the 5,6-dimethylbenzimidazole moiety coordinated to the cobalt ion in the α-axial position (1) (**Figure 1a**). The base-off conformation has been found only in a subset of Cbl-containing enzymes, but not in Cbl-binding proteins without enzymatic activity (1), such as the periplasmic substrate binding protein BtuF (19), the outer membrane transporter BtuB (20), and human Cbl-carriers intrinsic factor (21), haptocorrin (22), and transcobalamin (23). Enzymes that bind Cbl with the base-off conformation usually use a histidine residue as the α-axial ligand. In this way, the reactivity of the cobalt at the β-axial position is altered, allowing among others a variety of methyl-group transfer reactions (1). Therefore, the base-off binding mode by BtuMTd could indicate that the protein may exhibit enzymatic activity.

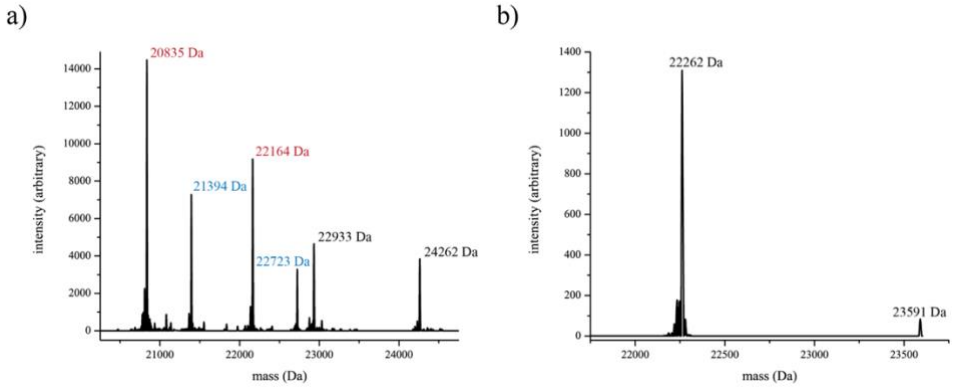

Figure 3: Mass spectrometry analysis of BtuM$_{Td}$_cHis8 and BtuM$_{Td}$_cEPEA bound to co-purified Cbl showing the loss of the β-ligand. a) BtuM$_{Td}$_cHis (native mass of 22905 Da) bound to Cbl yields multiple peaks. These peaks can be separated into three pairs of which the higher mass corresponds to the substrate-bound protein and the lower mass to the *apo* form. The mass differences are 1329 Da, which corresponds to the mass of Cbl without β-ligand. The masses labelled in black (22933 Da and 24262 Da) are the native protein with a formylated first methionine (adding 28 Da). The pair labelled in red (20835 Da and 22164 Da) and the pair labelled in blue (21394 Da and 22723 Da) correspond to truncated forms with loss of a 2098 Da C-terminal peptide (red) and 1539 Da C-terminal peptide (blue). The amino acid sequences of the lost peptides of the truncated versions are LMGTRRERHHHHHHHHH (red) and RERHHHHHHHH (blue). 3b) BtuM$_{Td}$_cEPEA (native mass 22234 Da) also shows the loss of the β-ligand . We observe the mass for formylated *apo* protein (22262 Da) and formylated substrate-bound protein (23591 Da). The difference between the two (1329 Da) is the mass of decyanated Cbl.

BtuM$_{Td}$ catalyzes decyanation of vitamin B12

Indeed, the structure of BtuM$_{Td}$ suggests that the protein can catalyze chemical modification of the substrate. We co-crystallized BtuM$_{Td}$ with cyano-Cbl, which contains a cyano-group as the β-ligand (1, 4). Cyano-Cbl is the most stable form of vitamin B12 (4) but, despite the tight binding of the β-ligand, in the crystal structure the cyano group is absent indicating protein-mediated decyanation. Consistent with decyanation and the presence of a cysteine ligand in BtuM$_{Td}$, the absorbance spectrum of Cbl-bound BtuM$_{Td}$ showed pronounced differences compared to that of free Cbl (18, 24) (**Figure 2b**). The characteristic absorption peak at 361 nm of Cbl is absent and two peaks with lower absorption appear around 330 nm and 370 nm. The absorption between 500 nm and 580 nm is lower than in free Cbl, and a new peak at 430 nm is present.

In place of the cyano-group the imidazole group of His207 from a neighboring BtuM$_{Td}$ molecule in the crystal is located at the β-axial position. His207 is the last histidine residue of the His$_8$ affinity-tag (His-

tag) engineered at the C-terminus of the protein (**Suppl. Figure 6**). Because crystal contacts may be non-physiological and the His-tag is a non-natural addition to the protein, we performed control experiments to exclude the possibility that decyanation is an artefact. First, we showed by mass spectrometry (MS) that the loss of the cyanide does not require crystal formation (**Figure 3a**). Second, we showed that decyanation also occurred by BtuM$_{Td}$ with a C-terminal Glu-Pro-Glu-Ala (EPEA)-tag instead of a His-tag (**Figure 3b**). Notably, the EPEA-tagged protein was active in the growth assay and also removal of the His-tag did not affect activity (**Suppl. Figure 2b and c).** Finally, binding of Cbl to BtuM$_{Td}$ with His-tag or EPEA-tag was accompanied by the same changes in absorption spectrum (**Figures 2b and 3b**). Therefore, we conclude that decyanation takes place regardless of crystal formation or presence of a His-tag.

Kinetics of the BtuM$_{Td}$ catalyzed decyanation reaction

To study the kinetics of BtuM$_{Td}$-catalyzed decyanation we used cobinamide (Cbi) instead of Cbl as substrate. Because Cbi does not contain the 5,6-dimethylbenzimidazole moiety (**Figure 1a**), it mimics the base-off conformation of cobalamin, which makes the compound suitable to study decyanation without interference from the slow conversion (25) of base-on to base-off Cbl. The absorption spectra of Cbl-bound and Cbi-bound BtuM$_{Td}$ are almost identical (**Figure 2c**), indicating identical coordination of the cobalt ion of Cbi at the α-axial and β-axial positions. MS analysis showed that binding of Cbi to BtuM$_{Td}$ also results in decyanation (**Suppl. Figure 7a**). To probe Cbi binding by BtuM$_{Td}$ we used isothermal titration calorimetry (ITC), which revealed dissociation constants for the His-tagged and EPEA-tagged protein of 0.65 ± 0.27 μM and 0.58 ± 0.13 μM (s.d. of the mean of technical triplicates), respectively (**Figure 4a**). It is noteworthy that we were unable to assay for Cbl-binding by ITC. We speculate that the conversion from base-on to base-off Cbl is so slow (25) that it may prevent detection of Cbl-binding by ITC. Additionally, the absence of the membrane environment also appears to preclude Cbl binding to purified BtuM$_{Td}$, as binding was observed only when the substrate was added before solubilization (**Figure 2b, c and Suppl. Figure 8**).

Because binding of cyanide to cobinamide causes a decrease in absorbance at 330 nm and an increase at 369 nm (24), we expected the opposite spectral changes upon decyanation. Addition of excess of *apo*-BtuM$_{Td}$

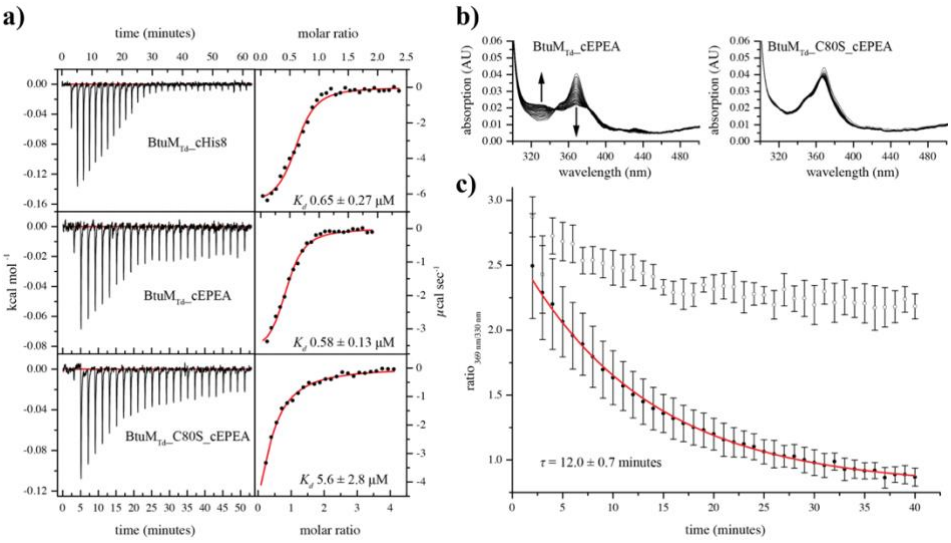

Figure 4: Cobinamide (Cbi) binding to BtuM$_{Td}$ and BtuM$_{Td}$-catalyzed decyanation. a) Representative ITC measurements of differently tagged BtuM$_{Td}$ constructs. BtuM$_{Td}$ with a C-terminal His-tag binds Cbi with a K_D value of 0.65 ± 0.27 µM (top). EPEA-tagged BtuM$_{Td}$ binds Cbi with essentially the same affinity of K_D 0.58 ± 0.13 µM (middle). For the EPEA-tagged mutant version BtuM$_{Td}$_C80S K_D = 5.6 ± 2.8 µM (bottom). All ITC experiments were performed as technical triplicates, error is s.d. b) Decyanation of Cbi catalyzed by EPEA-tagged BtuM$_{Td}$. Upon addition of an excess of BtuM$_{Td}$ to dicyano-Cbi, the substrate is slowly decyanated, which can be followed spectroscopically (left) with the main spectral changes indicated by the arrows. The mutant BtuM$_{Td}$_C80S, did not catalyze decyanation (right). c) Quantification (error bars are s.d. of technical triplicates) of decyanation reveals that the process is slow. The ratio of the absorption at 369 nm over 330 nm of BtuM$_{Td}$ (black dots) was plotted as function of time. A mono-exponential decay function was fitted to the data (red line) to extract τ = 12.0 ± 0.7 minutes (s.d. of technical triplicates), which is comparable to the decyanation rate of the His-tagged protein and the process follows pseudo-first order kinetics (**Suppl. Figure 7b and c**). The ratio of absorption obtained with the cysteine mutant (open dots), which does not catalyze decyanation, is shown for comparison.

(**Suppl. Figure 9a and b**) to a solution of Cbi indeed revealed time-dependent changes in absorbance consistent with a decyanation reaction (**Figure 4b and c**). Decyanation occurred with an apparent time constant of τ = 12.0 ± 0.7 minutes (s.d. from technical triplicates, **Figure 4c**), which is comparable to the rate observed in the human decyanating enzyme CblC (25, 26). We also tested Cbi binding and decyanation using mutant proteins C80A and C80S. While these mutants were unable to bind Cbl, they remained capable of binding Cbi as demonstrated by co-purification of the molecule with the protein (**Suppl. Figure 9c and d**). We measured the affinity of BtuM$_{Td}$_C80S to Cbi with ITC and found a dissociation constant of 5.6 ± 2.8 µM (s.d. of the mean of technical triplicates), which is an order of magnitude weaker than the wild-type (WT) protein. The

absorbance spectra of Cbi bound to the mutant proteins showed the characteristic features for cyano-Cbi, indicating that decyanation was abolished (**Suppl. Figure 9c and d**). Consistently, the decyanation assay with $BtuM_{Td}$_C80S did not reveal the slow spectral changes observed for the WT protein (**Figure 4b and c**). These results show that Cys80 is required for decyanation of Cbi and that binding and modification of this substrate are separate events: fast binding (detected by ITC) is followed by slow modification. The lack of detectable binding of Cbl to $BtuM_{Td}$_C80S (measured by lack of co-purification, **Suppl. Figure 9c and d**) may indicate that the cysteine is also required for base-on to base-off conversion, and that the base-on conformer binds with too low affinity for detection by co-purification. To understand $BtuM_{Td}$-catalyzed decyanation of Cbl and Cbi in more detail, we mutated conserved amino acids H28, D67, Y85, and R153 located in the binding pocket (**Suppl. Figure 3b**). Mutant D67A could not be purified, and was not analyzed further. Cbl-bound mutants H28A, Y85L, and R153A displayed the same spectral properties as the WT protein (**Suppl. Figure 10a**), and MS analysis showed that the binding of Cbl was accompanied by decyanation, indicating that the conserved residues are not essential for the reaction (**Suppl. Figure 10b-d**). Finally, to exclude that $BtuM_{Td}$ is merely a decyanating enzyme, and that the reaction product hydroxyl-Cbl is subsequently transported by another protein, we show that $BtuM_{Td}$ also mediates uptake of hydroxyl-Cbl in the growth assay (**Suppl. Figure 2d and e**).

Discussion

We showed *in vivo* that $BtuM_{Td}$ is a vitamin B12 transporter, which is consistent with the predictions based on bioinformatics analysis (5). Our work sheds light on the diversity of transport systems used for the uptake of vitamin B12. The outer membrane transporter BtuB is a TonB-dependent active transporter, which uses a different mechanism of transport than inner membrane proteins (1, 20). The well-studied inner membrane type II ABC transporter BtuCDF uses hydrolysis of ATP to pump Cbl into the cell like the ECF-transporter, ECF-CbrT (27). Both systems require a substrate binding protein and are multiprotein

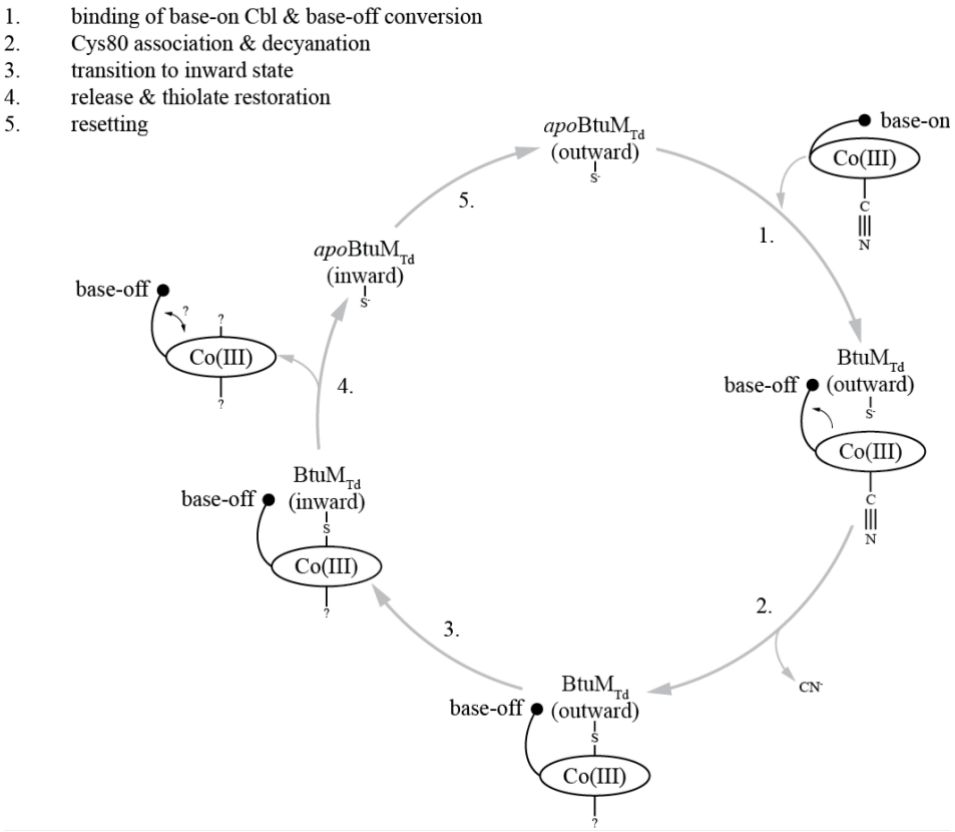

Figure 5: Proposed mechanism for of BtuM$_{Td}$ catalyzed decyanation of Cbl. Decyanation of the substrate that is in its base-on conformation at physiological pH in the periplasm with a trivalent Co-ion, binds to BtuM$_{Td}$ with its binding pocket exposed to the extracellular side (step 1). The cysteine replaces the α-ligand. We assume that the side chain of Cys80 is in its thiolate form allowing it to donate one electron to allow for a simple one-step reductive decyanation (step 2). We propose that the Co ion remains in its trivalent state (hexa-coordinate) throughout the reaction. We hypothesize that release of Cbl on the intracellular side (step 3) of the membrane and breaking of the Co-S bond is achieved by the reducing environment of the cell allowing the Cys80 to return in its thiolate state (step 4) making it accessible to undergo another reaction once the membrane protein has transitioned back to the outward facing conformation (step 5).

complexes (7, 8, 27, 28). BtuM$_{Td}$ on the other hand, must operate by a different mechanism because the protein lacks accessory components and the expected ATPase motifs of ABC transporters (10). BtuM$_{Td}$ structurally reassembles the S-components of ECF transporters. In ECF-transporters the S-components bind the transported substrate with high affinity and then associate with an ECF module for energizing transport. During the transport cycle, the S-components rotate (‘topple over’) in the membrane to bring the substrate from the outside to the cytoplasm. We hypothesize that BtuM$_{Td}$ mediates the translocation of Cbl through the membrane by a

similar toppling mechanism. Because $BtuM_{Td}$ does not require an ECF module, the transport mode may be facilitated diffusion along the concentration gradient of the substrate. In *T. denitrificans* and most other BtuM hosts, the $BtuM_{Td}$ gene co-localizes with *btuR*, which encodes for the cobalamin adenosyltransferase BtuR. This enzyme catalyzes the synthesis of 5'deoxyadenosyl-cobalamin and would offer a mechanism of metabolic trapping similar to what has been proposed for other vitamin transporters in bacteria (29).

Our work provides experimental evidence for a binding mode of Cbl, in which cysteine ligation and the base-off conformation are linked. This binding mode leads to decyanation of cyano-Cbl, for which we propose a reductive decyanation mechanism, which depends on Cys80 (17, 18) (**Figure 5**). The proposed decyanation mechanism differs from the mechanism used by CblC, where a flavin acts as reducing agent. In CblC the flavin donates two electrons resulting in the reductive decyanation (CN^-) and the reduction of the Co-ion (25, 26). For $BtuM_{Td}$, cysteine-catalyzed reductive decyanation would only result in the release of CN^-, but not in the reduction of the Co-ion.

Finally, $BtuM_{Td}$ likely combines two functions: transport of the substrate into the bacterial cell, and chemical modification of the substrate. Such combined functionality rarely occurs in transporters, and has been observed only in phosphotransferase systems (30). However, in that case the modification (phosphorylation) takes place on the cytoplasmic side of the membrane (30), whereas $BtuM_{Td}$ appears to modify on the periplasmic side of the membrane. Internalization of decyanated vitamin B12 may be relevant because environmental cyano-Cbl exists (26). A combination of decyanation and transport activity would make cyano-Cbl directly accessible for conversion into physiological forms, for example, by BtuR.

Materials and Methods

Bioinformatic identification of BtuM homologs & ECF-modules

The amino acid sequence of $BtuM_{Td}$ was used as a search query using the iterative jackHMMer algorithm (default settings) with the reference proteome database (31) until the search converged leading to 131 hits.

Within the genomes of the identified 131 organisms we screened for the presence of an ECF-module using the pHMMer algorithm (default settings) (31) with the amino acid sequence of the transmembrane component (ECF-T) from *Lactobacillus delbrueckii* (14) as a search query. Additionally, we used the SEED viewer (www. http://pseed.theseed.org) to verify the absence of any ECF-transporter in a subset of organisms (46 present in the SEED database) and also used this tool to find all ABC transporters in *T. denitrificans* to verify that none of these are an ECF-transporter.

Molecular Methods

For expression in *E. coli* MC1061 (32) a codon optimized version (Invitrogen) of *btuM* (Tbd_2719) from *Thiobacillus denitrificans* ATCC25259 with a C-terminal eight histidine affinity-tag or EPEA-tag was used and introduced into pBAD24 (33) with *NcoI* and *HindIII* restriction sites. A single glycine (Gly2) was introduced to be in-frame with the start-codon of the *NcoI* restriction site. Single amino acid substitutions and removal of the affinity tag were conducted using site directed mutagenesis. The complementation plasmid for expression of BtuC and BtuF was constructed using Gibson Assembly following the standard procedure (NEB). All constructs were checked for correct sequences by DNA sequencing. All primers are listed in **Suppl. Table 2**.

Construction of the ΔFEC strain

E. coli ΔFEC, was constructed by P1-mediated generalized transduction (27, 34, 35). In short: *E. coli* JW0154 (*ΔbtuF::Km*^{R}) was used as the basis for construction of *E. coli* ΔFEC. The kanamycin resistance cassette was removed using the FLP recombinase (36). The *metE::Km*^{R} locus from *E. coli* JW3805 and the *ΔbtuC::Km*^{R} locus of *E. coli* JW1701 was introduced (34, 35), resulting in *E. coli* ΔFEC (*ΔbtuF, ΔmetE, ΔbtuC::Km*^{R}). Colony PCRs based on three primer pairs (27) were used to verify *Km*^{R}-insertions, FLP-recombinase-mediated removal of *Km*^{R}-markers, and absence of genomic duplications.

Growth assays

The strains carrying various expression vectors were grown overnight at 37°C on LB-agar plates supplemented with 25 μg ml^{-1} kanamycin and 100

μg ml^{-1} ampicillin. M9 minimal medium (47.7 mM $Na_2HPO_4 \times 12H_2O$, 17.2 mM KH_2PO_4, 18.7 mM NH_4Cl, 8.6 mM NaCl) was supplemented with 0.4% glycerol, 2 mM $MgSO_4$, 0.1 mM $CaCl_2$, 100 μg ml^{-1} L-arginine, 25 μg ml^{-1} kanamycin and 100 μg ml^{-1} ampicillin. A single colony was picked and used to inoculate an M9-medium pre-culture supplemented with 50 μg ml^{-1} L-methionine (Sigma-Aldrich). The pre-culture was grown ~24 hours at 37°C, shaking in tubes with gas-permeable lids (Cellstar), and then used to inoculate the assay medium in a 1:500 ratio. The assay medium was supplemented with 0.00001% L-arabinose (Sigma-Aldrich) and either 50 μg ml^{-1} L-methionine, 0.01 nM, 1 nM and 5 nM cyano-cobalamin (Acros Organics), or 0.1 nM hydroxy-cobalamin (Sigma-Aldrich). 200 μl medium was added per well of a sterile 96 well-plate (Cellstar). Plates were sealed with a sterile and gas-permeable foil (BreatheEasy, Diversified Biotech). The cultures were grown for 1,000 minutes (1250 minutes for Cbi) in a BioTek Power Wave 340 plate reader at 37°C, shaking. The OD_{600} was measured every five minutes at 600 nm. All experiments were conducted as technical triplicates from biological triplicate. The displayed growth curves are the averages of all nine curves.

Western blotting

Cells grown in LB-medium were broken in 50 mM K-P_i pH 7.5 supplemented with 10% glycerol, 1 mM $MgSO_4$, 1 mM phenylmethylsulfonyl fluoride (PMSF) and DNaseI with glass beads in a tissue lyser at 50 hertz. The lysate was centrifuged for 10 min at 20,000×*g* and 4°C and the supernatant was used for further analysis. The samples analyzed by SDS-polyacrylamide gel electrophoresis followed by semi-dry western blotting. The primary antibody was mouse anti-Tetra·His Antibody, BSA-free from Qiagen (Cat.No. 34670) and the secondary antibody was anti-mouse IgG (whole molecule)−alkaline phosphatase conjugate antibody from Sigma Aldrich (Cat.No. A1902-1ML). The dilutions were 1:2,000 and 1:10,000, respectively. The full length blot from **Figure 1b** is included (**Suppl. Figure 2h**)

Overexpression and crude membrane vesicle preparation

All $BtuM_{Td}$ variants were overexpressed in *E. coli* MC1061. Overnight pre-cultures in LB-medium supplemented with 100 μg ml^{-1} ampicillin were diluted in a 1:100 ratio and allowed to grow at 37°C to an OD_{600} of 0.6 – 0.8. Expression was induced by addition of 0.05% L-arabinose for

three hours. Cells were harvested, washed with 50 mM K-P_i pH 7.5, and broken with a Constant Systems cell disruptor at 25 kpsi in 50 mM K-P_i pH 7.5 supplemented with 200 µM PMSF, 1 mM $MgSO_4$ and DNaseI. Cell debris were removed by centrifugation for 30 min with 25,805×*g* and 4°C. The supernatant was centrifuged for 2.5 hours at 158,420×*g* (average) and 4°C to collect crude membrane vesicles (CMVs). The CMV pellet was homogenized in 50 mM K-P_i pH 7.5 and used for purification.

Purification of $BtuM_{Td}$ for crystallization

His-tagged BtuM for crystallization was solubilized in buffer A (50 mM HEPES/NaOH pH 8.0, 300 mM NaCl, 0.05 mM cyano-Cbl, 1% n-dodecyl-β-maltoside (DDM) and 15 mM imidazole/HCl pH 8.5) for 45 minutes at 4°C with gentle movement. Insolubilized material was removed by centrifugation for 35 minutes at 219,373×*g* (average) and 4°C. The supernatant was decanted into a poly-prep column (BioRad) containing 0.5 ml bed volume superflow Ni^{2+}-NTA sepharose (GE healthcare) equilibrated with 20 column volumes (CV) buffer A containing additionally 3 mM dithiotreitol (DTT) and incubated for one hour at 4°C with gentle movement. Unbound protein was allowed to flow through and the column was washed twice with ten CV buffer A supplemented with 3 mM DTT and 0.35% n-nonyl-β-D-glucopyranoside (NG) and 60 mM or 90 mM imidazole/HCl pH 8.5. Bound protein was eluted from the column in four fractions of 0.5 ml (first) – 0.7 ml (others) with buffer A supplemented with 3 mM DTT 0.35% NG and 350 mM imidazole/HCl pH 8.5. The sample was centrifuged for five minutes at 20,000×*g* and 4°C to remove aggregates, and then loaded on a SD200 10/300 Increase SEC column (GE healthcare), which was equilibrated with 30 ml buffer B 50 mM HEPES/NaOH pH 8.0, 100 mM NaCl, 0.005 mM cyano-Cbl and 0.35% NG) and eluted in the same buffer while monitoring absorption at 280 nm and 361 nm.

Purification of His-tagged $BtuM_{Td}$

Purification of His-tagged protein for biochemical analyses was essentially performed as described above with the following adaptations. HEPES was replaced with 50 mM K-P_i pH 7.0 or 7.5 (for ITC and spectral analyses, respectively), NG was replaced with 0.04% DDM, and 100 mM NaCl was used throughout. For purification of the *apo* protein substrate

was omitted from all buffers. For spectral analyses of substrate-bound proteins substrate was omitted from buffer B.

Purification of EPEA tagged $BtuM_{Td}$

EPEA-tagged protein was purified as described above with the following adaptations. CaptureSelect™ C-tagXL Affnity Matrix (Thermo Fisher Scientific) was used. DTT and imidazole were omitted in all steps and 50 mM Tris/HCl pH 7.5 was used instead of K-P_i. The column was washed once with 10 CV buffer supplemented with 500 mM $MgCl_2$. Elution was done in four fractions of 0.5 (first) ml – 0.8 ml (others) in buffer containing 2 M $MgCl_2$.

Crystallization and phasing and structure determination

$BtuM_{Td}$ purified for crystallization was concentrated to between 1.1 mg ml^{-1} to 1.6 mg ml^{-1} with a 10,000 kDa cut-off Vivaspin concentrator (Sartorius) at 4,000×*g* at 2°C. The initial screening was done using a Mosquito robot (TTP Labtech), and a hit was found after one month in the H1 condition (50 mM Tris pH 8.5, 28% (v/v) PEG400) of the MemGold2 screen (Molecular Dimensions) at 4°C. Larger and better diffracting pyramid-shaped crystals were obtained at 8°C after three to four weeks in a crystallization buffer containing 25 mM Tris pH 8.5 and 25% to 30% (v/v) PEG400, 50 mM Tris pH 8.5 and 27% to 30% (v/v) PEG400 or 75 mM Tris pH 8.5 and 29% to 30% (v/v) PEG400, using the sitting drop vapor diffusion method (in MRC Maxi 48-well plate) and a 1:1 mixing ratio (2 µl final drop volume) of mother liquor and protein solution. Phases were obtained from crystals that were soaked for one minute with 100 mM Tb-Xo4 (37) (Molecular Dimensions) mother liquor solution (0.5 µl added directly to the drop). Diffraction data of the native crystals were collected at the Swiss Light Source (SLS) at PXI (X06SA) beamline (λ = 1.000 Å, T = 100 K) and two anomalous diffraction data sets were collected at the European Synchrotron Radiation Facility (ESRF) at beamline ID23-1 (λ = 1.400 Å and 1.476 Å, T = 100 K). Data were processed with XDS (38) and the two datasets containing anomalous information were merged and subsequently used to solve the structure with ShelX (39). Autobuild (40) was used to obtain a starting model, which was refined further with Phenix refine (41) with manual adjustments done in Coot (42). The model was used as an input to solve the phase problem for the native dataset, which was carried out with Phaser-MR (43). The model of the native data was

refined iteratively with Phenix refine (41) and manual adjustments were done in Coot (42). The Ramachandran statistics for the final model are 99.47% for favored regions, 0.53% for allowed regions and 0.00% for outliers. A stereo view of 2Fo–Fc electron density of the entire structure including the backbone trace molecule, the binding pocket and the Cbl-ligand is provided in **Suppl. Figure 5a-c**, respectively. All structural figures were prepared with an open-source version of pymol (https://sourceforge.net/projects/pymol/).

UV-Vis assay to determine decyanation of vitamin B12

All measurements were carried out in a Cary100Bio spectrophotometer (Varian) at room temperature and baseline corrected for buffer B in a quartz cuvette. To monitor the binding of dicyano-Cbi or cyano-Cbl by $BtuM_{Td}$ over time, every minute a spectrum was recorded between 260 nm and 640 nm for 40 minutes (Cbi, n = 3) or every 20 minutes for 12 hours (Cbl, n = 1)) at room temperature. For this measurement, a molar protein to substrate ratio of 5:1 (Cbi) or 1:1 (Cbl) was used. To obtain the apparent time constant, τ, the absorbance ratio of 369/330 nm was plotted against the time and fitted with a single exponential decay function in Origin 8. Decyanation assays with Cbi were conducted as technical triplicates and errors are standard deviations of the averaged ratios (if not specified otherwise).

ITC measurement with Cbi

Binding of dicyano-Cbi to purified $BtuM_{Td}$ was measured on a microcal200 ITC (GE healthcare) in high feedback mode. The cell temperature was set to 25°C with a reference power of 9.5 µcal sec^{-1}. During the measurement, the sample was stirred at 750 rpm and a 15-fold excess (WT) or 32.5-fold excess (C80S) of Cbi in the syringe was used over the protein concentration in the cell. The data was analyzed in Origin and experiments were done as technical triplicates (n = 3). The obtained dissociation constants were averaged and the error is the standard deviation of the replicates.

Mass spectrometry

$BtuM_{Td}$ variants and mutant proteins were purified as described above. $BtuM_{Td}$ proteins were diluted in a 1:1 (v/v) ratio with 0.1% formic acid

and 5 µl were injected into an Ultimate 3000-UPLC system (Dionex), connected to a Q-Exactive mass spectrometer (Thermo Fisher Scientific) and separated on a 2.1mm x 50mm Acquity UPLC BEHC18, 1.7 µm (Waters). Solvent A was H_2O with 0.1% formic acid and solvent B was acetonitrile with 0.1% formic acid. The following mobile phase gradient was delivered at a flow rate of 0.6 ml/min starting with a mixture of 60% solvent B for 1 minute. Solvent B was increased to 90% over 5 minutes with a linear gradient and kept at this concentration for 5 minutes. Solvent B was reduced to 60% in 0.1 minute and kept for 3.9 minutes resulting in a total elution time of 15 minutes. The column temperature was kept constant at 40°C. The mass spectrometer was operated in positive mode. Full scan MS spectra were acquired for 10 minutes from m/z 1000 to 2000 at a target value of 1×10^6 and a max IT of 500 ms with a resolution of 140000 at m/z 200. Scans were averaged using Xcalibur 4.0.27.42 Qualbrowser and the isotopically resolved MS spectrum was de-convoluted using the built-in Xtract algorithm.

Data availability

Data supporting the findings of this manuscript are available from the corresponding author upon reasonable request. Atomic coordinates and structure factors for the crystal structure of $BtuM_{Td}$ have been deposited in the Protein Data Bank under the accession code 6FFV. The mass spectrometry data has been deposited to the ProteomeXchange Consortium via the PRIDE partner repository with the dataset identifier PXD010024.

Acknowledgements

We appreciate the helpful advice from Dr. Stephanie Ruiz with the practical setup and analysis of the growth assay, we thank Dr. M. Majsnerowska (University of Groningen) for help with the construction of the EPEA-tag expression plasmids, and we would like to thank Prof. Dr. A.J.M. Driessen (University of Groningen) for the use of the ITC. We acknowledge the excellent advice, support and experimental work of the Interfaculty Mass Spectrometry Center at the Faculty of Science and Engineering of the University of Groningen. This work was supported by the European Molecular Biology Organization (EMBO; EMBO Short

Term Fellowship ASTF-382-2015 to S. Rempel), the Netherlands Foundation for the Advancement of Biochemistry (SSBN; SSBN Travel Grant to S. Rempel), the Netherlands Organization for Scientific Research (NWO Vici grant 865.11.001 to D.J. Slotboom), and the European Research Council (ERC; ERC Starting Grant 282083 to D.J. Slotboom). For technical support, we acknowledge the beamline personnel of PXI and ID 23-1 at SLS and ESRF, respectively.

References

1. Gruber K, Puffer B, Kräutler B. 2011. Vitamin B12-derivatives—enzyme cofactors and ligands of proteins and nucleic acids. *Chem. Soc. Rev.* 40(8):4346
2. Raux E, Schubert HL, Warren MJ. 2000. Biosynthesis of cobalamin (vitamin B12): a bacterial conundrum. *Cell. Mol. Life Sci.* 57(13–14):1880–93
3. Banerjee R V., Johnston NL, Sobeski JK, Datta P, Matthews RG. 1989. Cloning and sequence analysis of the Escherichia coli metH gene encoding cobalamin-dependent methionine synthase and isolation of a tryptic fragment containing the cobalamin-binding domain. *J. Biol. Chem.* 264(23):13888–95
4. Martens JH, Barg H, Warren M, Jahn D. 2002. Microbial production of vitamin B12. *Appl. Microbiol. Biotechnol.* 58(3):275–85
5. Rodionov DA, Vitreschak AG, Mironov AA, Gelfand MS. 2003. Comparative Genomics of the Vitamin B12 Metabolism and Regulation in Prokaryotes. *J. Biol. Chem.* 278(42):41148–59
6. Roth JR, Lawrence JG, Bobik T a. 1996. Cobalamin (coenzyme B12): synthesis and biological significance. *Annu. Rev. Microbiol.* 50:137–81
7. Locher K. P., Lee A. T. RDC. 2002. The E. coli BtuCD Structure: A Framework for ABC Transporter Architecture and Mechanism. *Science* 296(5570):1091–98
8. Cadieux N, Bradbeer C, Reeger-Schneider E, Köster W, Mohanty AK, et al. 2002. Identification of the periplasmic cobalamin-binding protein BtuF of Escherichia coli. *J. Bacteriol.* 184(3):706–17
9. DAVIS BD, MINGIOLI ES. 1950. Mutants of Escherichia coli requiring methionine or vitamin B12. *J. Bacteriol.* 60(1):17–28

10. Slotboom DJ. 2014. Structural and mechanistic insights into prokaryotic energy-coupling factor transporters. *Nat. Rev. Microbiol.* 12(2):79–87
11. Rodionov DA, Hebbeln P, Eudes A, Ter Beek J, Rodionova IA, et al. 2009. A novel class of modular transporters for vitamins in prokaryotes. *J. Bacteriol.* 91(1):42–51
12. Erkens GB, Berntsson RPA, Fulyani F, Majsnerowska M, Vujičić-Žagar A, et al. 2011. The structural basis of modularity in ECF-type ABC transporters. *Nat. Struct. Mol. Biol.* 18(7):755–60
13. Berntsson RP-A, ter Beek J, Majsnerowska M, Duurkens RH, Puri P, et al. 2012. Structural divergence of paralogous S components from ECF-type ABC transporters. *Proc. Natl. Acad. Sci.* 109(35):13990–95
14. Swier LJYM, Guskov A, Slotboom DJ. 2016. Structural insight in the toppling mechanism of an energy-coupling factor transporter. *Nat. Commun.* 7:11072
15. Finkenwirth F, Kirsch F, Eitinger T. 2013. Solitary bio Y proteins mediate biotin transport into recombinant Escherichia coli. *J. Bacteriol.* 195(18):4105–11
16. Genee HJ, Bali AP, Petersen SD, Siedler S, Bonde MT, et al. 2016. Functional mining of transporters using synthetic selections. *Nat. Chem. Biol.* 12:1015–22
17. Zhou J, Riccardi D, Beste A, Smith JC, Parks JM. 2014. Mercury methylation by HgcA: Theory supports carbanion transfer to Hg(II). *Inorg. Chem.* 53(2):772–77
18. Duléry V, Uhlich NA, Maillard N, Fluxà VS, Garcia J, et al. 2008. A cyclodecapeptide ligand to vitamin B12. *Org. Biomol. Chem.* 6(22):4134–41
19. Borths EL, Locher KP, Lee AT, Rees DC. 2002. The structure of Escherichia coli BtuF and binding to its cognate ATP binding cassette transporter. *Proc. Natl. Acad. Sci. U. S. A.* 99(26):16642–47
20. Shultis DD, Purdy MD, Banchs CN, Wiener MC. 2006. Outer Membrane Active Transport: Structure of the BtuB:TonB Complex. *Science* 312(5778):1396–99
21. Mathews FS, Gordon MM, Chen Z, Rajashankar KR, Ealick SE, et al. 2007. Crystal structure of human intrinsic factor: cobalamin complex at 2.6-A resolution. *Proc. Natl. Acad. Sci. U. S. A.* 104(44):17311–16

22. Furger E, Frei DC, Schibli R, Fischer E, Prota AE. 2013. Structural basis for universal corrinoid recognition by the cobalamin transport protein haptocorrin. *J. Biol. Chem.* 288(35):25466–76
23. Wuerges J, Geremia S, Fedosov SN, Randaccio L. 2007. Vitamin B12 transport proteins: crystallographic analysis of beta-axial ligand substitutions in cobalamin bound to transcobalamin. *IUBMB Life*. 59(11):722–29
24. Blackledge WC, Blackledge CW, Griesel A, Mahon SB, Brenner M, et al. 2010. New facile method to measure cyanide in blood. *Anal. Chem.* 82(10):4216–21
25. Koutmos M, Gherasim C, Smith JL, Banerjee R. 2011. Structural Basis of Multifunctionality in a Vitamin B 12 -processing Enzyme. *J. Biol. Chem.* 286(34):29780–87
26. Kim J, Gherasim C, Banerjee R. 2008. Decyanation of vitamin B12 by a trafficking chaperone. *Proc. Natl. Acad. Sci. U. S. A.* 105(38):14551–54
27. Santos JA, Rempel S, Mous ST, Pereira CT, ter Beek J, et al. 2018. Functional and structural characterization of an ECF-type ABC transporter for vitamin B12. *Elife*. 7:e35828
28. Hvorup RN, Goetz BA, Niederer M, Hollenstein K, Perozo E, Locher KP. 2007. Asymmetry in the Structure of the ABC Transporter-Binding Protein Complex BtuCD-BtuF. *Science* 317(5843):1387–90
29. Jaehme M, Guskov A, Slotboom DJ. 2014. Crystal structure of the vitamin B3 transporter PnuC, a full-length SWEET homolog. *Nat. Struct. Mol. Biol.* 21(11):1013–15
30. Cao Y, Jin X, Levin EJ, Huang H, Zong Y, et al. 2011. Crystal structure of a phosphorylation-coupled saccharide transporter. *Nature*. 473(7345):50–54
31. Finn RD, Clements J, Arndt W, Miller BL, Wheeler TJ, et al. 2015. HMMER web server: 2015 Update. *Nucleic Acids Res.* 43(W1):W30–38
32. Casadaban MJ, Cohen SN. 1980. Analysis of gene control signals by DNA fusion and cloning in Escherichia coli. *J. Mol. Biol.* 138(2):179–207
33. Guzman LM, Belin D, Carson MJ, Beckwith J. 1995. Tight regulation , modulation , and high-level expression by vectors containing the arabinose These include : Tight Regulation ,

Modulation , and High-Level Expression by Vectors Containing the Arabinose P BAD Promoter. *J. Bacteriol.* 177(14):4121–30

34. Miller J. 1972. Experiments in molecular genetics. In *Experiments in molecular genetics*. Cold Spring Harbor, NY: Cold Spring Harbor Laboratory
35. Thomason LC, Costantino N, Court DL. 2007. *E. coli* Genome Manipulation by P1 Transduction. *Curr. Protoc. Mol. Biol.* 1.17.1-1.17.8
36. Datsenko KA, Wanner BL. 2000. One-step inactivation of chromosomal genes in Escherichia coli K-12 using PCR products. *Proc. Natl. Acad. Sci.* 97(12):6640–45
37. Engilberge S, Riobé F, Di Pietro S, Lassalle L, Coquelle N, et al. 2017. Crystallophore: a versatile lanthanide complex for protein crystallography combining nucleating effects, phasing properties, and luminescence. *Chem. Sci.* 8(9):5909–17
38. Kabsch W, K. W, G. RRB. 2010. XDS. *Acta Crystallogr. Sect. D Biol. Crystallogr.* 66(2):125–32
39. Sheldrick GM. 2007. A short history of SHELX. *Acta Crystallogr. Sect. A Found. Crystallogr.* 64(1):112–22
40. Terwilliger TC, Grosse-Kunstleve RW, Afonine P V., Moriarty NW, Zwart PH, et al. 2007. Iterative model building, structure refinement and density modification with the PHENIX AutoBuild wizard. *Acta Crystallogr. Sect. D Biol. Crystallogr.* 64(1):61–69
41. Adams PD, Afonine P V, Bunkóczi G, Chen VB, Davis IW, et al. 2010. PHENIX: A comprehensive Python-based system for macromolecular structure solution. *Acta Crystallogr. Sect. D Biol. Crystallogr.* 66(2):213–21
42. Emsley P, Lohkamp B, Scott WG, Cowtan K. 2010. Features and development of Coot. *Acta Crystallogr. Sect. D Biol. Crystallogr.* 66(4):486–501
43. McCoy AJ, Grosse-Kunstleve RW, Adams PD, Winn MD, Storoni LC, Read RJ. 2007. Phaser crystallographic software. *J. Appl. Crystallogr.* 40(4):658–74

Supplementary Information

Supplementary tables

Suppl. Table 1: RMSD comparison between full length $BtuM_{Td}$, ThiT, BioY, and FolT.

Values in Å	**$BtuM_{Td}$**	**ThiT**	**BioY**	**FolT**
$BtuM_{Td}$	0.0	3.1	3.2	3.1
ThiT	3.1	0.0	2.8	2.6
BioY	3.2	2.8	0.0	2.9
FolT	3.1	2.6	2.9	0.0

Suppl. Table 2: Primer list used in this study.

Primer name	**Sequence (5'-3')**
BtuM_opt_NcoI_frwd	GGTCCATGGGTCTGAATC
BtuM_NcoI_long_frwd	GGTCCATGGGTCTGAATCTGACCCGTCGTCAGCAGATTGC
BtuM_Td_opt_C80S_frwd	GTTAGCGATTTTTCTGTTAGTCCGGC
BtuM_Td_opt_C80S_rev	GCCGGACTAACAGAAAAATCGCTAAC
BtuM_Td_opt_C80A_frwd	GGTGTTAGCGATTTTGCGGTTAGTCCGGCATATTG
BtuM_Td_opt_C80A_rev	CAATATGCCGGACTAACCGCAAAATCGCTAACACC
BtuM_Td_opt_H28A_frwd	GACCCGTAGCCATGCTTGGGCAAGCATTC
BtuM_Td_opt_H28A_rev	GAATGCTTGCCCAGCGATGGCTACGGGTC
BtuM_Td_opt_D67A_frwd	GATTGCAGCAAGCGTTGTTATTGCTTATGTTG
BtuM_Td_opt_D67A_rev	CAGGTAATTGCAACATAAGCAATAACAACG
BtuM_Td_opt_Y85L_frwd	GTTAGTCCGGCACTTTGGCTGCTG
BtuM_Td_opt_Y85L_rev	GCAGCCAAAGTGCCGGACTAACAC
BtuM_Td_opt_R153A_frwd	CAGGTCTGGTGCTGGCTCTGGAAAAATAC
BtuM_Td_opt_R153A_rev	GTATTTTTCCAGAGCCAGCACCAGACCTG
BtuM_Td_opt_rev	GCCAAGCTTTCATTAACGTTCACGACGGG
BtuM_Td_cEPEA-HindIII_rev	GATAAGCTTTCATTATGCCTCTGGTTCACGTTCACGACGGG
BtuC_frwd	GCAGGAGGAATTCACCATGCTGACACTTGCCCGC
BtuC_rev	GAATTCCTCCTATTGATTACTAACGTCCTGCTTTTAACAATAACCAG
BtuF_frwd	GACGTTAGTAATCAATAGGAGGAATTCACCATGGCTAAGTCACTGTTCAGG
BtuF_rev	GCCAAAACAGCCAAGCTTTTACTAATCTACCTGTGAAAGCGCATTAC
pBAD24_frwd	TTAAAGCTTGGCTGTTTTGGCG
pBAD24_rev	GGTGAATTCCTCCTGCTAGC
Seq_frwd	CTCTACTGTTTCTCCATACCCG
Seq_rev	GCTGAAAATCTTCTCTCATCCG

Supplementary Figures

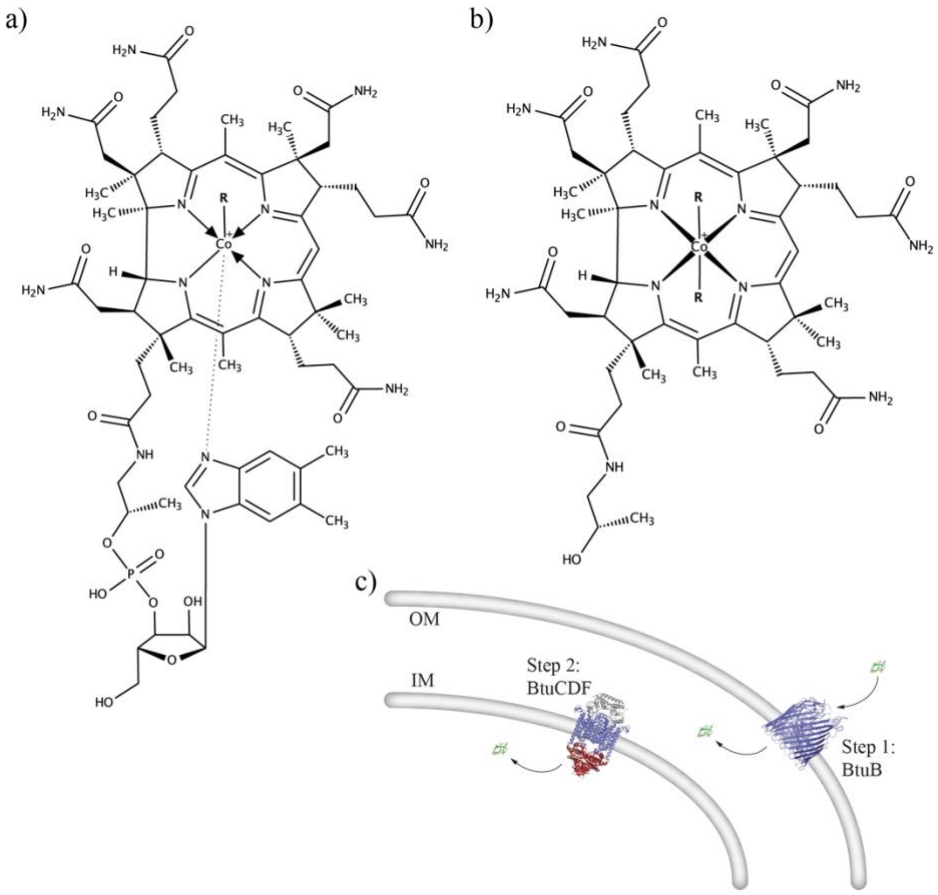

Suppl. Figure 1: Structure of cobalamin and cobinamide and *E. coli* Cbl uptake pathway. a) Structural formula of cobalamin (Cbl) where R can be a cyano group (cyano-Cbl), a hydroxyl group (OH-Cbl), a methyl-group (CH3-Cbl) or a 5'-deoxyadenosyl group (ado-Cbl). The latter two are two of three biologically active variants of the vitamin. The third variant is found in epoxyqueuosine oxidoreuctases, which bind Cbl in an 'open conformation' where R is a water and Cbl is bound in the base-off conformation and its cobalt ion is kept penta-coordinate (in contrast to the 'normal' hexa-coordinate) and thus in its divalent state. b) The Cbl precursor cobinamide (Cbi) has two variable groups, R. In this study, di-cyano Cbl was used. c) The uptake of Cobalamin in *E. coli* requires the translocation of Cbl (green) over the outer (OM) and inner (IM) membrane. BtuB is the TonB-dependent outer membrane active transporter (PDB: 2GSK) and BtuCDF (PDB: 4FI3) is a type II ABC-importer. Together they form the full BtuBCDF transport pathway. In our deletion strain, *E. coli* ΔFEC, the *btuB* gene locus is still present.

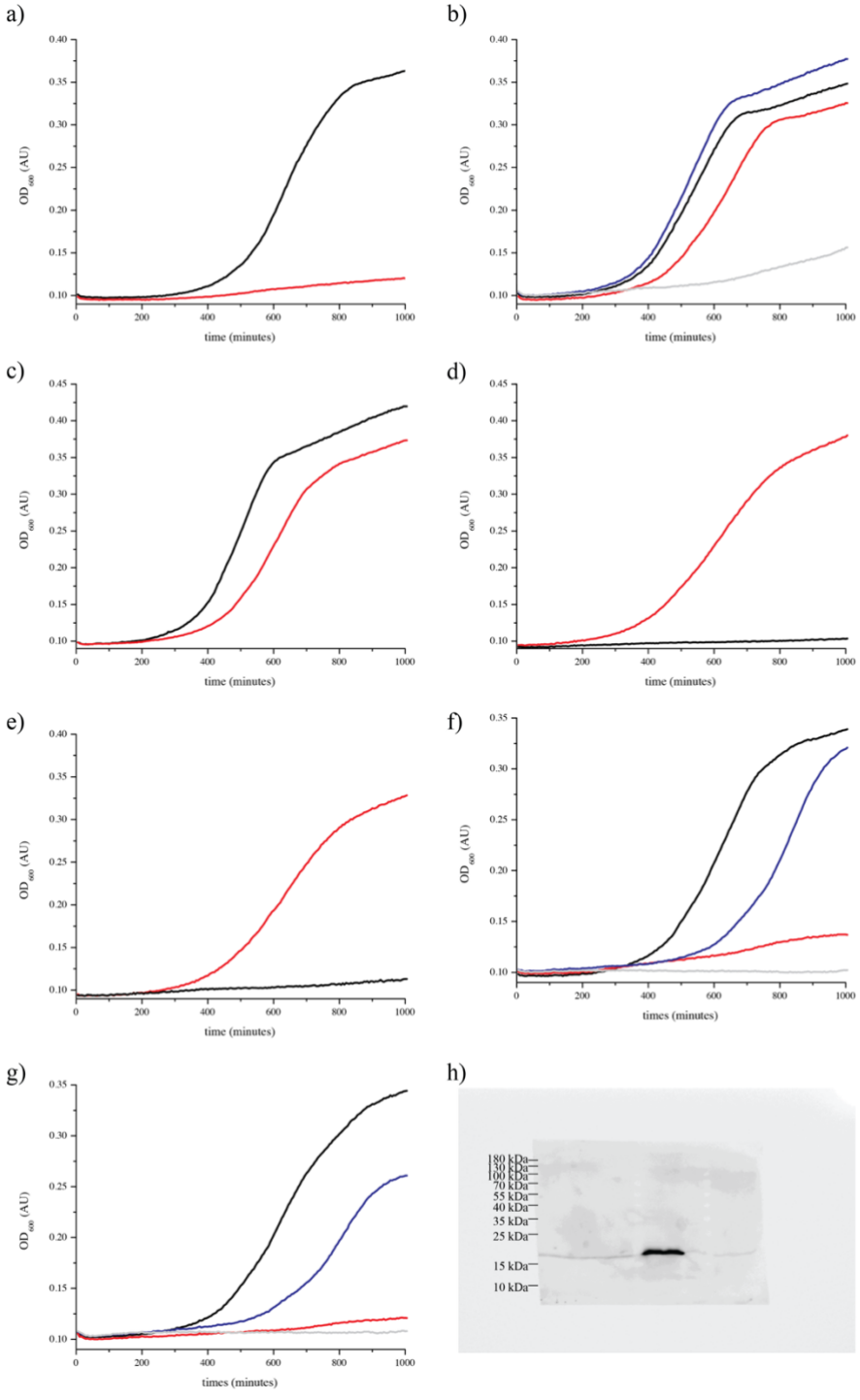
a)
b)
c)
d)
e)
f)
g)
h)
OD600 (AU)
time (minutes)
times (minutes)
180 kDa
130 kDa
100 kDa
70 kDa
55 kDa
40 kDa
35 kDa
25 kDa
15 kDa
10 kDa

Suppl. Figure 2: Growth assay in the presence of OH-Cbl and Cbi and using extreme Cbl concentrations. All growth curves are averages of biological triplicates each consisting of technical triplicates. a) *E. coli* ΔFEC without expression plasmid can grow in the presence of 50 µg/ml L-methionine (black line) but not in the presence of 1 nM Cbl (red line). b) Growth of *E. coli* ΔFEC expressing EPEA-tagged versions of $BtuM_{Td}$. In the presence of 50 µg/ml L-methionine both wild-type and C80S mutant grow (black and blue line, respectively), whereas in the presence of 1 nM Cbl only $BtuM_{Td}$ (red line) can grow and the C80S mutant does not exhibit substantial growth (grey line). c) Growth of tag-less $BtuM_{Td}$ expressing cells shows that the His-tag does not affect activity of $BtuM_{Td}$ *in vivo* in the presence of either L-methionine (black line) or Cbl (red line). d) Growth assay in the presence of 0.1 nM OH-Cbl of cells expressing BtuCDF (red line) and control carrying the empty expression vector (black line). e) Growth assay in the presence of 0.1 nM OH-Cbl of wild-type $BtuM_{Td}$ expressing cells (red line) and the C80S mutant (black line). f) At Cbl concentrations of 5 nM both BtuCDF expressing cells (black line) and empty expression vector carrying cells (blue line) grow whereas 0.01 nM Cbl is insufficient to sustain grow for either BtuCDF expressing cells (red line) or cells carrying pBAD24 (grey line). g) For cells expressing His-tagged $BtuM_{Td}$ (black and red lines) and BtuMTd_C80S (blue and grey lines) under the same conditions as in e) we observe the same behavior. h) Full length western blot of the inset in **Figure 1b**.

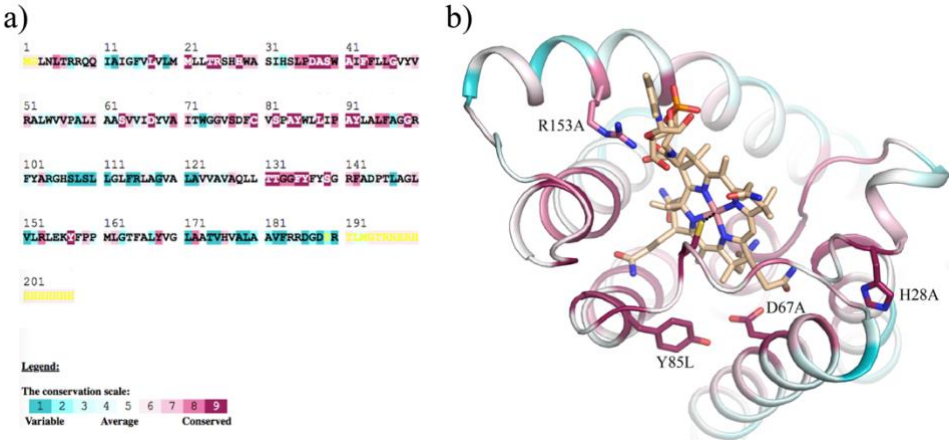

Suppl. Figure 3: Sequence conservation in the BtuM family. a) Amino acid sequence of $BtuM_{Td}$ with color key showing the degree of conservation (yellow residues with insufficient data). Residue Cys80 is completely conserved. b) View from the periplasmic side of the membrane on the $BtuM_{Td}$ binding pocket. The coloring of residues by conservation was mapped on the structure using the ConSurf Server. Four residues were chosen and mutant protein variants were constructed,

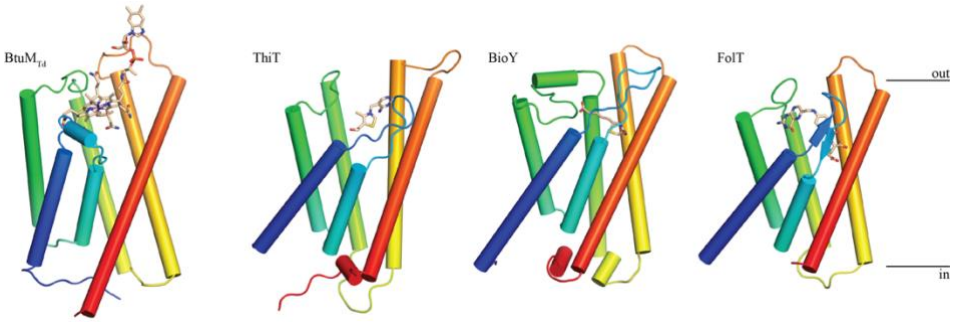

Suppl. Figure 4: Comparison of BtuM$_{Td}$ to three other S-components. Structural alignment of BtuM$_{Td}$ with three S-components ThiT, BioY and FolT (pdb-codes 3RLB, 4DVE and 5D0Y, respectively) shows that the overall fold is the same. Also, the substrate-binding site is located at the same position. RMSD values between are listed in **Suppl. Table 1**.

Suppl. Figure 5: Stereo view images of the main chain traced electron density of BtuM$_{Td}$ and its binding pocket and vitamin B12. a) Stereo view image of the full-length ribbon traced model with its corresponding 2fo-fc density map (grey) at 2σ (residues 3-182 and 202-207) and 0.5σ (residues 1-2 and 183-201). b) The same model as in (a) focused on the binding pocket including Cbl and its corresponding 2fo-fc density (grey) at 2σ. c) Stereo view on Cbl and Cys80 with their 2fo-fc density map (grey) at 2σ.

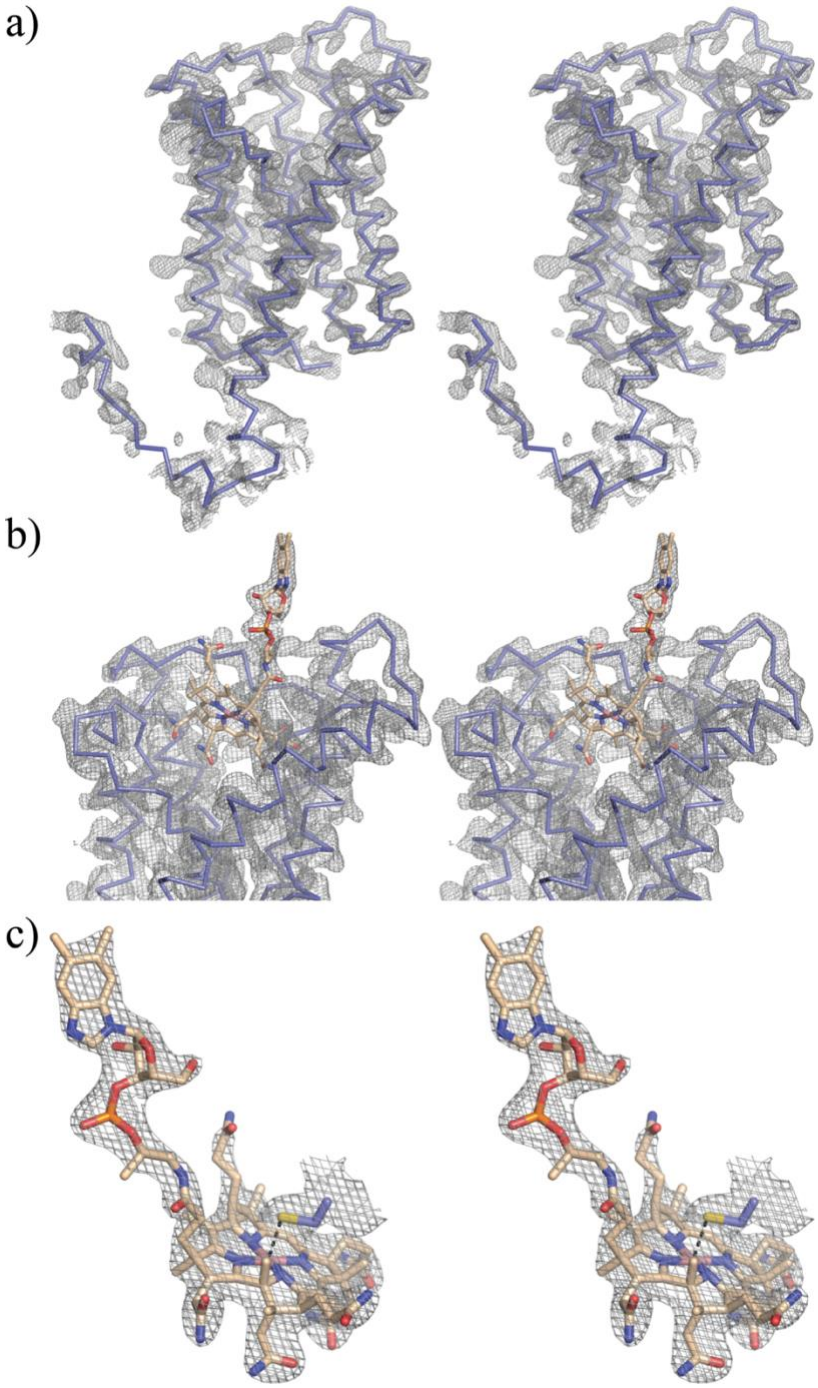
a)
b)
c)

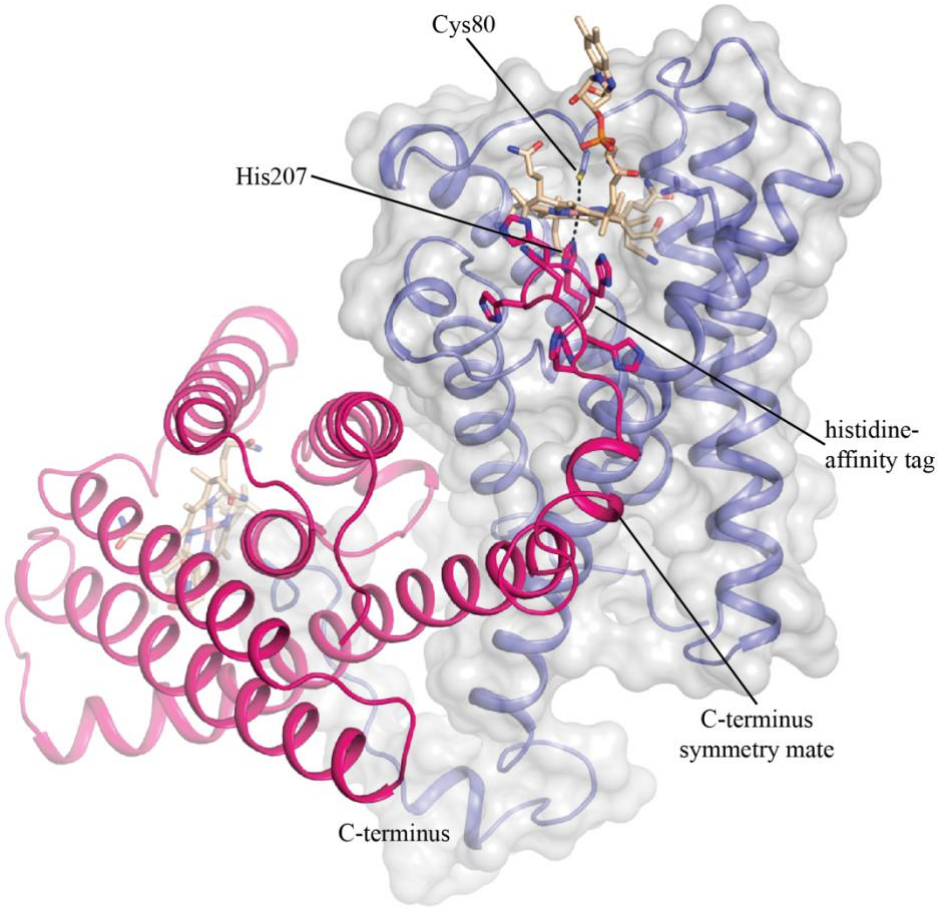

Suppl. Figure 6: BtuM$_{Td}$ and its neighboring symmetry mate in the crystal. The two symmetry mates (blue and pink) align almost antiparallel allowing the C-terminal histidine-affinity tags to mutually enter into each other's binding pocket. The last His207 then binds the Co-ion of Cbl.

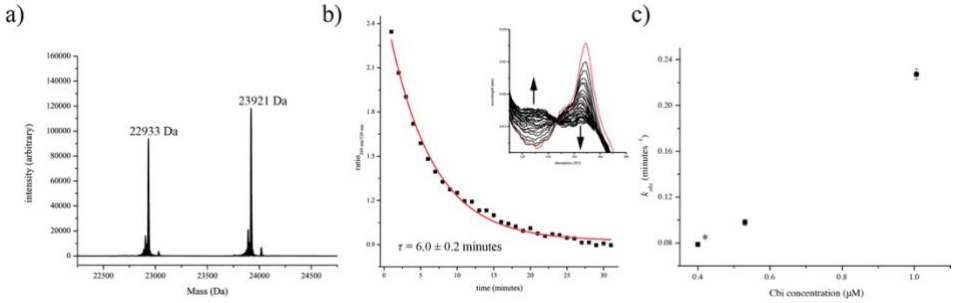

Suppl. Figure 7: High resolution mass spectrum of BtuM$_{Td}$ bound to Cbi and decyanation of Cbi by His-tagged BtuM$_{Td}$. a) The formylated *apo* protein with M_w of 22933 Da (similar to Supplementary Figure 7 a) and a peak for the substrate bound protein (23921 Da) are visible. The difference of the two masses is 988 Da, close to the mass of decyanated Cbi of 990 Da; because dicyano-Cbi was added during the purification (MW of 1042 Da) the data indicates that the protein removed both cyano groups. b) Spectral changes of a 5:1 His-tagged BtuM$_{Td}$ (0.5 – 1.3 μM) to Cbi molar ratio mixture were monitored over time (starting spectrum red line). The absorption increased at 330 nm and decreased at 369 nm. These changes are consistent with removal of cyanide from the substrate. His-tagged BtuM$_{Td}$ and EPEA-tagged BtuM$_{Td}$ behaved similarly (compare **Figure 3b and c**). c) Decyanation assay with a fixed concentration (4 μM) of EPEA-tagged BtuM$_{Td}$ with increasing concentrations of Cbi (* value from single experiment, other points averaged from triplicates with standard deviation as the error of the mean) showing that the decaynation process follows the kinetics of a pseudo-first order binding reaction.

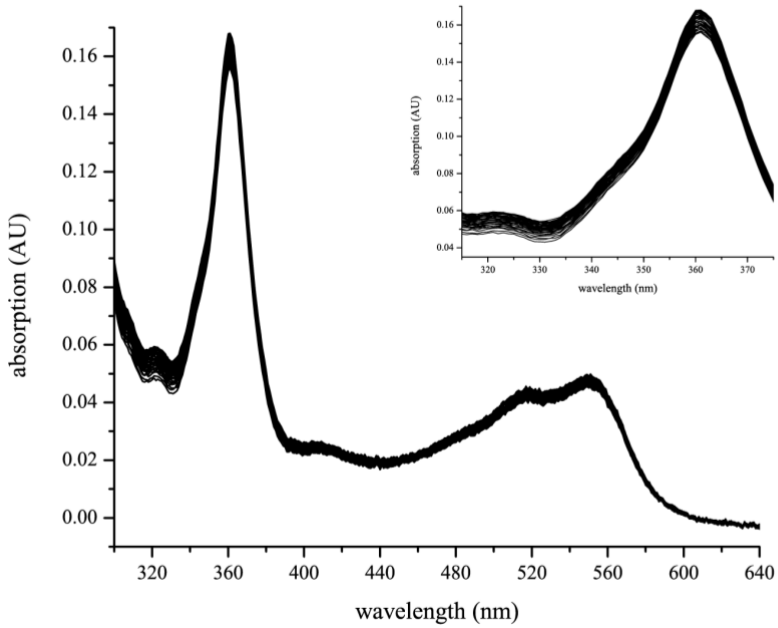

Suppl. Figure 8: Monitoring cyano-Cbl binding by BtuM$_{Td}$ by spectral changes. Similar to the experiment in **Suppl. Figure 7b** spectral changes in BtuM$_{Td}$_cHis8 upon substrate binding were followed over time. A molar ratio of substrate to protein of 1:1 was used and spectra were taken every 20 minutes for 12 hours. Because binding would lead to the spectral changes observed in **Figure 2b**, we conclude that we do not observe binding.

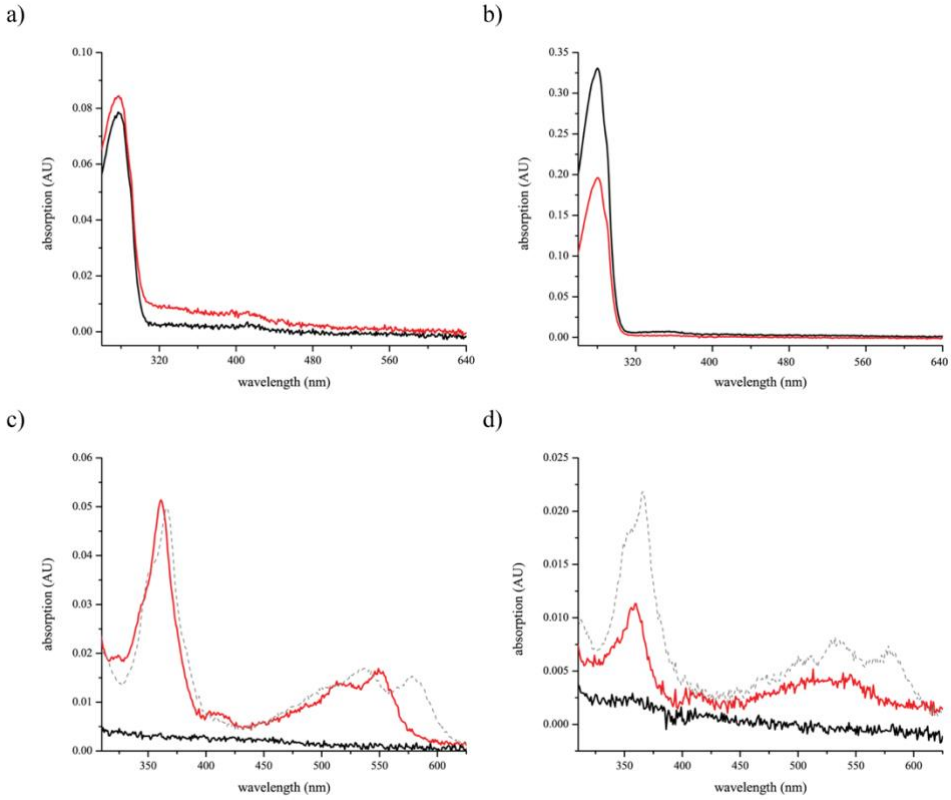

Suppl. Figure 9: Absorption spectra of *apo* BtuM$_{Td}$ and mutants C80A and C80S. a) Absorption spectra of *apo* EPEA-tagged BtuM$_{Td}$ (black line) and BtuM$_{Td}$_C80S (red line) showing that the protein purifies in its *apo* state when no substrate is added. (b) The absorption spectra of His-tagged BtuM$_{Td}$_C80A (black line) and C80S (red line) purified in the presence of Cbl show that no substrate is bound. c) and d) The two mutant variants BtuM$_{Td}$_C80A and C80S were purified in conditions where wild-type BtuM$_{Td}$ binds Cbl and Cbi. BtuM$_{Td}$_C80A c) and BtuM$_{Td}$_C80S d) did not bind Cbl (black line, same data as in b) but still bound Cbi (red line). Binding of Cbi did not lead to the spectral changes as observed for the native protein (compare **Figure 2b and c**). Spectra of 2 μM c) and 1 μM d) unbound Cbi (dashed grey line) are included for comparison.

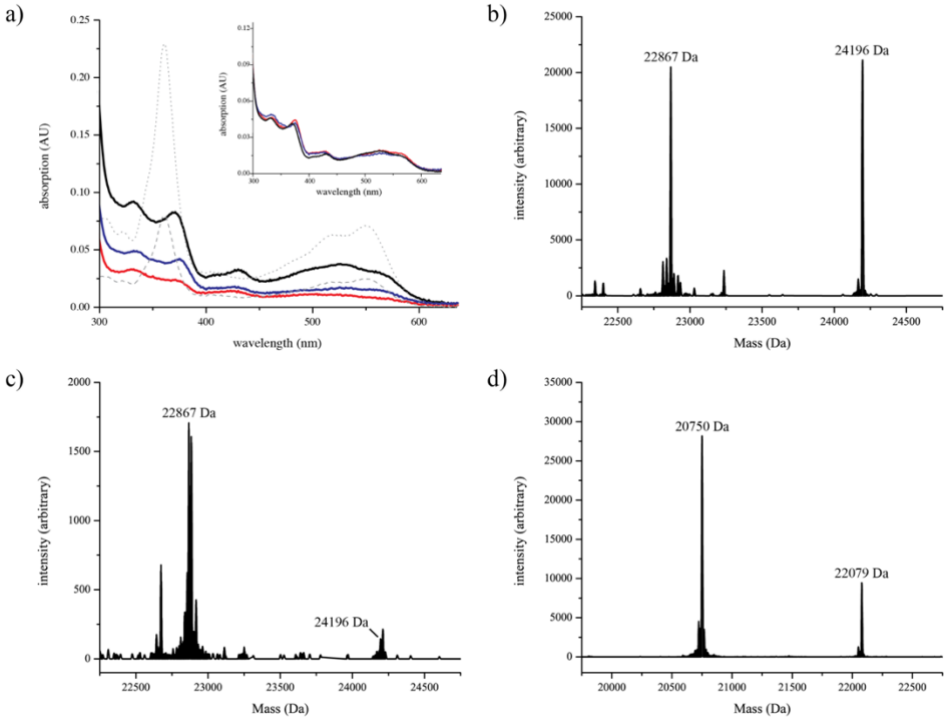

Suppl. Figure 10: Absorption spectra and high-resolution mass spectra of BtuM$_{Td}$ mutants bound to Cbl. a) The absorption spectra of Cbl bound to BtuM$_{Td}$_H28A (black line, 8.7 µM), Y85L (red line, 3.1 µM), and R153A (blue line, 4.4 µM) show the characteristic changes of cysteine binding and decyanation. For comparison spectra of free Cbl are shown at concentrations of 3 µM and 8.5 µM, grey dashed and dotted line, respectively. The inset shows scaled spectra of the mutants to emphasize that spectral changes caused by binding to mutants of BtuM$_{Td}$ are essentially the same (inset) and apparent differences are caused by different concentrations. b) Mass spectrum of BtuM$_{Td}$_H28A shows two peaks corresponding to the formylated *apo* protein (22867 Da) and the formylated, Cbl-bound protein (24196 Da). The mass difference of 1329 Da is consistent with decyanation. c) Same for the Y85L mutant d) Same for the R153A mutant.

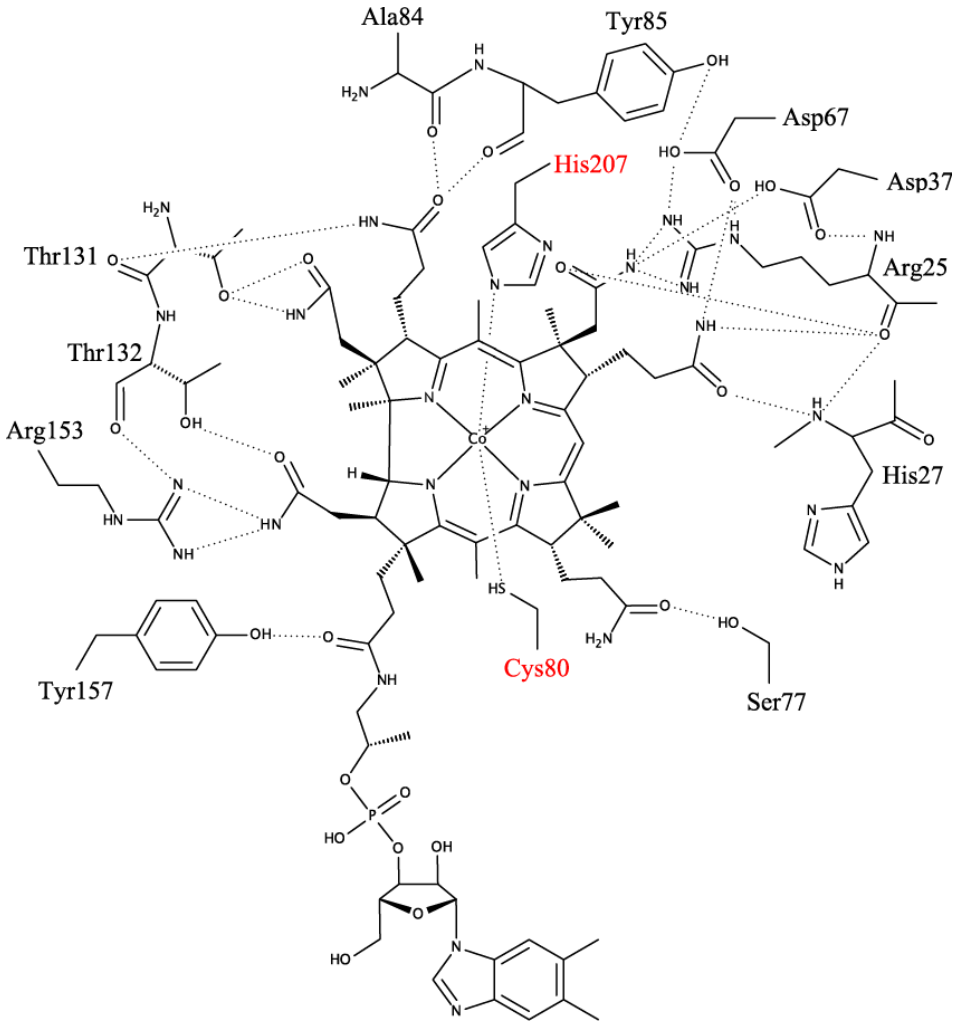

Suppl. Figure 11: Depiction of hydrogen bond network in the binding pocket of Cbl with BtuM$_{Td}$. Next to the major interactions of the sulphur and nitrogen of Cys80 and His207 with the cobalt ion of Cbl there are a variety of side chain and backbone interactions with corrin-ring decorating moieties.

Chapter 4

On the role of modifications for the oligomeric state of the vitamin B12 transporter BtuM

Rempel, S.[1], Robinson, A.[2,3], de Gier J.W.[4], and Slotboom, D.J.[1,2]

[1]*Groningen Biomolecular and Biotechnology Institute (GBB), University of Groningen, The Netherlands*

[2]*Zernike Institute for Advanced Materials, University of Groningen, The Netherlands*

[3]*current address: School of Chemistry, Faculty of Science, Medicine and Health, University of Wollongong, Australia*

[4]*Department of Biochemistry and Biophysics, Stockholm University, Sweden*

Abstract

S-components are subunits of ECF-type ABC transporters, which act as their membrane-embedded substrate-binding proteins. The transport mechanism of ECF-type ABC transporters requires toppling of the S-component in the membrane, for which the tripartite ECF-module is thought to be essential. BtuM is a recently discovered solitary S-component that catalyzes uptake of Vitamin B12 into Gram-negative proteobacteria, without the use of an ECF module. The mechanism of transport used by this solitary S-component is unclear. It may involve the toppling motion, but it is debated whether such movement can take place in the absence of an interacting membrane protein partner. Here, we investigated if BtuM adopts a higher oligomeric state, which could facilitate toppling. We find that BtuM is a monomer both *in vitro* and *in vivo*. Additionally, based on the recently reported crystal structure of BtuM, we show that the presence of an engineered C-terminal Histidine-tag promotes dimerization, showing that engineered proteins a prone to exhibit artefactual behavior.

Introduction

Energy coupling factor (ECF-) type ABC-transporters are a relatively recent addition to the versatile ATP binding cassette (ABC) transporter super-family. They are found only in prokaryotes, primarily in Gram-positive bacteria of the Firmicutes group (1). ECF-transporters contain two ATPases and two transmembrane proteins, an architecture shared will all other ABC-transporters, like the type I maltose or type II vitamin B12 (cobalamin, Cbl) importers, MalGFK or BtuCDF, respectively, which additionally require a soluble substrate binding protein. However, the membrane subunits in the ECF-type transporters have different functional properties. One of the transmembrane subunits has evolved into a membrane embedded substrate binding protein, called S-component (2–5). In a subset of ECF-transporters, the S-component dynamically associates with the rest of the transporter, called ECF-module, that is comprised of two ATPases and the transmembrane protein ECF-T. Structural analyses have revealed that the S-component, which mediates substrate-specificity, can topple by almost 90° in the membrane, likely aided by ECF-T, and thereby shuttles the substrate through the membrane (1, 6, 7).

Recently, BtuM from *Thiobacillus denitrificans*, which previously had been predicted to be a new type of Cbl transporter, has been biochemically and structurally characterized, confirming that it is indeed a novel class of vitamin B12 transporters (8, 9). Intriguingly, $BtuM_{Td}$ is a S-component that catalyzes Cbl-transport *in vivo* without an accompanying ECF-module (9). The same has been shown before for a small group of solitary BioY proteins, which is an S-component that transports biotin (10). Differently from BtuM homologs, BioY can also be found as a non-solitary S-component, in which case transport of the substrate depends on the presence of the ECF-module (1, 10). Thus, the question arises, what transport mechanism is used by solitary S-components. It was speculated that transport is achieved by toppling of the solitary S-component without the aid of the ECF-module (9). However, toppling of S-components in ECF transporters is believed to depend on the interaction with the ECF module, presumable via the 'greasy' gliding surface provided by the transmembrane domain ECF-T (7), which raises the question how a solitary protein may topple over. It is possible that solitary S-components form oligomeric assemblies, in which one of the two protomers could translocate the substrate by toppling, using the other protomer as the

'gliding surface', in analogy to the full complex. It was claimed before that for BioY a higher oligomeric state is the functional state (11). Because non-solitary S-components are known to be monomeric when dissociated from the full complex (12–14), we investigated if $BtuM_{Td}$ forms oligomers *in vitro*, using size exclusion multiangle laser light scattering (SEC-MALLS) analyses, or *in vivo*, using single molecule fluorescence microscopy. Our findings show that $BtuM_{Td}$ is monomeric *in vitro* and *in vivo*.

Results

In vitro *oligomeric state determination using SEC-MALLS*

To determine the oligomeric state, we purified a C-terminally His-tagged version of $BtuM_{Td}$ ($BtuM_{Td}$_cHis8) in the *apo* and substrate-bound states. Using SEC-MALLS, we probed in detergent solution the oligomeric state. For the *apo* protein, we observed a symmetrical elution profile pointing towards a single oligomeric species (**Figure 1a**). The determined profile profile pointing toward a single oligomeric species (**Figure 1a**). The determined weight was ~23 kDa, which is close to the theoretical molecular weight of 22.9 kDa, and thus *apo* $BtuM_{Td}$_cHis8 is monomeric (**Figure 1a**). In contrast, the substrate-loaded protein exhibited an elution profile that had an additional shoulder at a slightly earlier elution volume (**Figure 1b**). The measured molecular weight of the protein in the main peak was 23 kDa, but the earlier eluting species was determined to be ~46 kDa, and thus contained dimeric $BtuM_{Td}$_cHis8 (**Figure 1b**). Because the crystal structure of Cbl-bound $BtuM_{Td}$_cHis8 showed that the imidazole moiety of the last, C-terminal His-tag histidine side chain can insert into the binding pocket of a neighboring $BtuM_{Td}$ molecule in the crystals, and make contact with the cobalt ion of Cbl (9), we concluded that the dimer formation upon substrate-binding may be an artefact. Therefore, we engineered a tobacco edge virus (TEV-) cleavage site between the native protein sequence and the His-tag ($BtuM_{Td}$_cTEV-His8). We conducted the same experiments with TEV-cleaved $BtuM_{Td}$ ($BtuM_{Td}$-cut) and found that both *apo* and substrate-loaded $BtuM_{Td}$-cut eluted with symmetrical elution profiles during SEC-MALLS resulting in monomeric species of ~23 kDa under both conditions (**Figure 1c and d**).

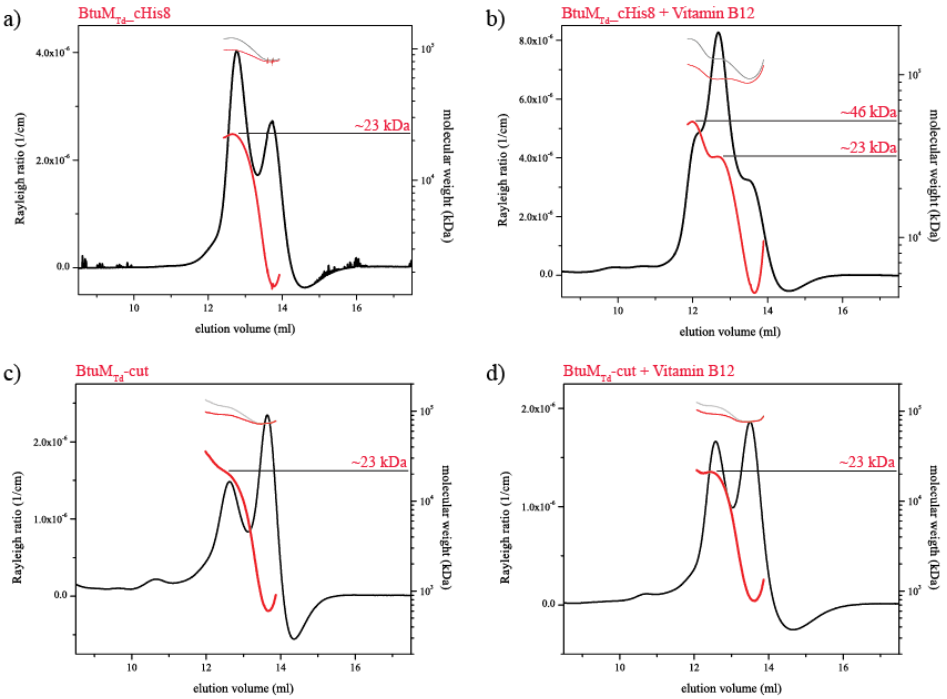

Figure 1: SEC-MALLS analysis of BtuM$_{Td}$. The Rayleigh ratio is plotted against the elution volume (black) and molecular weights (MW) of the protein (red, thick), the micelle (red, thin), and the conjugate (light grey) are shown for regions of interest. a) BtuM$_{Td}$_cHis8 in its *apo* state elutes as a single peak followed by an empty n-dodecyl-β-D-maltoside (DDM) micelle. The measured MW is ~23 kDa (theoretical MW is 22.9 kDa). b) same as a) but with vitamin B12-bound protein. A shoulder appears at an earlier elution volume showing partial dimer formation of ~46 kDa. c) same as in a) but with His-tag free BtuM$_{Td}$-cut after TEV treatment, resulting also in a monomer. d) same as in b) but with His-tag free BtuM$_{Td}$-cut after TEV treatment. In the absence of the His-tag no partial dimer formation occurs.

In vivo *oligomeric state determination using single-molecule fluorescent bleaching microscopy*

The SEC-MALLS results in combination with the crystal structure indicate that BtuM$_{Td}$ exists as a monomer *in vitro* (9). To further corroborate that BtuM$_{Td}$ is monomeric, we aimed to investigate the oligomeric state of BtuM$_{Td}$ *in vivo*. *In vivo* experiments do not suffer from potential effects of the detergent micelle on the oligomeric state. We used single-molecule fluorescent bleaching microscopy, which requires the presence of a fluorescent Ypet protein, which was fused C-terminally to BtuM$_{Td}$_cHis8 (BtuM$_{Td}$_cHis8-Ypet) including a flexible linker (15). Because the His-tag is wedged in between BtuM$_{Td}$ and Ypet we reason that the last histidine residue is sterically blocked by Ypet from binding to

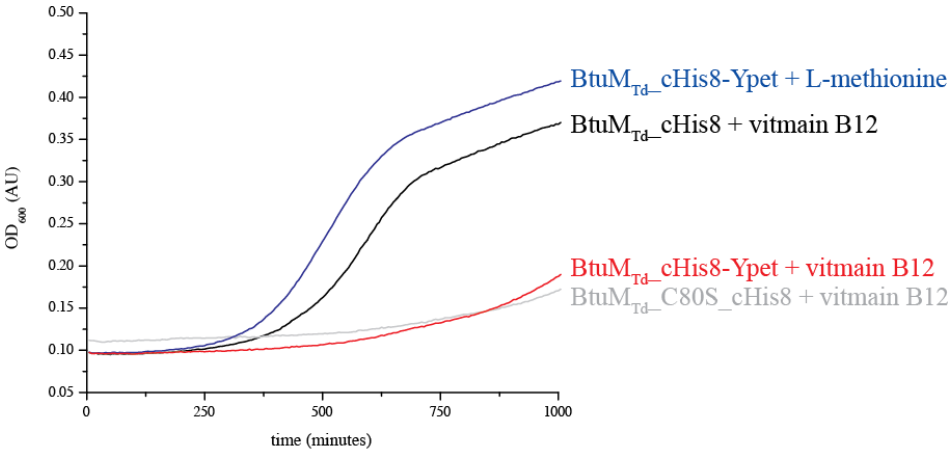

Figure 2: Growth assay with $BtuM_{Td}$_cHis8-Ypet. The *E. coli* triple knock-out strain carrying the indicated expression constructs in the presence of either 1 nM vitamin B12 or 50 mg ml^{-1} L-methionine. Expression of $BtuM_{Td}$_cHis8 (positive control, black line) leads to growth in the presence of vitamin B12, whereas $BtuM_{Td}$_C80S_cHis8 (negative control, grey line) cannot sustain growth under these conditions. Expression of $BtuM_{Td}$_cHis8-Ypet also cannot support growth in the presence of vitamin B12 (red line) and only in the presence of L-methionine (blue line) these cells grow.

Cbl of a second $BtuM_{Td}$ molecule. We used an *E. coli* triple knock out strain (*E. coli* ΔFEC) like previously described (9, 16, 17). In brief, deletions of *btuF* and *btuC* abolish endogenous Cbl uptake, and deletion of the Cbl-independent methionine synthase forces the strain to synthesize L-methionine *via* a Cbl-requiring route. Thus, the strain depends on a Cbl transporter when no L-methionine is supplied in the growth medium. The fusion affected activity of $BtuM_{Td}$ (**Figure 2**) but nonetheless expression was present allowing for *in vivo* oligomeric state determination. We expressed $BtuM_{Td}$_cHis8-Ypet at low levels to obtain single foci that are required for analysis with ISbatch (batch-processing platform for data analysis of live-cell single-molecule microscopy images) (18) and followed bleaching of the fusion protein in the absence or presence of 2 mM Cbl in the growth medium. This method allows to determine the number of protomers in a complex, which is equal to the number of bleaching steps and can be derived from the expression $n = I_{foci}\ I_{step}^{-1}$ (where n is the number of protomers and I is the intensity of the foci and the bleaching step, respectively) (19). Thus, we expect for monomeric or dimeric $BtuM_{Td}$_cHis8-Ypet one or two bleaching steps, respectively (and so on for higher oligomers). When $BtuM_{Td}$_cHis8-Ypet was expressed without the presence of Cbl and was thus in its *apo* form, we only could

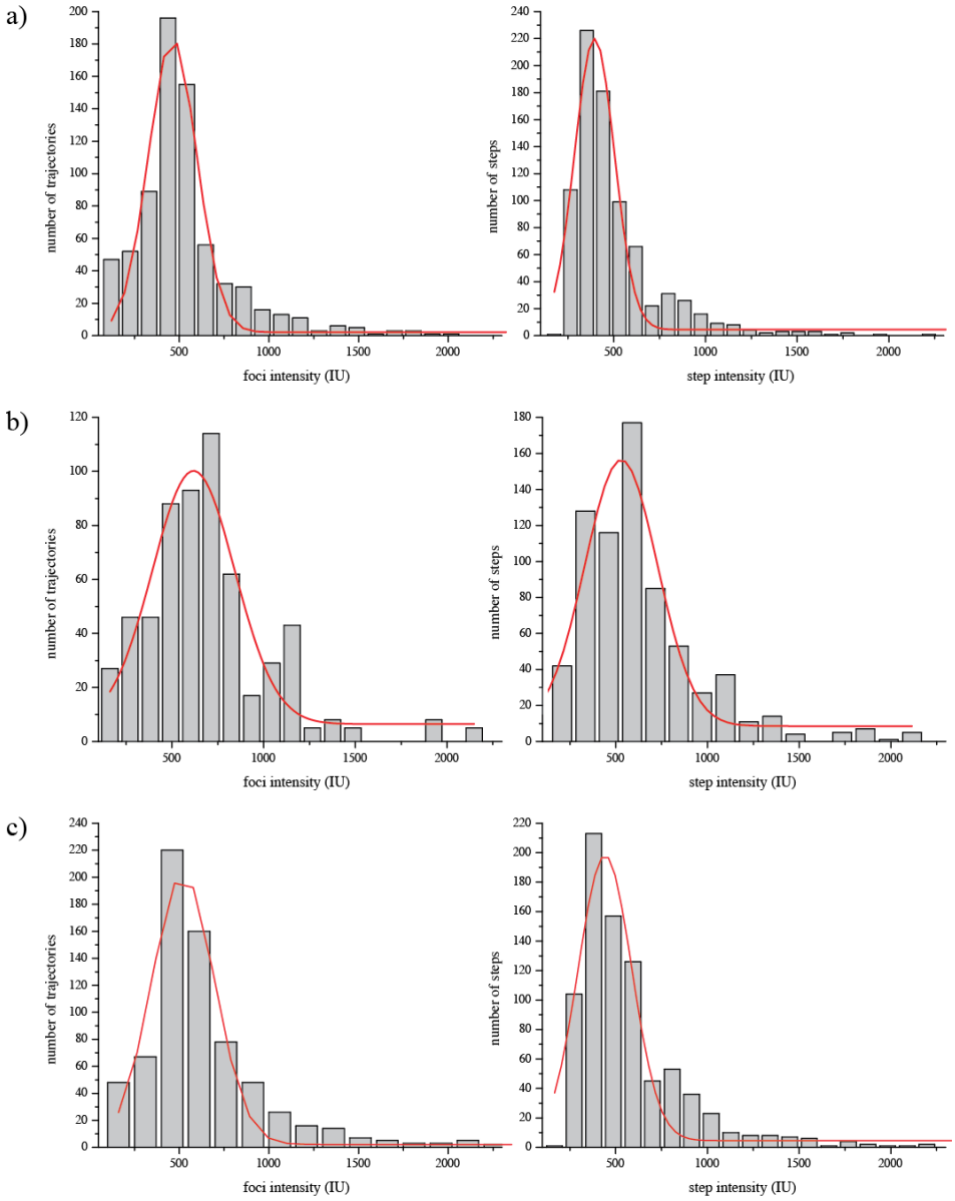

Figure 3: Single molecule *in vivo* oligomeric state determination. a) In the *apo* state (n = 376), $BtuM_{Td}$_cHis8-Ypet foci have a mean intensity of 462.7 intensity unit (IU, σ = 133.7 IU), which bleach with a mean step size intensity of 395.1 IU (σ = 108.6 IU. b) In the presence of 2 mM Cbl (n = 799), the mean foci intensity is 617.8 IU (σ = 197.7 IU), which bleach with a mean step size intensity of 529.4 IU (σ = 224.6 IU). Because low expression may hamper dimer formation, the L-arabinose concentration was increased in the presence of substrate (1 ng *apo* and 7.5 ng with Cbl). In both cases foci bleach in a single steps, meaning that $BtuM_{Td}$ is monomeric. c) As a positive control LacY_eYFP was probed under the same condition as *apo* $BtuM_{Td}$. The foci of n = 726

find single bleaching step events and hence observed only monomeric $BtuM_{Td}$ (**Figure 3a**). Because normally the inducer concentration is chosen such that only one focus per cell appears to facilitate analysis, low expression levels may hamper oligomerization in the presence of substrate. Therefore, the L-arabinose concentration was increased when Cbl was added to $BtuM_{Td}$_cHis8-Ypet expressing cells. Also under these conditions we only observe single bleaching step events, indicating that no higher oligomer is present (**Figure 3b**). As a monomeric control, we used LacY (20) fused to eYFP (LacY-eYFP) and also observed As a monomeric control, we used LacY (20) fused to eYFP (LacY-eYFP) and also observed only the expected monomeric species (**Figure 3c**).

Discussion

We investigated the oligomeric state of the solitary S-component, $BtuM_{Td}$ with two techniques, SEC-MALLS and *in vivo* single-molecule fluorescent bleaching experiments. SEC-MALLS analysis shows that *apo* $BtuM_{Td}$ is monomeric, but partial dimer formation occurs in the substrate-bound state of the His-tagged construct. If the affinity-tag is absent, no dimerization is present, which can be explained by crystal contacts in the structure of $BtuM_{Td}$. In the crystal, two $BtuM_{Td}$ molecules align almost antiparallel, and the His-tag of one $BtuM_{Td}$ binds to the bound Cbl substrate of the other $BtuM_{Td}$ protein and *vice versa* (9). The partial dimer formation in detergent solution likely is a similar artificial assembly, because it can only be observed when Cbl, the anchoring point of the His-tag, is bound to $BtuM_{Td}$. Therefore, the addition of the His-tag causes an artefact. The unnatural nature of the change in oligomeric state was corroborated using an *in vivo* approach, which showed that $BtuM_{Td}$ is monomeric under substrate-free and substrate-bound conditions. Although the fusion to a fluorescent Ypet protein affects the activity of $BtuM_{Td}$, the *in vivo* oligomeric state determination is of value, since *in vivo* experiments offer a more physiological environment, especially for membrane proteins that otherwise are kept in detergent solution. It is possible that the Ypet fusion may sterically interfere with dimer formation, forcing $BtuM_{Td}$ to be monomeric in the single-molecule experiments, but there is also the possibility that the Ypet fusion interferes with the proposed toppling mechanism of transport (9), not affecting the

Figure 4: Consensus sequence of BtuM homologs. BtuM homologs (224 in total) were identified and aligned using the iterative jackHMMER search engine (30). Conservation scores were assigned in Jalview (31) ranging from high (blue) to low (grey) with the corresponding consensus sequence of all homologs. The part of the sequence corresponding to helix H1 in $BtuM_{Td}$ is marked (between red lines) showing that the A-X-X-X-A motif is not part of the BtuM homolog consensus sequence.

oligomeric state, and only thereby rendering $BtuM_{Td}$ inactive in the growth assay. If the latter is true, the microscopy results are valid.

In conclusion, only the complementary use of techniques, ruling out methodological effects on the oligomeric state (detergent micelles and membrane environment on the one hand, and unmodified $BtuM_{Td}$ and Ypet fusion protein on the other hand), allows for the conclusion that $BtuM_{Td}$ is monomeric. The results also demonstrate, that modifications can greatly alter the behavior of a protein, in unexpected ways as demonstrated by the His-tag binding to the substrate that is bound to a second $BtuM_{Td}$ molecule (9), or the fusion to a fluorescent protein. Therefore suitable control experiments must be included to show that any non-natural modifications are not altering the native properties of a protein, which has been done here with the complementary approach of techniques.

Investigation into the oligomeric state of S-components has been done for the biotin-specific, isolated S-component BioY from *Rhodobacter capsulatus* ($BioY_{Rc}$), RibU (riboflavin-specific), ThiT (thiamin-specific), and BioY from *Lactococcus lactis* ($BioY_{Ll}$) (11–14, 21). Only for $BioY_{Rc}$,

Kirsch *et al.* and Finkenwirth *et al.* claimed that the S-component exists as a higher oligomer (11, 21). However, the authors prepared homo $BioY_{Rc}$ tandem fusion proteins and only with these fusions a higher oligomeric state occurred that otherwise could not be observed (11). In contrast, the homologous $BioY_{Ll}$ was shown to be monomeric, like ThiT and RibU (12–14). Because S-components share a highly conserved fold (12, 14, 22–26), and in combination with our results, showing that non-physiological modifications can result in non-natural behavior, we hypothesize that $BioY_{Rc}$ is also monomeric.

But the question remains what properties make solitary S-components and non-solitary S-components, which strictly require an ECF-complex for transport, so different (9, 10, 17)? For example, the Cbl-specific S-component CbrT strictly requires an ECF-module, whereas Cbl-specific $BtuM_{Td}$ does not (9, 17). One difference is an interaction motif between S-component and the transmembrane domain of the ECF complex. S-components that require the full complex have a conserved motif (A-X-X-X-A where 'X' is any amino acid) in the first transmembrane helix H1 (5, 14), which is absent in $BtuM_{Td}$. A multi-sequence alignment of all identifiable BtuM homologs (now 224 homologs, previously 131 (9)) shows that none of these carries this motif (**Figure 4**). Therefore, it appears that BtuM homologs have evolved to transport substrate independently of an ECF-module and are a distinct within the family of S-components. Additionally, because $BtuM_{Td}$ appears to have lost the necessity for an ECF-module and also features enzymatic activity, decyanating cyano-cobalamin before transport (9), the S-component fold seems to be a versatile chassis for a variety of functions, ranging from membrane-embedded high affinity substrate binding proteins for structurally and chemically diverse compounds, over solitary, independent transporters, to enzyme-like function (1, 5, 9, 10). Similarly, also the over 800 G-protein coupled receptors (GPCRs), of which all structures solved have a conserved fold, have a hugely diverse set of different ligands (27). Thus, also the GPCR fold allows for a variety of functions and it seems, although the diversity of structural folds in membrane proteins may be limited due to membrane environment constraints (28, 29), their functionality may not follow this restriction.

Materials and Methods

Sequence analysis

$BtuM_{Td}$ sequences and alignments were obtained as described before (9, 30). The sequences were aligned in Jalview (31) to obtain the consensus sequence of BtuM homologs.

Molecular methods

The expression plasmid for $BtuM_{Td}$_cHis8 (pBAD24_B tuM_{Td}_cHis8) was constructed before (9). The pBAD24_$BtuM_{Td}$_cTEV-His8 expression vector was constructed using restriction cloning with overhanging primers (forward primer with *NcoI*-site 5'-GGTCCATGGGTCTGAATCTGACCCGTCGTCAGCAGATTGC-3' and reverse primer with TEV-His8 site, stop-codon, and *HindIII*-site 5'-AATAAGCTTTCATTAGTGGTGGTGATGGTGATGATGATGTCCC TGAAAGTACAGATTCTCACGTTCACGACGGGTG-3') to insert the TEV cleavage site with *NcoI* and *HindIII* restriction sites. The vector for the expression of the fluorescently tagged $BtuM_{Td}$ (pBAD24_$BtuM_{Td}$_cHis8-Ypet) was constructed using the Gibson Assembly kit (NEB) and a flexible linker (15) was inserted after the His-tag and Ypet ($BtuM_{Td}$_GibsAssem forward primer 5'-AGCAGGAGGAATTCACCAATGGGTCTGAATCTGACC-3', $BtuM_{Td}$_ GibsAssem reverse primer 5'-GCCGACATATGATGGTGATGGTGGTG-3', Ypet_GibsAssem forward primer 5'-CACCATCATTCGGCTGGCTCCGCTGC-3', Ypet_GibsAssem reverse primer 5'-GATCCCCGGGTACCATCATTAGAGCTCTTTGTACAATTCATTC ATACCC-3', the backbone forward primer 5'-TGGTACCCGGGGATCCTC-3', and the backbone reverse primer 5'-TGGTGAATTCCTCCTGCTAGC-3'). All constructs were checked by sequencing for correctness.

Overexpression, purification, TEV-cleavage and SEC-MALLS analysis

Substrate-free or substrate-bound $BtuM_{Td}$_cHis8 and $BtuM_{Td}$_cTEV-His8 were overexpressed and purified in DDM and K-P_i buffer as previously described (9). TEV cleavage was initiated with Ni^{2+}-NTA immobilized

protein after washing by the addition of 500 µl SEC-buffer and 30 µl TEV protease (Promega, 8,000 units). The reaction was incubated for 21 hours at 4°C on a moving platform. Cleaved protein was eluted without imidazole and used for SEC purification as described (9). SEC-MALLS was performed as described before (13, 32). The analysis of the data requires the extinction coefficient of the protein. For *apo* protein the amino acid derived extinction coefficient (ε_{280} = 40,910.0 M^{-1} cm^{-1}, Protparam online tool) was used. Because cobalamin absorbs strongly at 280 nm and binding to $BtuM_{Td}$ changes the spectrum (9) of the substrate, the extinction coefficient was determined experimentally. The absorption of Cbl-bound $BtuM_{Td}$ was measured at 280 nm with purified protein in buffer supplemented with 50 µM Cbl and the protein concentration was determined using a bicinchoninic acid (BCA). The resulting extinction coefficient of $BtuM_{Td}$ bound to Cbl at 280 nm calculated with Lambert-Beer's law is ε_{280} = 53581.9 M^{-1} cm^{-1}.

Cell preparation for microscopy

Escherichia coli MC1061 (33) carrying pBAD24_$BtuM_{Td}$_cHis8-Ypet or _LacY-eYFP were pre-cultured overnight in EZ rich defined medium (Teknova) supplemented with 0.2% (v/v) glycerol and 100 µg ml^{-1} ampicillin at 37°. The pre-culture was used to inoculate the main culture in a 1:1,000 ratio that was supplemented with 1 ng ml^{-1} (*apo*) or 7.5 ng ml^{-1} (Cbl) L-arabinose. The main culture (500 µl) was grown at 37°C until visible growth could be detected by eye. For *apo* $BtuM_{Td}$ and LacY formaldehyde (Sigma Aldrich) was added to a final concentration of 3.7% (v/v) and the culture was incubated for ten minutes at room temperature. Cells were washed once with the same volume EZ medium and used for imaging. For substrate-bound $BtuM_{Td}$ cells were first washed in three-times the volume of a 2 mM cyano-cobalamin (Acros Organics) and 50 mM K-Pi pH 7.0 solution with 15 minutes incubation at 37°C prior to formaldehyde addition. Cells were washed with the 2 mM cyano-cobalamin and 50 mM K-Pi pH 7.0 solution and used for imaging.

Growth assay

The growth assay with $BtuM_{Td}$_cHis8, $BtuM_{Td}$_C80S_cHis8, and $BtuM_{Td}$_cHis8-Ypet was done as described before (9, 17).

Single molecule microscopy for in vivo *oligomeric state determination*

High Precision 24x60 mm cover slips were cleaned by sonication in 5 M KOH for one hour, washed extensively with ddH_2O, dried, and functionalized by addition of 0.1% (w/v) in ddH_2O poly-L-lysine solution (Sigma-Aldrich) for five minutes at room temperature. Residual poly-L-lysine solution was removed by rinsing with ddH_2O. After drying, a droplet of cell suspension was applied and imaged on a home-build, fully automated, inverted single molecule microscope (Olympus IX-81, *apo* $BtuM_{Td}$ and LacY or Olympus IX-83, substrate-bound $BtuM_{Td}$) for 100 ms with 1 frame ms^{-1}. Excitation was provided by a coherent laser at 514 nm (Sapphire). Data analysis was conducted in ImageJ with the ISbatch plugin on flattened and discoidal filtered images (18). Obtained trajectories were binned and plotted in Matlab. Fitting with normal distribution was done in OriginPro8.

Acknowledgments

We would like thank Prof. Dr. B. Poolman, University of Groningen, for the use of the microscope and Dr. H. Ghodke, University of Wollongong, for the Ypet containing plasmid. We would like to acknowledge the help with scripting provided by I.L. Rempel, Groningen University Hospital (UMCG), and Dr. J.M.H. Goudsmits, University of University of Technology Sidney). The pBAD24_LacY-eYFP plasmid was a generous gift from Dr. J.T. Mika.

References

1. Rodionov DA, Hebbeln P, Eudes A, Ter Beek J, Rodionova IA, et al. 2009. A novel class of modular transporters for vitamins in prokaryotes. *J. Bacteriol.* 91(1):42–51
2. ter Beek J, Guskov A, Slotboom DJ. 2014. Structural diversity of ABC transporters. *J. Gen. Physiol.* 143(4):419–35
3. Oldham ML, Chen J. 2011. Crystal structure of the maltose transporter in a pretranslocation intermediate state. *Science*

332(6034):1202–5
4. Hvorup RN, Goetz BA, Niederer M, Hollenstein K, Perozo E, Locher KP. 2007. Asymmetry in the Structure of the ABC Transporter-Binding Protein Complex BtuCD-BtuF. *Science* 317(5843):1387–90
5. Slotboom DJ. 2014. Structural and mechanistic insights into prokaryotic energy-coupling factor transporters. *Nat. Rev. Microbiol.* 12(2):79–87
6. Xu K, Zhang M, Zhao Q, Yu F, Guo H, et al. 2013. Crystal structure of a folate energy-coupling factor transporter from Lactobacillus brevis. *Nature*. 497(7448):268–71
7. Wang T, Fu G, Pan X, Wu J, Gong X, et al. 2013. Structure of a bacterial energy-coupling factor transporter. *Nature*. 497(7448):272–76
8. Rodionov DA, Vitreschak AG, Mironov AA, Gelfand MS. 2003. Comparative Genomics of the Vitamin B12 Metabolism and Regulation in Prokaryotes. *J. Biol. Chem.* 278(42):41148–59
9. Rempel, S., Colucci, E., de Gier, J.W., Guskov, A., Slotboom DJ. 2018. Cysteine-mediated decyanation of vitamin B12 by the predicted membrane transporter BtuM. *Nat. Commun.*, pp. 1–8
10. Finkenwirth F, Kirsch F, Eitinger T. 2013. Solitary bio Y proteins mediate biotin transport into recombinant Escherichia coli. *J. Bacteriol.* 195(18):4105–11
11. Kirsch F, Frielingsdorf S, Pohlmann A, Eitinger T, Ziomkowska J, Herrmann A. 2012. Essential amino acid residues of BioY reveal that dimers are the functional S unit of the Rhodobacter capsulatus biotin transporter. *J. Bacteriol.* 194(17):4505–12
12. Berntsson RP-A, ter Beek J, Majsnerowska M, Duurkens RH, Puri P, et al. 2012. Structural divergence of paralogous S components from ECF-type ABC transporters. *Proc. Natl. Acad. Sci.* 109(35):13990–95
13. Erkens GB, Slotboom DJ. 2010. Biochemical characterization of ThiT from lactococcus lactis: A thiamin transporter with picomolar substrate binding affinity. *Biochemistry*. 49(14):3203–12
14. Zhang P, Wang J, Shi Y. 2010. Structure and mechanism of the S component of a bacterial ECF transporter. *Nature*. 468(7324):717–20
15. Moolman MC, Krishnan ST, Kerssemakers JWJ, van den Berg A, Tulinski P, et al. 2014. Slow unloading leads to DNA-bound β2-

sliding clamp accumulation in live Escherichia coli cells. *Nat. Commun.* 5:5820
16. Cadieux N, Bradbeer C, Reeger-Schneider E, Köster W, Mohanty AK, et al. 2002. Identification of the periplasmic cobalamin-binding protein BtuF of Escherichia coli. *J. Bacteriol.* 184(3):706–17
17. Santos JA, Rempel S, Mous ST, Pereira CT, ter Beek J, et al. 2018. Functional and structural characterization of an ECF-type ABC transporter for vitamin B12. *Elife*. 7:e35828
18. Caldas VEA, Punter CM, Ghodke H, Robinson A, Van Oijen AM. 2015. ISBatch: A batch-processing platform for data analysis and exploration of live-cell single-molecule microscopy images and other hierarchical datasets. *Mol. Biosyst.* 11(10):2699–2708
19. Leake MC, Chandler JH, Wadhams GH, Bai F, Berry RM, Armitage JP. 2006. Stoichiometry and turnover in single, functioning membrane protein complexes. *Nature*. 443(7109):355–58
20. Costello MJ, Escaigell J, Matsushitaji K, Viitanenii P V, Menick DR, Kabackii HR. 1987. Purified lac Permease and Cytochrome o Oxidase Are Functional as Monomers. *J. Biol. Chem.* 262(35):17072–82
21. Finkenwirth F, Neubauer O, Gunzenhäuser J, Schoknecht J, Scolari S, et al. 2010. Subunit composition of an energy-coupling-factor-type biotin transporter analysed in living bacteria. *Biochem. J.* 431(3):373–80
22. Erkens GB, Berntsson RPA, Fulyani F, Majsnerowska M, Vujiĉić-Žagar A, et al. 2011. The structural basis of modularity in ECF-type ABC transporters. *Nat. Struct. Mol. Biol.* 18(7):755–60
23. Swier LJYM, Guskov A, Slotboom DJ. 2016. Structural insight in the toppling mechanism of an energy-coupling factor transporter. *Nat. Commun.* 7:11072
24. Zhao Q, Wang C, Wang C, Guo H, Bao Z, et al. 2015. Structures of FolT in substrate-bound and substrate-released conformations reveal a gating mechanism for ECF transporters. *Nat. Commun.* 6:
25. Josts I, Almeida Hernandez Y, Andreeva A, Tidow H. 2016. Crystal Structure of a Group I Energy Coupling Factor Vitamin Transporter S Component in Complex with Its Cognate Substrate. *Cell Chem. Biol.* 23(7):827–36
26. Yu Y, Zhou M, Kirsch F, Xu C, Zhang L, et al. 2014. Planar substrate-binding site dictates the specificity of ECF-type nickel/cobalt transporters. *Cell Res.* 24(3):267–77

27. B. Gacasan S, L. Baker D, L. Parrill A. 2017. G protein-coupled receptors: the evolution of structural insight. *AIMS Biophys.* 4(3):491–527
28. Feng X, Barth P. 2016. A topological and conformational stability alphabet for multipass membrane proteins. *Nat. Chem. Biol.* 12(3):167–73
29. Von Heijne G. 2006. Membrane-protein topology
30. Finn RD, Clements J, Arndt W, Miller BL, Wheeler TJ, et al. 2015. HMMER web server: 2015 Update. *Nucleic Acids Res.* 43(W1):W30–38
31. Waterhouse AM, Procter JB, Martin DMA, Clamp M, Barton GJ. 2009. Jalview Version 2-A multiple sequence alignment editor and analysis workbench. *Bioinformatics*. 25(9):1189–91
32. Slotboom DJ, Duurkens RH, Olieman K, Erkens GB. 2008. Static light scattering to characterize membrane proteins in detergent solution. *Methods*. 46(2):73–82
33. Casadaban MJ, Cohen SN. 1980. Analysis of gene control signals by DNA fusion and cloning in Escherichia coli. *J. Mol. Biol.* 138(2):179–207

Chapter 5

Summary and perspective on vitamin B12 transport

Abstract

Vitamin B12 is only produced by a subset of bacteria and archaea, making ~50% of prokaryotes auxotrophic for vitamin B12, which need to take up the compound by yet to identify transport systems. In 2003 and 2009, two systems, BtuM and ECF-CbrT, respectively, where predicted by Rodionov, *et al*. to be potential vitamin B12 transporters. BtuM has no sequence identity to any known protein and ECF-CbrT belongs to the energy coupling factor (ECF-) type ABC transporter family. Using *in vivo* growth assays with recombinant *Escherichia coli* strains and BtuM from *Thiobacillus denitrificans* ($BtuM_{Td}$) we showed that $BtuM_{Td}$ indeed is a vitamin B12 transporter. The high-resolution crystal structure and spectroscopic data revealed that an unusual thiolate coordination between a cysteine residue and the cobalt ion of vitamin B12 allows for chemical modification of the substrate, which is unprecedented in vitamin B12-transport proteins. Additionally, we confirmed that ECF-CbrT from *Lactobacillus delbrueckii* transports vitamin B12 and its precursor cobinamide. Kinetic studies and binding measurements reveal that the rate limiting step for transport by ECF-CbrT is substrate translocation and that the transporter is promiscuous for different vitamin B12 variants. The crystal structure of the complex in an *apo*, post-substrate release state shows is similar to previously resolved states of other ECF-transporters, with minor alterations that may point toward a slightly different intermediate in the transport cycle. Our results indicate that transport of this biologically unique and important vitamin is mechanistically not uniformly accomplished and potentially paves the way for the discovery and description of more uncharacterized vitamin B12 transporters like ABCD4, BtuN, and Rv1819c.

Summary

All cells need to constantly and specifically exchange molecules with their surroundings, either to expel metabolic waste products and toxic compounds, or to take up nutrients to sustain growth, proliferation, and survival in an everchanging environment. This crucial aspect of life is served by membrane spanning transport proteins. These transporters must have a variety of different characteristics to be able to fulfil their role: In the direction of transport, transport proteins need to bind their substrate, then undergo a dynamic transition to expose the substrate loaded binding site to the other side. Differently from facilitating transporters, active transporters, which use a driving force to catalyze transport additionally need to render their binding site to a low affinity state to release the substrate. Next, reorientation of the empty carrier must occur, whilst preventing leakage of substrate or other cellular compounds. To avoid the latter, transporters alternatingly expose the substrate binding site to the sides of the membrane and close the substrate binding site with gates. This alternating access mechanism of transport is achieved by four currently known mechanisms. The rocker-switch mechanism, where the protein alternatingly opens and closes the substrate binding site around a hinge region, the gated pore mechanism, where gates open alternatingly with a fully occluded intermediate state, the elevator mechanism, which is similar to the gated pore, but also involves shuttling transitions of a transport domain through the membrane relative to a scaffold domain, and, finally, toppling, where the gated substrate binding site is moved from one side to the other by a rotation of the transporter by ~90° (1–3).

S-components of energy coupling factor (ECF-) type ABC transporters are the only known membrane proteins that employ the toppling mechanism, which makes them a distinct group in the ABC transporter superfamily (3, 4). ABC transporters catalyze transport of their substrates at the expense of ATP hydrolysis and either catalyze export or import of substrates, which comprise a vast variety of chemically and structurally unrelated compounds (4, 5). While exporters consist of nucleotide binding domains and transmembrane domains, importers are thought to strictly require a substrate binding protein. ECF-transporters that are strict importers are no exception from this rule and need a substrate binding protein for transport, which differs from other ABC-importer substrate binding proteins in that it is a membrane protein and topples over to move the substrate through the membrane (3, 4, 6). Additionally, in a subset of ECF-transporters

several S-components with different substrate-specificities can dynamically associate with the rest of the complex, which is thus referred to as the ECF-module (3, 6).

ECF-type ABC transporter are a relatively recent addition to ABC-transporters. These systems were formally described for the first time in 2009 and it was concluded from genomic context analyses that the substrates are in large parts micronutrients, like B-type vitamins (6). One of the predicted substrates is vitamin B12 (cobalamin) (6). Cobalamin is an intriguing molecule from a chemical, metabolic, and transporter point of view. It is considered the largest and most complex 'small molecule' (7). Probably because of its complexity and thus its energetically costly biosynthesis, only a small number of prokaryotes can synthesize cobalamin *de novo*, leaving ~50% of prokaryotes vitamin B12 auxotrophs, which require an uptake system (8). However, until recently the only characterized cobalamin transporter was the *Escherichia coli* ABC transporter BtuCDF, and not all cobalamin auxotrophs carry a homolog. Instead, a subset of these auxotrophic bacteria has the genes for the predicted vitamin B12 specific ECF-transporter, ECF-CbrT (8–10).

Using an *E. coli* triple knock out strain (*E. coli* ΔFEC) that no longer can import cobalamin via BtuCDF due to genomic deletions of *btuF* (substrate binding protein) and *btuC* (transmembrane domain), and requires the vitamin to be able to synthesize L-methionine because the independent route is also abolished by deletion of *metE* (cobalamin independent methionine synthase, MetE), we showed that ECF-CbrT from *Lactobacillus delbrueckii* is a vitamin B12 transporter (10, 11). *In vitro* experiments with into proteoliposomes reconstituted ECF-CbrT and substrate binding studies, allowed for the further elucidation of substrate specificity, transport kinetics, and determination of the rate limiting step of transport: As expected for an ABC transporter, the system strictly requires the presence of Mg-ATP to fuel transport. ECF-CbrT catalyzes the uptake of several cobalamin analogs (cyano-cobalamin, hydroxyl-cobalamin, methyl-cobalamin, and 5'-deoxyadenosylcobalamin; the latter two are the physiological active variants) and the cobalamin precursor cobinamide, but not the structurally related compound hemin (7). Uptake occurs with a K_M of 2.1 ± 0.4 nM and V_{max} of 0.06 ± 0.01 nmol mg^{-1} s^{-1}. Because the S-component CbrT binds its substrates with a affinities that are in the same range, the rate limiting step for transport is substrate translocation and not substrate capture (10).

A high-resolution X-ray structure of the full ECF-CbrT complex was determined at 3.4 Å resolution and showed the same overall conformation as previously determined structures of other ECF-transporters (10, 12–16). ECF-CbrT is in the *apo* inward-oriented, post substrate release state and exhibits subtle differences to previous structures (10, 12–16). First, one of the gating loops (loop L3) of CbrT occludes the predicted binding site, which may represents an intermediate state in the transport cycle, which is marginally closer to resetting of the transporter compared to other structures (10, 12–16). After substrate release, at which state all gating loops are pried open, these loops eventually have to close, because the S-component has to topple back to expose its binding site to the exterior of the cell. If the gates would remain open during reorientation, the hydrophilic binding site would be exposed to the hydrophobic membrane environment, which would make toppling impossible. Secondly, the ECF-CbrT structure shows when compared to the structure of ECF-FolT2 (15), which both have exactly the same ECF-module, that different S-components (CbrT and FolT2) are accommodated by flexibility in the transmembrane domain relative to its cytosolic coupling domain of ECF-T (scaffold protein in the ECF-module) (10).

Using the same recombinant *E. coli* ΔFEC strain as before, we also showed, that BtuM from *Thiobacillus denitrificans* ($BtuM_{Td}$) that was predicted in 2003 is a vitamin B12 transporter (8, 17). The transporter has no sequence similarity to any other known protein but, intriguingly and surprisingly, the high-resolution X-ray crystal structure at 2.0 Å resolution revealed, that $BtuM_{Td}$ is structurally similar to S-components. It does not make use of an ECF module, and therefore qualifies as a solitary S-component, capable of ECF-module independent transport, as evidenced by the heterologous expression in the growth assay, and absence of an ECF-module in the original host. Additionally, BtuM homologs do not carry an interaction motif, that is used by non-solitary S-components to interact with ECF-T. Because solitary S-components presumably use a toppling mechanism to achieve transport (17), it is disputed whether a protein partner, like for example in a multimer, is required to facilitate the toppling movement. Therefore, we investigated the oligomeric state with *in vitro* (SEC-MALLS; size exclusion chromatography-multi angle laser light scattering) and *in vivo* (single-molecule fluorescent microscopy) experiments, which strongly suggest that $BtuM_{Td}$ is monomeric.

The crystal structure of $BtuM_{Td}$ additionally revealed an unprecedented binding mode of vitamin B12 that is linked to chemical modification of the substrate prior to transport, which is a rare feature among membrane transporters (17). The main distinguishing feature in the binding mode of $BtuM_{Td}$ is the cysteine to cobalt ion ligation on the α-face (see chapter 3, Figure 1a for schematics of vitamin B12 architecture and nomenclature) of the corrin ring. This for native proteins unprecedented interaction, replaces the intramolecular coordination of the cobalt ion, that makes use of the 5,6-dimethylbenzimidazole ribonucleotide moiety, resulting in conversion of cobalamin into its base-off conformation. The cysteine residue is invariably conserved among BtuM homologs and is essential for transport activity. The cysteine to cobalt ion ligation also results in decyanation of cyano-cobalamin at the β-axial position. To study this enzymatic modification and to prevent interference from base-on to base-off conversion, cobinamide instead of cobalamin was used for assays with detergent solubilized $BtuM_{Td}$. Cobinamide lacks the 5,6-dimethylbenzimidazole ribonucleotide moiety and therefore mimics the base-off conformation of cobalamin. The decyanation reaction is slow with an apparent time constant of $\tau = 12.0 \pm 0.7$ minutes and the only critically involved residue appears to be the conserved cysteine residue. Because cobinamide binding could also be measured with isothermal titration calometry (ITC), which is an assay that probes much quicker events, it was concluded that substrate binding with a K_D between 0.58 – 0.65 μM and decyanation are separate events. A mutant version of $BtuM_{Td}$, where the cysteine is replaced with a serine, still binds cobinamide (albeit with a ~10-fold lower affinity), but cannot modify the substrate, further corroborating that events are separate. Additionally, this mutant can no longer bind cobalamin, which implies that the cysteine is also involved in converting the vitamin into its base-off conformation (17).

In conclusion, two previously predicted vitamin B12 transporters were structurally and biochemically characterized. This study sheds light on the diversity of membrane transport for cobalamin and it illustrates, that *in vivo* screening is a powerful tool to both screen and pivotally characterize novel vitamin B12 uptake systems. While ECF-CbrT appears to be a 'conventional' ABC-transporter uptake system, which could be characterized with standard methodology, $BtuM_{Td}$ required and will require a diverse approach to elucidate its function that, next to its transporter activity, also includes enzymatic activity. This work may form the basis to better understand transport by solitary S-components, the

potential involvement of cellular redox potential in transport (see below), and how molecular machines have evolved to serve the individual uptake needs of various types of cells for vitamin B12.

Perspective on vitamin B12 transport

The future in vitamin B12 transport potentially holds intriguing fundamental discoveries, but also particular questions, that are discussed in the following paragraphs, will further our understanding of specific systems. Fundamentally, new cobalamin transporters that evaded detection or characterization, could vastly expand our understanding of membrane protein transport. For example, humans possess an ABC-transporter, ABCD4, that transports vitamin B12 (18). A study showed that it is localized in the lysosomal membrane of the cell. ABCD4 then transports cobalamin, which has been liberated from its protein-chaperone by proteolysis inside the lysosomal compartment, into the cytosol of the cell (18, 19). This casual notion has serious consequences on what we believe is true about ABC-transporters. Mammals are thought to exclusively have ABC-exporters (5), but, because the lysosomal compartment is devoid of ATP, the nucleotide binding domains of ABCD4 must be in the cytosol and, thus, direction of transport cannot be that of an ABC-exporter. Therefore, ABCD4 could be a mammalian ABC-importer. Hence, not only in bacteria, where BtuN may be a periplasm spanning vitamin B12 transporter, BtuM may add the redox potential as a driving force for transporters, or Rv1819c that may be an ABC importer with an exporter type fold (all see below), but also in humans with clinically relevant targets, curiosity driven basic research will result in findings, which will shape and further our basic understanding of membrane (ABC) transporters.

ECF-CbrT

Although the group II ECF-transporter for vitamin B12, ECF-CbrT, has been intensively structurally and biochemically characterized (10), several key questions remain. Because there are also group I homologs of the system, called CbrTUV (6), it is likely and tempting to assume that these systems also represent functional vitamin B12 transporters. This remains to be shown. An attempt to detect activity of CbrTUV from *Brochothrix*

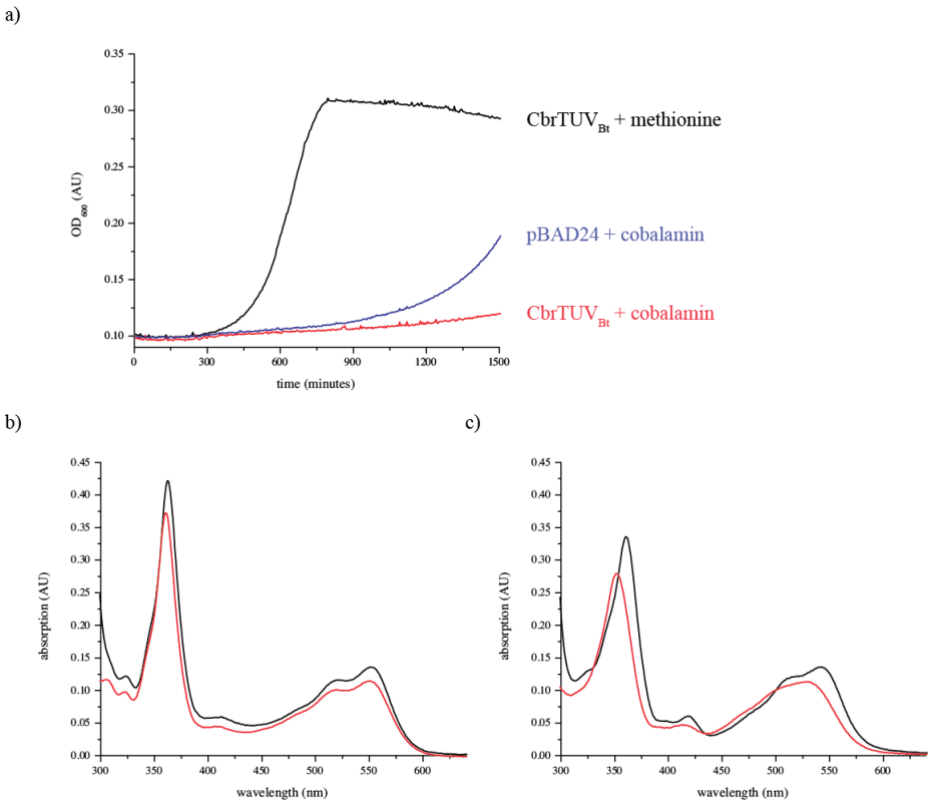

Figure 1: Growth assay with CbrTUV from *Brochothrix thermosphacta* and spectra of substrate bound *Lactobacillus delbrueckii* CbrT. a) Growth assay with *E. coli* ΔFEC expressing the predicted group I ECF-transporter for vitamin B12, CbrTUV, showing that it cannot sustain growth in the presence of cobalamin (red), similar to the negative control (blue). In contrast, when expressing CbrTUV in the presence of L-methionine (black), cells grow. b) Absorption spectra of CbrT, bound to cyano-cobalamin (black) compared to 15 μM unbound substrate (red). c) same as in b) but with hydroxyl-cobalamin.

thermosphacta in *E. coli* ΔFEC failed however (**Figure 1a**), potentially due to poor expression behavior. Using homologs from other organisms is a promising route to circumvent this problem. Next, the location of the cobalamin binding site in CbrT has only been hypothesized based on the common structural architecture of S-components and the presence of a deep cavity in CbrT in the context of the full complex structure, which is decorated with conserved amino acid residues (10). A mutational analysis or an X-ray structure of CbrT in complex with cobalamin will show the location and, in the case of the latter, how vitamin B12 is bound. The binding mode is of particular interest in light of the unusual binding mode of $BtuM_{Td}$ (17), although there is experimental evidence hinting that neither base-off conversion, nor direct interaction with the cobalt ion

occurs (**Figure 1b and c**). Thus, CbrT may exhibit a for substrate binding proteins 'conventional' binding mode, which does not allow for modification of the substrate. Finally, because cobalamin strongly absorbs visible light, ECF-CbrT in combination with size exclusion co-elution experiments may be a suitable model system to investigate under which conditions dissociation of CbrT from the full complex occurs, similar to what has been done for ECF-RibU in the past (20). In short, the current working model of ECF-type transport assumes, that ATP-binding leads to release of the S-component from the ECF-module. If ECF-CbrT is purified in the presence of ATP and cobalamin, released CbrT would bind Cbl, which is detectable due to the strong absorption of the vitamin at 361 nm.

BtuM$_{Td}$

BtuM$_{Td}$ supposedly represents a novel class of transporter. Not surprisingly, many basic questions remain to be answered (17). The most puzzling and unresolved finding is that BtuM$_{Td}$ binds cobalamin only when added before solubilization, but with such high affinity that it stays bound throughout the purification and subsequent experiments, such as crystallization or electron spray mass spectrometry. We excluded that the essential cysteine is modified in the *apo* protein using mass spectrometry, which may prevent substrate binding, leaving the major difference between the unpurified and purified protein the membrane environment. Extensive ITC binding studies with different cobalamin analogs were carried out on crude membrane vesicles containing overexpressed BtuM$_{Td}$ in analogy to CbrT binding studies, but no binding could be observed. To rule out that too low expression levels obscure binding detection, cobinamide, whose binding to BtuM$_{Td}$ can be detected with ITC, was used as a positive control in the crude membrane vesicle ITC experiments. Because cobinamide binding was not observed with crude membrane vesicles, the expression level may be too low to use this type of experiment. Therefore, binding studies in reconstituted systems may be more suitable, but two questions remain: does BtuM$_{Td}$ retain its ability to bind cobalamin during the purification procedure that precedes reconstitution, and is the defined proteoliposome environment suitable to support binding (see below)? At this point, the only statement that can be made with relative certainty, is that the α-ligand prevents cobalamin binding to *apo* BtuM$_{Td}$ in detergent solution in contrast to cobinamide that lacks it and binds to BtuM$_{Td}$. This means that conversion of cobalamin to base-off is part of the binding step and suggests that BtuM$_{Td}$ binds its

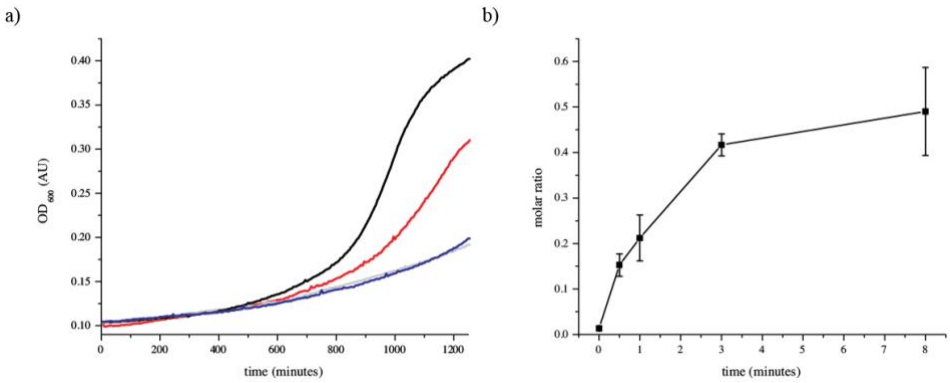

Figure 2: Growth assay of BtuM$_{Td}$ with cobinamide and uptake assay with reconstituted BtuM$_{Td}$. a) Growth of *E. coli* ΔFEC in the presence of 1 nM Cbi. Cells expressing BtuCDF (black line) or BtuM$_{Td}$ (red line) grow readily or 'intermediate', respectively. Cells expressing mutant BtuM$_{Td}$_C80S (blue line) and cells carrying the empty expression vector (grey line) show poorer growth. b) Uptake assay without proton and sodium gradient and with ^{57}Co-cobinamide (0.25 µM radiolabeled, four times diluted) and reconstituted BtuM$_{Td}$ (1.5 µg per time point) in proteoliposomes. The molar ratio does not exceed one, showing that there is either no accumulation or only binding of substrate to the protein.

substrate with an induced fit binding mode. This mode is in contrast to a conformational selection binding mode, where BtuM$_{Td}$ only binds cobalamin that already has adopted the base-off conformation. This mode however seems to be unlikely, because at physiological pH cobalamin essentially exists only in the base-on conformation and it is still bound by insolubilized BtuM$_{Td}$.

All studies with BtuM$_{Td}$ concerning ligand binding and enzyme kinetics were carried out with cobinamide (17), however it is not clear if it is a transported substrate. Growth assays in the presence of cobinamide were performed, but the experimental setup of the assay and interpretation of the results are not straight forward and unconvincing, respectively (**Figure 2a**). Therefore, an *in vitro* transport assay is required. BtuM$_{Td}$ was reconstituted into proteoliposomes and activity was observed with ^{57}Co-cobinamide (not with ^{57}Co-cobalamin), but the molar ratio of activity never exceeded one (**Figure 2b**). Thus, it cannot be distinguished between substrate binding and transport. Considering the working hypothesis that BtuM$_{Td}$ may be a high-affinity facilitator, showing *in vitro* uptake would be extremely challenging. Nonetheless, experiments with whole cells, right side out vesicles and counter-flow experiments were conducted, however unsuccessfully.

Finally, based on the cysteine-ligation and the proposed thiolate-mediated decyanation of cobalamin, which implies a redox-mechanism, another hypothesis is, that $BtuM_{Td}$ may use the redox potential of the cell to bias translocation of the substrate toward the inside of the cell. The reducing environment inside the cell allows to break the cysteine to cobalt ion bond between $BtuM_{Td}$ and cobalamin, thereby 'pulling' the substrate inside the cell. A way to measure this hypothesis may be to include reduced glutathione inside proteoliposomes, or use a system to maintain a $NAD/NADH^+$ ratio in the proteoliposome lumen, which would mimic the reducing properties of the cellular compartment.

BtuN

In the same study that predicted BtuM as a new vitamin B12 transporter, another protein, BtuN, was also predicted as such (8). From an amino acid sequence point of view, BtuN is fascinating. The protein has no sequence similarity to any other known protein, it comprises four predicted transmembrane helices, carries large extracellular loops, and a mirrored architecture. We probed BtuN from *Pseudomonas stutzeri* in the growth assay with *E. coli* ΔFEC, but found it to not support cobalamin dependent growth (**Figure 3a**). This could have several reasons next to not being cobalamin transporter. For example, *btuN* from *P. stutzeri* has a high GC-content (70%) that may interfere with expression in *E. coli* ΔFEC. Because *btuN* is co-localized with *btuB* (encodes the outer membrane active cobalamin transporter, BtuB) and carries large periplasmic loops, it may form a periplasmic space spanning complex with BtuB, which likely would require co-expression of the two genes from the same organism during the growth assay. However, another simple way to show implication in cobalamin transport, could be to show co-elution during purification. However, initial purification experiments showed that both expression and purification conditions require optimization.

Rv1819c

Rv1819c from *Mycobacterium tuberculosis* experienced growing attention since it was shown that it constitutes a vitamin B12 transporter in this organism (21). Because cobalamin uptake plays a role during *M. tuberculosis* pathogenesis, Rv1819c is of pharmacological interest (22). But also from a basic science perspective, the transporter is intriguing. Because from its predicted secondary structure, Rv1819c falls into the

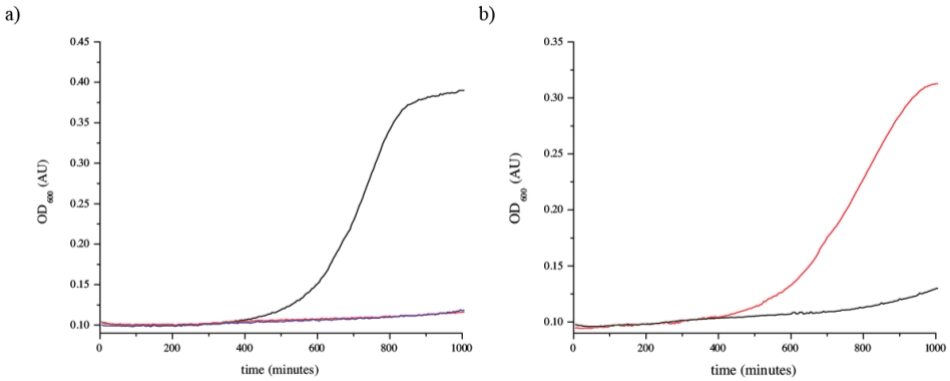

Figure 3: Growth assay with BtuN from *Pseudomonas stutzeri* and Rv1819c from *Mycobacterium tuberculosis*. a) *E. coli* ΔFEC expressing BtuN from *P. stutzeri* (red line) or carrying the empty expression vector (pBAD24, blue line) cannot grow. Only in the presence of 25 mg ml^{-1} L-methionine the BtuN expressing strain grows (black). b) Expression of *M. tuberculosis* Rv1819c in *E. coli* ΔFEC supports growth in the presence of 1 nM cobalamin (red line). In contrast, the ATP hydrolysis incapable mutant version Rv1819c_E578G cannot support cobalamin dependent growth (black line), showing that substrate transport is ATP dependent.

ABC-exporter fold. Therefore, Rv1819c may represent a new type of ABC-import with the exporter-type fold, that may be independent of a substrate binding protein (no genetic co-localization with a substrate binding protein, which would make it the first importer without one). Additionally, if Rv1819c really exhibits the ABC-exporter fold, it could mean, that direction of transport in ABC-exporters is determined on which side of the membrane the high affinity and low affinity binding site is located.

The activity of Rv1819c as a cobalamin transporter was confirmed in the growth assay (**Figure 3a**), and, moreover, with the Walker B motif glutamate-mutant it was shown that transport is ATP-dependent (**Figure 3b**). This mutant is known to inhibit ATPase hydrolysis in ABC transporters, and thereby inactivating transport. Because the major novelty lies in the elucidation of the structure of Rv1819c, we aimed for a single particle cryo-EM approach (in collaboration with Dr. C. Gati, Stanford University), which is hampered by the poor biochemical performance of the protein. Purification requires the presence of high amounts of detergent, several times above the critical micelle concentration, which causes a detrimentally high background during cryo-EM imaging. In an attempt to circumvent laborious purification optimization, the *E. coli* homolog YddA was probed for cobalamin transport. YddA is an ABC-

transporter of unknown function and was tested in the growth assay, but did not support cobalamin dependent growth.

References

1. Jardetzky O. 1966. Simple allosteric model for membrane pumps
2. Forrest LR. 2013. (Pseudo-)symmetrical transport
3. Slotboom DJ. 2014. Structural and mechanistic insights into prokaryotic energy-coupling factor transporters. *Nat. Rev. Microbiol.* 12(2):79–87
4. ter Beek J, Guskov A, Slotboom DJ. 2014. Structural diversity of ABC transporters. *J. Gen. Physiol.* 143(4):419–35
5. Davidson AL, Dassa E, Orelle C, Chen J. 2008. Structure, Function, and Evolution of Bacterial ATP-Binding Cassette Systems. *Microbiol. Mol. Biol. Rev.* 72(2):317–64
6. Rodionov DA, Hebbeln P, Eudes A, Ter Beek J, Rodionova IA, et al. 2009. A novel class of modular transporters for vitamins in prokaryotes. *J. Bacteriol.* 91(1):42–51
7. Gruber K, Puffer B, Kräutler B. 2011. Vitamin B12-derivatives—enzyme cofactors and ligands of proteins and nucleic acids. *Chem. Soc. Rev.* 40(8):4346
8. Rodionov DA, Vitreschak AG, Mironov AA, Gelfand MS. 2003. Comparative Genomics of the Vitamin B12 Metabolism and Regulation in Prokaryotes. *J. Biol. Chem.* 278(42):41148–59
9. Locher K. P., Lee A. T. RDC. 2002. The E. coli BtuCD Structure: A Framework for ABC Transporter Architecture and Mechanism. *Science* 296(5570):1091–98
10. Santos JA, Rempel S, Mous ST, Pereira CT, ter Beek J, et al. 2018. Functional and structural characterization of an ECF-type ABC transporter for vitamin B12. *Elife*. 7:e35828
11. Cadieux N, Bradbeer C, Reeger-Schneider E, Köster W, Mohanty AK, et al. 2002. Identification of the periplasmic cobalamin-binding protein BtuF of Escherichia coli. *J. Bacteriol.* 184(3):706–17
12. Xu K, Zhang M, Zhao Q, Yu F, Guo H, et al. 2013. Crystal structure of a folate energy-coupling factor transporter from Lactobacillus brevis. *Nature*. 497(7448):268–71
13. Wang T, Fu G, Pan X, Wu J, Gong X, et al. 2013. Structure of a bacterial energy-coupling factor transporter. *Nature*.

497(7448):272–76
14. Zhang M, Bao Z, Zhao Q, Guo H, Xu K, et al. 2014. Structure of a pantothenate transporter and implications for ECF module sharing and energy coupling of group II ECF transporters. *Proc. Natl. Acad. Sci. U. S. A.* 111(52):18560–65
15. Swier LJYM, Guskov A, Slotboom DJ. 2016. Structural insight in the toppling mechanism of an energy-coupling factor transporter. *Nat. Commun.* 7:11072
16. Bao Z, Qi X, Hong S, Xu K, He F, et al. 2017. Structure and mechanism of a group-I cobalt energy coupling factor transporter. *Cell Res.* 27(5):675–87
17. Rempel, S., Colucci, E., de Gier, J.W., Guskov, A., Slotboom DJ. 2018. Cysteine-mediated decyanation of vitamin B12 by the predicted membrane transporter BtuM. *Nat. Commun.*, pp. 1–8
18. Coelho D, Kim JC, Miousse IR, Fung S, Du Moulin M, et al. 2012. Mutations in ABCD4 cause a new inborn error of vitamin B12metabolism. *Nat. Genet.* 44(10):1152–55
19. Wuerges J, Geremia S, Fedosov SN, Randaccio L. 2007. Vitamin B12 transport proteins: crystallographic analysis of beta-axial ligand substitutions in cobalamin bound to transcobalamin. *IUBMB Life*. 59(11):722–29
20. Karpowich NK, Song JM, Cocco N, Wang DN. 2015. ATP binding drives substrate capture in an ECF transporter by a release-and-catch mechanism. *Nat. Struct. Mol. Biol.* 22(7):565–71
21. Gopinath K, Venclovas C, Ioerger TR, Sacchettini JC, McKinney JD, et al. 2013. A vitamin B_{12} transporter in Mycobacterium tuberculosis. *Open Biol.* 3(2):120175
22. Gopinath K, Moosa A, Mizrahi V, Warner DF. 2013. Vitamin B(12) metabolism in Mycobacterium tuberculosis. *Future Microbiol.* 8(11):1405–18

Addendum

Layman terms summaries in Dutch and German

Nederlandse samenvatting voor de leek

Deutsche Zusammenfassung für Laien

List of publications and achievements

Acknowledgments

Nederlandse samenvatting voor de leek

Bacteriën hebben voor hun overleven essentiële stoffen nodig die ze niet zelf kunnen produceren. Dit betreft verscheidene chemische categorieën van substraten, waarvan vitamines een belangrijk deel uitmaken. Daarom is het nodig dat de laatstgenoemde moleculen met hulp van speciale transportsystemen in de bacteriecel worden opgenomen, want, zoals alle cellen, zijn ook bacteriële cellen van hun milieu gescheiden door een membraan. In dit membraan bevinden zich membraaneiwitten, die de uitwisseling van alle benodigde stoffen mogelijk maken en zo het overleven van de bacterie garanderen. Voor veel stoffen die getransporteerd worden, waaronder vitamine B12, zijn de verantwoordelijke membraaneiwitten nog niet bekend. Ongeveer 50% van de bacteriën hebben een transporteiwit nodig om vitamine B12 te kunnen transporteren. Bij de start van het promotietraject dat tot voorliggend proefschrift heeft geleid, was er echter slechts één transporter hiervoor bekend terwijl dit eiwit niet in al deze bacteriën voorkomt. In 2003 en 2009 zijn er twee transporteiwitten ontdekt, BtuM en ECF-CbrT, waarvan werd voorspeld dat het bacteriële vitamine B12 transporters zijn. Er was echter geen experimenteel bewijs hiervoor.

ECF-CbrT hoort bij de Energy-Coupling Factor (ECF) transporter familie, die een onderdeel van de ABC-transporter superfamilie (ATP-binding cassette) uitmaakt. ABC-transporters maken de opname van een groot aantal verschillende stoffen mogelijk, en begruiken daarbij cellulaire energie in de vorm van ATP . In het geval van BtuM was het niet duidelijk welk soort transporter dit membraaneiwit is, aangezien BtuM geen gelijkenis heeft met andere bekende transporteiwitten.

Tijdens mijn promotieonderzoek heb ik een speciale, gemodificeerde bacteriestam geconstrueerd, die het mogelijk maakt om te testen of een membraaneiwit een verantwoordelijk is voor vitamine B12 transport. In het geval dat ik in deze bacteriestam één van de veronderstelde vitamine B12 transporters introduceerde, konden deze gemodificeerde bacteriën groeien in omstandigheden waaronder de opname van vitamine B12 noodzakelijk was. Dit experiment toonde aan dat BtuM en ECF-CbrT daadwerkelijk twee nieuwe vitamine B12 transporters zijn.

Door middel van röntgenkristallografie was het mogelijk om de driedimensionale structuren van BtuM en ECF-CbrT te bepalen. De

structuur van ECF-CbrT toont aan dat het een typische ECF-transporter betreft. Dit was verrassend aangezien vitamine B12 aanzienlijk groter is in vergelijking met andere stoffen die door ECF-transporters getransporteerd worden, waardoor je aanpassingen verwacht. De structurele gelijkenis met andere ECF transporters was echter niet geheel onverwacht omdat de structuur van deze famile van eiwitten goed geconserveerd is. Verder was het mogelijk ECF-CbrT in proteoliposomen te reconstitueren, wat betekent dat de gezuiverde transporter weer in een membraanomgeving wordt gebracht. Proteoliposomen zijn kleine blaasjes, die door een membraan omgeven worden. Deze proteoliposomen maken het mogelijk om onder verschillende condities te bepalen hoeveel radioactief gelabeld vitamine B12 geïmporteerd wordt in de lumen van de proteoliposomen door ECF-CbrT. Bovendien zijn ATP moleculen benodigd als energiebron voor het importeren van het substraat, wat voor een ABC-transporter te verwachten is. Ten slotte was het door middel van een combinatie van technieken mogelijk om aan te tonen dat de traagste stap in de gehele transportreactie de translocatie van vitamine B12 is, en niet bijvoorbeeld het binden van het substraat, wat voorafgaat aan de translocatie.

In het begin van mijn project was het niet duidelijk tot welk soort transporters BtuM behoorde. De kristalstructuur van BtuM toonde aan dat BtuM dezelfde structuur heeft als een S-component. S-componenten zijn normaal gesproken een onderdeel van ECF-transporters, dat zorgt voor de binding met het bijpassende substraat (bijvoorbeeld vitamine B12), waardoor het getransporteerd kan worden. Dit resultaat is verrassend en van groot belang aangezien alle bacteriën die BtuM als vitamine B12 transporter gebruiken, de overige eiwitten missen om een compleet ECF-transporter complex te kunnen vormen. Daarom vertegenwoordigt BtuM een nieuwe soort transporter van ECF-module onafhankelijke S-componenten. Verder bleek dat BtuM niet alleen verantwoordelijk is voor het transporteren van vitamine B12, maar dat het tevens zorgt voor chemische modificatie van het substraat. Dit is voor transporters zeer ongebruikelijk, aangezien ze normaal alleen maar aan het substraat binden en het vervolgens transporteren. Het enige andere bekende opnamesysteem, waar tevens chemische modificatie van het substraat gekatalyseerd wordt tijdens de transportreactie, zijn phosphotransferasesystemen. BtuM katalyseert een reactie waarbij het cyanide ligand van het cyanide-bevattende vitamine B12 molecuul, wat ook bekend staat als cyanocobalamine, verwijderd wordt.

Cyanocobalamine is de meest stabiele vorm van vitamine B12, maar het is niet biologisch actief en moet eerst door de cel omgezet worden om actief te worden. Dit maakt de modificatie van cyanocobalamine, gekatalyseerd door BtuM, nuttig aangezien de cel de geïmporteerde cyanide-vrije cobalamine direct kan gebruiken. Ten slotte is de verwijdering van cyanide een langzaam proces. Het humane enzym CblC, dat soortgelijke reacties katalyseert, heeft een overeenkomstige reactiesnelheid wat mogelijk aangeeft dat dit soort reacties over het algemeen langzame processen zijn.

Deutsche Zusammenfassung für Laien

Bakterien benötigen für ihr Überleben essentielle Substanzen, die sie nicht selbst herstellen können, wie zum Beispiel Spurenelemente, aber auch Vitamine. Viele dieser Substanzen müssen Letztere mit speziellen Transportsystemen in die Bakterienzelle aufgenommen werden, da wie alle Zellen auch Bakterien von einer Membran umgeben sind, die sie von ihrer Umwelt trennt. Eingebettet in diese Membran sind spezialisierte Membranproteine, die den Austausch von allen Substanzen, die das Bakterium zum Überleben benötigt, ermöglichen. Für den Transport von vielen Substanzen sind die notwendigen Membrantransporter noch nicht bekannt, was unter anderem auf Vitamin B12 zutrifft. Ungefähr die Hälfte aller bekannten Bakterien benötigen einen Vitamin B12 Transporter, dennoch ist bisher nur ein Transporter für dieses Vitamin bekannt, den wiederum nicht alle dieser Bakterien besitzen. 2003 und 2009 wurden in theoretischen Studien zwei potentielle Vitamin B12 Transporter, die BtuM und ECF-CbrT heißen, identifiziert und es wurde vorhergesagt, dass diese eventuell neue, bakterielle Vitamin B12 Aufnahmesysteme sind. Dafür fehlte bisher jedoch jeglicher experimenteller Nachweis.

ECF-CbrT gehört zu der ECF-Transporter Familie (Energie Kopplungsfaktor), die ein Teil der ABC-Transporter Superfamilie (ATP Bindekassette) sind, welche den Transport von vielen verschiedenen Substanzen ermöglichen und dafür Energie aus dem Stoffwechsel der Zelle in Form von ATP-Molekülen verbrauchen. Bei BtuM war es nicht klar um was für eine Art Transporter es sich handelt, da BtuM keinerlei Ähnlichkeit mit anderen, bekannten Membranproteinen hat.

In meinem Doktorprojekt habe ich einen speziell modifizierten Bakterienstamm konstruiert, mit dem es möglich ist zu testen, ob ein Membranprotein ein Vitamin B12 Transporter ist. Wenn man es diesem Bakterienstamm ermöglicht die hypothetischen Vitamin B12 Transporter zu besitzen und es sich auch tatsächlich um Aufnahmesystem für Vitamin B12 handelt, können die modifizierten Bakterien unter bestimmten Bedingungen wachsen, ansonsten sterben sie. Mit dieser Methode konnte nachgewiesen werden, dass BtuM und ECF-CbrT zwei neue Vitamin B12 Transporter sind.

Mit Hilfe von Röntgenkristallographie konnten die dreidimensionalen Strukturen von BtuM und ECF-CbrT bestimmt werden. Die Struktur von ECF-CbrT zeigt, dass ECF-CbrT ein typischer ECF-Transporter ist. Zusätzlich war es möglich ECF-CbrT in Proteoliposome zu rekonstituieren, d.h. den aufgereinigten Transporter wieder in eine Membranumgebung, die eine Zelle imitiert, einzufügen. Proteoliposome sind kleine Sphären, die von einer definierten Membran gebildet werden. Mit diesen Proteoliposomen ist es möglich zu messen unter welchen Bedingungen, wie viel radioaktiv markiertes Vitamin B12 durch ECF-CbrT in das Lumen der Proteoliposome importiert wird. Hierdurch konnte gezeigt werden, dass ATP Moleküle als Energiequelle für den Import benötigt werden, was für einen ABC-Transporter wie ECF-CbrT zu erwarten ist. Zusätzlich konnten wir, in Kombination mit anderen Techniken bestimmen, dass der langsamste Schritt in der Transportreaktion die eigentliche Translokation von Vitamin B12 durch die Membran ist, und nicht etwa das Binden von Vitmain B12, was immer der erste Schritt der gesamten Transportreaktion ist.

BtuM war zu Beginn des Projekts ein unbeschriebenes Blatt, und es war nicht klar um was für eine Art von Transporter es sich handelt. Mit der Kristallstruktur konnte geklärt werden, dass BtuM den gleichen Aufbau hat wie S-Komponenten, die normalerweise ein Teil von ECF-Transportern sind und dort die Aufgabe haben das entsprechende Substrat (z.B. Vitamin B12) zu binden damit es transportiert werden kann. Dieses Ergebnis ist überraschend und von großer Bedeutung, weil alle Bakterien, die BtuM als Transporter für Vitamin B12 besitzen, nicht die restlichen Komponenten besitzen um einen kompletten und funktionstüchtigen ECF-Transporter zu bilden. Deshalb repräsentiert BtuM eine neue Transporterklasse von ECF-Modul unabhängigen S-Komponenten. Zusätzlich stellte sich heraus, dass BtuM nicht nur Vitamin B12

transportiert, sondern das Vitamin auch chemisch modifiziert, was für Transporter, die normalerweise ausschließlich ihr Substrat transportieren um es der Zelle zur Verfügung zu stellen ohne es zuvor zu verändern, außerordentlich selten ist. Die einzigen bisher bekannten Transportsysteme, die ihr Substrat während der Transportreaktion chemisch modifizieren sind Phosphotransferasesysteme. BtuM katalysiert die Entfernung eines Cyanidmoleküls von Vitamin B12, das auch Cyanocobalamin heißt. Cyanocobalamin ist die stabilste Form von Vitamin B12, aber nicht biologisch aktiv und muss erst in z.B. Methylcobalamin oder Adenosylcobalamin umgewandelt werden. Deshalb macht es Sinn, dass BtuM auch substratmodifizierende Eigenschaften besitzt, weil es dem Bakterium Vitamin B12 zur Verfügung stellt, das sofort in biologisch aktive Analoge umgewandelt werden kann. Zusätzlich konnte gezeigt werden, dass das Entfernen des Cyanidmoleküls für enzymatische Reaktion sehr langsam abläuftkjguhr. Aber, da ein menschliches Enzym, das CblC heißt und die gleiche Reaktion (Decyanierung) katalysiert, scheint diese Art von Reaktion generell langsam aber ausreichend für lebende Zellen zu sein.

List of publications

4. **Rempel, S.**, Stanek, W.K., Slotboom, D.J. ECF-type ABC-transporters. *In press, Annual Reviews in Biochemistry (will be published in June 2019, issue 88).*

3. **Rempel, S.**, Colucci, E., de Gier J.W., Guskov, A., Slotboom, D.J. Cysteine-mediated decyanation of vitamin B12 by the predicted membrane transporter BtuM. *Nat. Commun.* **9**, 1–8, 3038 (2018).

2. Santos, J.†, **Rempel, S.†**, Mous, S.T.M., Pereira, C.T., ter Beek, J., de Gier, J.W., Guskov, A., Slotboom, D.J. Functional and structural characterization of an ECF-type ABC transporter for vitamin B12. *eLife.* **7**, e35828 (2018).

† equal contribution

1. Jensen, S., Guskov, A., **Rempel, S.**, Hänelt, I., Slotboom, D.J. Crystal structure of a substrate-free aspartate transporter. *Nat. Struct. Mol. Biol.* **20**, 1224–26 (2013).

Achievements

3. DFG (German Science Foundation) fellow at the 7th FEBS special meeting 'ATP-Binding Cassette (ABC) Proteins: From Multidrug Resistance to Genetic Diseases' (2018)

2. SSBN (Stichting Stimulering Biochemie Nederland) grantee to attend the Gordon Research Seminar and Gordon Research Conference 'Membrane Transport' (2017)

1. EMBO (European Molecular Biology Organisation) short-term fellow (2015)

Acknowledgments

As I come to the end of my thesis, I would like to express the gratitude to those, who were part of this journey. Because I am a 'cold blooded German' (Hylkje J. Geertsema), this is no easy task for me, so it may sound a bit dry. I would like to thank **Dirk** for the opportunity to start painting on the 'white canvas' of uncharacterized vitamin B12 transporters and giving me the freedom to develop the projects as I thought would be the best way forward. I enjoyed the frank and open discussions. Also many thanks to my co-promotor **Bert**, whose questions still make me sweat, but are always valuable input and advice. I also would like to thank my **reading committee**, Prof. S.J. Marrink, and Prof. A.J.M. Driessen from the University of Groningen, and Prof. M.A. Seeger from the University of Zürich for the assessment of my thesis. Next, as it turned out, the expertise and help from Prof. **J.W. de Gier** with the construction of the triple knockout *E. coli* strain during my stay in Stockholm, was absolutely essential to this work, and I would like to thank him for that. I also would like to thank **Joana**, **Albert**, and all the other **authors**, who contributed to the publications in this book or hopefully soon to be published results, for their work, dedication, and help. In the hopefully soon to be published category falls **Andrew**, who's expertise in bacterial *in vivo* single molecule fluorescent microscopy made a very challenging project look easy – unfortunately we were not able to write it up yet. I am also extremely happy and thankful, and never want to miss the time with my paranymphs **Gianluca** and **Alisa**, who made the years much more pleasant, showed me my passion for new hobbies, drinks, and as a 'final' act helped me through my defense ceremony. In that line, I would also like to mention and thank **Weronika**, who was a great companion in the lab and on many work trips like the summer school in Croatia (yes, it was work, definitely!). It was an honor to be your paranymph and you are still being missed by many in the lab. I also would like to mention **Joris**, who now made his way literally around the world, was a great supervisor and source of inspiration with his physics point of view on our biochemistry projects. **Emanuela**, you were an exceptional student who helped and dealt with a very difficult project excellently and I am convinced you will continue to do so in your PhD. The same is true for **Sandra**. I also want to acknowledge the help of **Mark** and **Denise** for their Dutch input in this thesis and all other **students** who worked together with me. I would like to acknowledge **all members** of the Membrane Enzymology group, past and present, who shared expertise, help, stories, drinks, and the lab,

especially **Ria** and **Gea**, **Dorith**, **Morten**, **Cristina**, **Gert**, and **Michiel**, **Marysia** and **Stephanie**. Finally, I would like to thank my family, for their support. I would most definitely not be at this point without you. At last but not least, I sincerely hope I have not forgotten anyone, who deserved to be in this list, and I want to make clear that a PhD is not only the effort of a sole person. So, if you think you should have been mentioned here, I apologize sincerely.